eman ta zabal zazu

Universidad del País Vasco
Euskal Herriko Unibertsitatea

Department of Analytical Chemistry

Assessment of conservation state of gothic wall paintings: from scientific diagnostic to a new monitoring approach

Report to complete for the International PhD degree

Ilaria Costantini

February 2019

ACKNOWLEDGMENTS

I am very grateful to its research group of the Department of Analytical Chemistry, Ikerkuntza eta Berrikuntza Analitikoa (IBeA).

This PhD work has been developed thanks to the financial support received from:

- CTP projects (ref CTP09-P04 and CTP12-P10) founded by Working Community of the Pyrenees, Basque Government.
- project IT-742-13 for Consolidated Research Groups, funded by the Basque Country Government.

My thankfulness goes also to the technical support provided by Dr. Alfredo Sarmiento (in the Singular Coupled Multispectroscopy Laboratory, LASPEA), Dr. Javier Sanguesa (in the X-Ray Service of Rocks and Minerals Unit), from the Research General Services of the UPV/EHU (SGIKER) and Dr. Xabier Murelaga (Department of Stratigraphy and Palaeontology of the University of the Basque Country). MONARIS research group from the University of Pierre et Marie Curie (UPMC, Paris, France) is also gratefully acknowledged

In addition, I am grateful to *Diputación Foral de Álava*, and to Valderejo Natural Park. In also thank Dra. Maria Dolores Rodriguez Lazo (Department of Painting in Faculty of Fine Arts, University of the Basque Country).

I would also like to express my gratitude to Dr. Fernando Benito Lopez (Analytical Microsystems & Materials for Lab-on-a-Chip Group, University of the Basque Country) for giving me the opportunity to use your knowledge for my investigation.

I would like to thank Dr Pier Paolo Lottici and Dr. Danilo Bersani for trust in me and for introducing me in the IBeA research group, Dr. Juan Manuel Madariaga for giving me the opportunity to do this PhD, and my supervisor Dr. Kepa Castro for the support and the dedication to carry out this work.

I would also like to thank all researchers forming part of the IBeA group for the professional and human support and for the good friendships born during the years.

INDEX

CHAPTER 1

Introduction

Cultural Heritage represents the basis of our identity, the legacy that the past civilizations have left us and, for this reason, we must protect it for the future generations. The preservation of our heritage is a current topic of great interest, in particular due to the increase in the last 30-40 years of threatening factors, such as environmental contamination, due to the industrialization, wars and political instability.

The term “Cultural Heritage” usually indicates objects and buildings that have a historical, artistic and monetary value, although also the intangible heritage that includes traditions, knowledge, dialects, etc. is part of it. It is a dynamic concept, because new discoveries from all over the world enrich it every day.

Different types of objects, books, archaeological pieces, paintings, statues, oil and wall paintings, porcelain, jewellery and textiles belong to the cultural heritage and each item is composed of different materials, organic and inorganic, which have a variable aging that affect its durability. Undoubtedly, the most threatened artworks are all those in the open air, as well as those that are kept in places where it is not possible to have a controlled atmosphere, such as architectural works, statues, fountains and wall paintings inside churches and castles [1, 2].

1.1 Multianalytical approach for the study of environmental stressors

The factors that promote the deterioration may be intrinsic or extrinsic to the work of art. For example, several studies have shown that the instability and the reactivity to the atmospheric agents of some pigments employed on wall paintings can cause aesthetic damage [3]. Many examples of chromatic variations are known in the literature, the most frequent being of blackening of lead based pigments such as minium and lead white [4], or the degradation of malachite [5], cinnabar [6] or natural earths [7]. In the recent work by Coccato *et al.* [8] the effect of different parameters on the stability of most common medieval pigments were shown underlining the complexity in the conservation of polychrome artworks.

Additionally, the formation of soluble salts, in form of carbonate, sulphate and nitrate, represents one of the most evident and dangerous cause of degradation for a porous building material, on the surface (efflorescence) or within the porous structure (subefflorescence), although the stone has been considered for centuries one of the most resistant materials [9]. The variations in temperature in presence of water, both infiltration of rainwater or risen by capillarity, cause cycles of salt crystallization and hydration and dehydration provoking the contraction and expansion of the material, which over time, undergoes micro fractures and subsequently disintegrates [10]. In particular, the formation of nitrate salts, such as ammonium nitrate, is one of the major causes of disintegration of carbonaceous materials since ammonium ions are highly reactive species and can attack the alkaline substances of which the masonries are composed [11]. The identification and study of nitrate salts that may be caused by natural factors, such as the degradation of organic material in soil, or of anthropic nature following the wet deposition of NO_x gases in areas with a high level of environmental pollution, is a fundamental step for the protection of building materials, stones, plasters and bricks [12].

Moreover, the interaction between objects and structures and atmospheric pollutants is increasingly studied due to the high levels of air contamination present in many European cities. Air pollution is characterized by the high level of acidic gases, which in presence of the water rain become into acids (H_2CO_3, H_2SO_4, HNO_3) [13, 14]. The action of these acidic compounds favours the degradation of the building materials and ancient and modern artworks in the open air [15]. These processes cause, in most cases, the presence of thick black crusts that ruin the appearance of the artefacts and that are very hard to remove [16] (Figure 1.1).

Figure 1.1: Black crusts visible in the Erechteion in the Achropolis of Athens due to the atmospheric pollutions of the city.

An example of the harmful influence of atmospheric agents on works of art is the archaeological site of Pompeii (Italy). In fact, as shown by several recent studies, both the building materials and the wall paintings of the Roman *domus*, which had been preserved over the centuries buried by the pyroclastic material generated from the eruption of Vesuvius, have suffered a sharp deterioration after the excavation campaigns that brought them to light due to continuous exposure to atmospheric agents [17]. Thus, it is very important to study the best methodologies of preservation before exhibiting an artefact, a painting or an archaeological remain.

In addition, several studies have shown that in certain environmental conditions of temperature, humidity, type of support [18] and presence of light [19], the historical and modern building materials can represent a suitable substrate for biological colonization [20, 21]. The carotenoid organic pigments (β-carotene, zeaxanthin and astaxanthin) present in photosynthetic organisms are the most common molecules identified on substrates and are the main responsible for the aesthetic damage due to the formation of green, pink or brown patinas on the surfaces of the artefacts [22].

A well know study by Ciferri [23] on the damage caused by the presence of microorganisms on cultural heritage shows very extensively the most widespread species on organic and inorganic substrates and the damage that they are able to promote. Indeed, although it may seem that the presence of biological patinas exerts only an aesthetic damage, microorganism such as fungi or lichens can penetrate into the material on which they have grown, with hyphae and thallus respectively, causing cracks. In addition, from the point of view of chemical damage, oxalic acid ($H_2C_2O_4$), secreted by microorganisms, reacts with the calcium carbonate of the substrate causing the formation of calcium oxalate that, depending on the degree of hydration, is recognized as whewellite ($CaC_2O_4{\cdot}H_2O$) or weddellite ($CaC_2O_4{\cdot}2H_2O$), two insoluble mineral species that contribute to the formation of salt efflorescence [24].

A well know study by Edwards *et al.* [25], was carried out on the frescoes of Palazzo Farnese, Caprarola, Italy, where, due to the chemical and structural damage caused by the massive colonization of lichens (*Dirina massiliensis forma sorediata*), around the 80% of the Renaissance frescoes were destroyed in some areas. The analyses indicated a significant chemical activity in lichen encrustations, in which some metabolic products such as erythrine, lecanoric acid and polyphenolic acids were identified together with calcium oxalate hydrate, formed by the irreversible reaction of oxalic acid with the calcium carbonate of the substrate [26]. On the other hand, some studies have highlighted the presence of calcium oxalate resulting from the degradation of organic binder's media [27].

Being this the state-of-the-art, it is interesting to see the way in which all mentioned degradations perception has changed, as well as the philosophy in which conservation and restorations works are carried out.

In past years, the evaluation of the conservation status of an artefact was carried out by curators and restorers according to an empirical method developed over the years without carrying out chemical-physical investigations. This lack of materials knowledge sometimes led to wrong diagnosis and to unsuitable restoration interventions accordingly. In this way, rather than protect a work of art these interventions worsened its aesthetics and reduced its durability in time. Only in a few cases the analytical techniques were used, for example, to verify the suitability and effectiveness of chemical products used in cleaning procedure [28].

During the last decade, due to the increase of decay’s factors, it has been necessary to operate with a renewed attitude and a great attention has been paid to the study of materials. For this reason, different professionals - conservators, restorers and diagnosticians - have shared their historical, artistic and scientific knowledge to characterize and study not only the original materials but also especially the degradation products, and consequently, identify the factors that caused them. Therefore, it has been sometimes possible to reduce these factors and choose the best restoration and conservation treatment. This was possible especially thanks to the development of new non-invasive diagnostic methodologies, sometimes adapted from other scientific fields, that have been employed for the study of Cultural Heritage. Currently, restoration interventions are carried out only after a chemical study of materials and each artwork is considered as an individual case.

In this sense, portable and mobile diagnostic techniques are the most adequate tools with considerable advantages for the study of works of art. Thanks to them, it has been possible to extend the scientific study to the so-called immobile works of art that cannot be transported to the laboratory and consequently cannot be analysed by benchtop instruments. Nowadays, statues, architectural works and wall paintings can be analysed *in situ* without taking away any sample, and therefore neither the appearance nor the integrity of the artefact under study is affected because the techniques are completely non-invasive. Moreover, the results are obtained almost immediately, thus, it is possible to decide the right intervention method during the study campaigns, sparing time.

There is some confusion in the literature with regard to the terminology around portable devices, even though some efforts has been done, such as a publication by Bersani *et al.* [29], which tried to clarify the terminology indicating the different types of non-destructive techniques and the instruments defined as “mobile instrumentation” or portable instrumentation. The most important fact is that with such kind of portable devices it is possible to perform *in situ* analyses.

The most used *in situ* techniques for application in analytical archaeometry are the spectroscopic techniques [30], such as X-ray fluorescence (XRF), Fourier transform infrared spectroscopy (FT-IR) and Raman spectroscopy. Since the mid-80s, Raman spectroscopy has become the most used technique for the molecular study of artefacts of historical and artistic interest [31, 32], especially for direct [33] and *in situ* analysis [34]. The use of a portable Raman spectrometer connected to a micro probe allows a non-destructive approach towards the work of art, if the laser power is under control to avoid thermal degradation [35]. Its reliability in the characterization of ancient [36] and modern pigments [37], organic compounds [38] and degradation products [39] is reported in many studies concerning cultural heritage.

Even *in situ*, Raman spectroscopy presents a high standard performance and it is capable to distinguish among polymorphs of the same compound. An example of this is the work of Prieto- Taboada *et al*. [40], which showed for the first time the attribution of Raman bands belonging to five different polymorphic species of calcium sulphate ($CaSO_4.2H_20$, $CaSO_4.½.H2O$, γ-$CaSO_4$, β-$CaSO_4$, α-$CaSO_4$), confirming the importance of Raman spectroscopy for the study of degradation products found on the surfaces of wall paintings containing calcium sulphate.

Together with Raman spectroscopy, XRF spectroscopy is also a very valuable technique for *in situ* analyses since it provides the elemental composition being used generally as the first screening of the materials [41]. As well as XRF spectroscopy, laser-induced breakdown spectroscopy (LIBS) is another technique devoted to the elemental characterization of materials, and presents some advantages over the XRF approach, like the possibility to detect light elements. However, LIBS is still not used as often as XRF although a detailed study was reported more than fifteen years ago by Anglos [42].

In addition to the success of portable instrumentation, researches have showed that the best results are obtained when portable techniques are supported by laboratory analyses. In these cases, portable techniques have been fundamental to identify the areas of interest in which perform further micro-sampling without unnecessarily affecting the underlying surfaces. Through the use of laboratory techniques, such as scanning electron microscope combined with energy-dispersive X-ray spectroscopy (SEM-EDS), micro X-ray fluorescence (μ-XRF), X-ray diffraction (XRD) [43] or chromatographic techniques (PY-GC-MS, GC-MS) [44], it is possible to obtain information that could not be obtained only by *in situ* analysis. In fact, the signal obtained by *in situ* analysis, depending on the technique used, can provide information that relates not only to the surface but also to the underlying layers, making more complex the interpretation of the results. For this reason, SEM, micro-XRF and Raman imaging techniques have revealed to be very useful to obtain the elemental and molecular distribution of compounds in a sample, especially if it has been previously embedded in resin to be analysed as a cross section to identify the stratigraphic distribution of compounds in the layers [45, 46]. This preparation of the sample is particularly important in the case of wall paintings as they are characterized by a succession of different layers, in particular in the case of the fresco technique, which needs some substrate preparation layers (arriccio and intonaco), above which the paint layer is applied. Moreover, during its history, wall paintings may be subjected to restoration interventions and new materials from the modern era, pigments, consolidating materials and varnishes can be found on the surface.

Thus, thanks to the point by point analysis carried out using laboratory instruments, the materials that make up each pictorial layer can be well characterized as well as the presence of possible degradation products.

Indeed, among the immovable artefacts, the wall paintings are undoubtedly one of the most studied categories because they are the most at risk due to the permanent interaction with the surrounding environment. Therefore, the study of these artworks provides information not only about the raw materials but also about the environment in which they are located. In this way an explanation of the reactions between the original compounds and the chemicals in the environment can be explained and the subsequent adequate restoration procedures can be applied [47].

1.2 Medieval wall paintings

After the revaluation of medieval art, excellent results have been obtained in recent years concerning the study of wall paintings. The medieval era covers a very long period that includes almost a millennium of art history. According to the most widespread periodization, the Middle Ages would start in 476 AD, the year of the fall of the Western Roman Empire, and would end in 1492, the year of the discovery of America. Generally, the main currents that are recognized by the art historians include a phase following Early- Christian art, Byzantine art, pre-Romanesque and Romanesque, and Gothic. However, the attempt to classify them in main periods and styles could be complex due to local currents that spread to different locations in Europe and in the Middle East.

The strong break with the classical art from which it strongly differs for the symbolic character, in contrast to the realism, was the main cause of lack of appreciation that it had especially in the Renaissance period in which with “Renaissance” it was usual to indicate a rebirth of the arts after the dark medieval ages [48]. This denigration for an art that was considered of a lower level, and therefore, not worthy of being safeguarded, was the main cause of abandon of medieval art and even of its voluntary destruction in the phenomenon of iconoclasm when many works of art were lost forever. The icons were burned and the mosaics were destroyed as well as the wall paintings inside the churches. In some cases, these were covered under layers of plaster or hidden with altarpieces.

Around the middle of the 19th century, medieval art conceived as a true artistic current was rediscovered, thanks above all to the influence of romantic culture promoted by writers such as John Ruskin, Eugène Viollet-le-Duc, and Pugin, because they were the first to question the conservation of the architectural heritage that arose in the Middle Ages and consequently also the treasures located inside them.

Although the paintings preserved in the castles had the purpose of celebrating the nobility, those located inside the churches and the monasteries had an educational function and represented the material instrument that connected the believers to God. Unfortunately, many of them are at risk of conservation and for this reason several studies have been carried out in recent years and have allowed to bring to light pictorial cycles belonging to this era and the historical-artistic studies have rediscovered new meanings of enigmatic paintings until now unknown.

This introduction aims to show the results obtained in the last twenty years in the study of medieval wall paintings through the use of portable non-destructive and micro-destructive techniques, highlighting their reliability in the characterization of original materials and modern materials used during restoration work carried out in modern times. Thanks to the study of the materials that compose the pictorial layers it has been possible to obtain important information about the identification of pictorial techniques as well as the determination of the period of execution, the studies of provenance of the raw materials and the attribution to an author or a studio. In particular, the numerous works that have underlined the usefulness of the scientific approach for the diagnostic of the conservation state of the paintings thanks to the identification of degradation products caused by the impact of natural and environmental stressors will be mentioned along this chapter.

1.3 Characterization of mediaeval wall painting's materials

1.3.1 Study of antique pigments

At first, the analytical techniques were mainly used for the characterization of original materials of medieval wall paintings. The compositions of plasters for the identification of the execution techniques and the pigments used were studied in depth, especially through the use of laboratory techniques applied on fragments for surface analysis or in cross-section.

Certainly, the research group headed by H.G.M. Edwards was one of the first to prove the reliability of spectroscopic techniques for the study of works of art. One of his first researches on the study of medieval works involved the use of Fourier transform Raman spectroscopy for the identification of pigments on red samples of English medieval wall paintings [49] where the signals of vermilion (HgS) on a substrate of calcium carbonate and siliceous material were identified. In addition, a mixture of vermilion and red iron oxide (α-Fe_2O_3) was found approximately mixed in a ratio of 1:3 from a comparison of intensity of spectra of standard pigments.

Numerous researches were carried out on the study of medieval wall paintings preserved in the religious buildings in the north of Spain. The construction of churches and monasteries in the Middle Ages in this area was due to the need to provide an accommodation to pilgrims who stopped in villages along the way heading to Santiago de Compostela in Galicia (Spain). It is precisely through the comparison of some fragments taken from two churches in the province of Castilla y León (Spain), that was verified by Edwards *et al.* [50] an antique controversy regarding the use of the term "minium" with which both cinnabar and red lead were defined. This work showed the potential of the FT-Raman spectroscopy for the identification and quantification of ancient pigments used in the mixture through the construction of calibration curves. The confusion in the interpretation of ancient recipes for pigment blends is unavoidable and was exacerbated by the practice of adulteration of cinnabar with red lead generally for economic reasons.

However, the research carried out on the murals of the Church of Saints Cosmo and Damian at Basconcillos del Tozo [51] (Castilla y León, Spain) demonstrated a hierarchical application in the use of red pigments in which the most important biblical figures were painted with pure cinnabar while mixtures of cinnabar and red lead or red ochre were employed in other areas. Moreover, thanks to the application of FT-Raman spectroscopy, two types of cinnabar were identified from two different locations, one of which, from the Almadén mine, is supposed to be considered more precious for its use in the paintings. The same pigment was found also in some microsamples taken from the wall paintings from the thirteenth century Convento de la Peregrina, Sahagún (León, Spain) [52].

Of particular interest are the studies conducted on microsamples from murals in the monastery of Saint Baudelio [53] located to the south of the Duero river. The chromatic palette composed of haematite, charcoal/soot, litharge, goethite, minium and copper salt (probably malachite or verdigris) was completely different from the one found in the northern paintings in which cinnabar, realgar, orpiment, barytes and lapis lazuli were present. This discovery would confirm the theory of art historians that the monastery of Saint Baudelio was colonized by an enclosed monastic order, so the materials employed were limited only to those minerals available locally.

Another similar case is represented by medieval frescoes located in the Palencia region of Spain [54]. Some fragments from four churches, belonging to different periods (from fifteenth century to twelfth century) and with influences of different pictorial schools were studied and only in one case cinnabar was used.

Some researchers have highlighted the lack of availability of raw materials in the Middle Ages and the difficulty of the purchase for economic reasons. This problem did not concern only the availability of red pigment such as cinnabar and was remarkable for the blue pigments. Indeed, since they were imported from Germany (azurite ($2Cu(CO_3)_2\ Cu(OH)_2$)) or from Afghanistan (lapis lazuli ($Na_8(Al_6Si_6O_{24})S_n$)) they were expensive and therefore were reserved for important areas of wall paintings. Indeed, in the iconographic tradition, the use of the blue pigment takes on a symbolic value - it was used to paint the Virgin's mantle - as shown in the study of blue fragments from medieval mural paintings in the South West of France [55]. Thanks to spectrocolorimetric analysis and microanalysis with SEM-EDS, the use of copper based pigments was pointed out, lapis lazuli and azurite (non-local source), employed for the most important figures, while aerinite (local), a rare blue Fe(II)/Fe(III)-containing aluminosilicate from the Pyrenees region, was used for the background. In the absence of these pigments, the artists resorted to using more accessible pigments, carbon black or lime white for example.

The same blue pigment aerinite was used for the painting of Romanesque frescoes in the Pyrenean region of Catalonia and in Andorra [56] and its use was probably dictated both by local availability and by economic factors. A detailed work published by Pérez-Arantegui *et al.* [57] has allowed to obtain new analytical data concerning the microstructure and the chemical composition of the aerinite pigment identified on Romanesque wall paintings in Aragón (Spain).

The use of azurite for blue areas and posnjakite ($Cu_4(SO_4)(OH)_6 \cdot H_2O$) and atacamite ($Cu_2(OH)_3Cl$) for green decorations was confirmed also by the study of fragments from the mural paintings of the Tournai Cathedral, (Belgium) [58]. In other cases, as in the Peć Monastery [59], a black layer of coal was identified under a layer of green and blue colour in order to obtain a more intense blue hue, a typical method applied in Byzantine times.

A series of wall paintings dating from the Romanesque period to the 16th century were uncovered during restoration projects at the Pyrenean Church of Santa Eulàlia of Unha in the Val d'Aran (Spain) [60]. The study through different analytical, elemental and molecular techniques showed the use of traditional colours of the medieval period (haematite, goethite, vermilion, red lead, carbon black and calcite) and a variation of the palette based on the period of realization of the works. Only in Romanesque paintings the aerinite was identified and for the first time its spectra were shown in the context of a work of art. On the other hand, surprisingly, in the 16th century wall paintings a mixture of lime white and charcoal black was identified to obtain a "blue colour".

In fact, the work by Daniel *et al*. [55] highlighted the use of pigments suggested by a different conception of colour in the medieval period that does not differ from theories of contemporary colours. The false blues were used because some grey shades could be perceived as bluish. In this work the false-blue was considered a typology and a classification of it was proposed.

The use of false-blue was also found in early medieval frescoes of the Longobard temple of Cividale del Friuli (Italy) [61] in which the blue colour is given by the diffusion properties of the black and white particles of lime and carbon black respectively. In this work a particular technique of achievement was underlined. In fact, SEM images identified the use of textile fibres incorporated in the pictorial film. Considering the scarce availability of cotton in Europe in the Middle Ages it can be assumed that this material was imported by the workers of oriental origin.

Pigment analyses have sometimes revealed the money available for the execution of the paintings. For example, in the case of the study of 14th century wall paintings from the Church of the Holy Mother of God Hodegetria (Serbia) [59], Raman spectroscopy showed that the artist's palette was exceptionally limited, consisting of inexpensive pigments of local origin, testifying that the founder member did not belong to a noble family.

On the contrary, the multi-analytical study based on the use of elemental and molecular techniques, - employed in the study of materials used for the decoration of the monastery of Žiča [62] (Serbia), - was fundamental for the identification of expensive pigments such as lapis lazuli and cinnabar, as well as gilding with golden tin, which confirmed the desire of the Serbian aristocracy to assert its economic power. This was also the case of the materials found in the Gothic wall painting of the Dominican Monastery in Ptuj (Slovenia) [63], where the use of expensive pigments such as azurite and cinnabar indicated a wealthy client. Moreover, of great interest was the discovery of the lead–tin yellow type I in the wall paintings belonging to 14th century since, until that moment it was considered that it appeared on the market only in the first half of the 15th century.

In the study by Edwards *et al.* [64] on a post-medieval wall painting in the church of St. Peter and St. Paul at Upton (United Kingdom), an unusual palette of pigments was identified, which included expensive pigments such as cinnabar and lapis lazuli and materials from the nineteenth century such as barites and chrome yellow. The hypothesis formulated by the researchers is that an ancient mural painting could have been repainted in modern times. A similar research using micro-Raman spectroscopic was reported by Minceva-Sukarova *et al.* [65] on the study of pigments used in medieval wall painting in Sveta Bogorodica church in Lešok (North- Western Macedonia) in which a distinction was made between original and new materials from two layer paint from the 17th and from the 19th century.

Thanks to technological development, new portable instruments have been tested to make direct measurements on the artworks for the identification of pigments and the execution techniques. They have proved to be particularly suitable for archaeometric study, above all because of their non-invasive feature. This means that sampling can be avoided since the portable instrumentation allows to perform a satisfactory investigation of the material. Although some pitfalls have been pointed out in the use of mobile instrumentation (the instrumental set-up, the positioning of the probe head and stability problems for vibrations of the scaffold, problems related to environmental conditions [66] or to the presence of some materials [67]), the spectroscopic portable techniques have been the most used ones for the study of the conservation state of wall paintings in the last years.

The completely non-destructive work carried out by using only mobile tools (X-ray fluorescence and Raman spectroscopy) to examine the 15th century mediaeval vault paintings in the Our Lady's Cathedral (Antwerp, Belgium) [68] can be used as an example of the difficulties that during an *in situ* analysis can arise. In fact, the Raman signals from calcium carbonate, belonged to small particles left after removing the layer of plaster applied over the paintings during the iconoclast wave, made difficult the characterization of the pigments by Raman spectroscopy. Despite this, lead white, calcite, gypsum, lead tin yellow, and vermilion were identified.

Another research work carried out completely in non-invasive way by using just a portable XRF analyser, concerned the study of medieval wall paintings of Yemrehanna Krestos Church, Ethiopia [69]. This research was the first research of Ethiopian wall paintings. The correlation between the element concentration and the multivariate statistical analysis was used to identify the most probable compounds and to classify the groups of pigments used. Some authors state that the *in situ* ED-XRF analyses are, in most cases, sufficient to guide *in situ* conservation and restoration interventions, as shown by Ferrero *et al.* [70] in the study of a wall painting of the 14th and 15th centuries. The identification of inorganic key elements allowed the characterization of the pigments and the techniques used by the artists. This approach, however, is sometimes criticized because the same elemental composition can belong to different molecular composition, thus, data misinterpretation can occur.

1.3.2 Further than *in situ* analysis

Although some researches have shown that it is possible to obtain exhaustive results only through the use of portable techniques, other publications had underlined the need to continue the study through laboratory analysis. In this sense, the portable techniques are extremely useful for identifying a particular area in order to minimize the sampling.

The simultaneous use of portable XRF and Raman spectroscopies was tested for the study of the range of pigments used in the mural paintings and frescos of the Little Christopher chamber in the Main Town Hall of Gdańsk, Poland [71]. Subsequently, the statistical processing of the spectra was applied to minimize the number of sample extractions to complete the study using micro-Raman spectroscopy in the laboratory. The presence of copper, lead, iron, mercury and calcium together with traces of antimony, cadmium, barium and molybdenum, was in accordance with the composition of the identified pigments by Raman spectroscopy.

In order to solve the problem of the lack of written source concerning the techniques of execution of Nubian wall paintings [72], different analytical techniques such as portable X-ray fluorescence, laser ablation inductively coupled plasma mass spectrometry and Raman spectroscopy were applied to identify the raw materials and distinguish the use of different pigments. The use of complementary techniques made it possible to observe some variations in the composition of the pigments in samples from different archaeological sites and were useful for evaluating the existence of possible variations among the local Nubian workshops.

The comparison between the materials used in different wall paintings belonging to the same area can be useful for the identification of the origin of the workers or for the attribution to an artist as shown in the work by Lampakis *et al.* [73] where thanks to the combined use of micro-Fourier transform infrared and micro-Raman spectroscopy some fragments of Byzantine wall paintings from three Thessalian monasteries (Greece) were studied. The similarities in the materials and in the technique supported the hypothesis that the same artist may have worked in the three churches. On the other hand, the vibrational techniques FT-IR and μ- Raman were employed on fragments from the medieval Monastery of Karaach-Teke [74] in which it was evident the Byzantine influence on the technology and the thematic-aesthetic features of Byzantine iconography in Bulgaria. In the research on Russian-Byzantine wall paintings from Sweden [75], dating back to the 12th century, the isotopic composition of lead pigments was studied using a mass spectrometer to clarify the provenance of the materials found in the paintings. The results showed that the materials were not only locally sourced but rather came from both Russia and Germany as well.

In another study [76], the natural origin of azurite and malachite found in some murals was demonstrated by the presence of copper and zinc arsenates, while artificial malachite was identified by uniform spherulitic particles.

In the same way the objective of the study of wall paintings preserved within two Byzantine churches in Kastoria, (Greece) [77] was to find similarities in the materials to hypothesize the presence of a single hand in the realization of the paintings. Thanks to the use of SEM-EDS and Raman spectroscopy on fragments, similar pigments were identified for both churches. However, the wall paintings could not be attributed to a single iconographer due to some differences noted for the realization of the green tone that in one case was obtained from green earth and in the other from mixtures of iron oxides and calcite.

A similar approach was employed for the comparative evaluation of the results obtained studying the materials of wall paintings in the Protaton church [78] and in the Thessaloniki cathedral [79] by non-invasive analysis with XRF, mid-FT-IR, UV-Vis diffuse reflectance spectroscopy and laboratory analyses using micro-FT-IR, SEM-EDS and micro-Raman spectroscopy, which had strengthened the hypothesis of the attribution of the paintings to the same Panselinos School.

The results of the research by Cheilakou *et al.* [80] on the study of Byzantine wall paintings from Rethymno, Crete, demonstrated the reliability of the portable non-invasive technique of diffuse reflectance spectroscopy (FORS) for the *in situ* characterization of pigments used in wall paintings, also thanks to the comparison with the information obtained with laboratory techniques such as ESEM-EDS, ATR-FT-IR and micro-Raman spectroscopy. The same FORS technique was successfully used together with X-ray fluorescence spectrometry and Raman spectroscopy also in the study of mural paintings attributed to Giacomino di Ivrea in Valle d’Aosta (Italy) [81]. From a technical point of view, FORS and XRF confirmed their wide potential as preliminary methods for the identification of pigments, reducing the need to use other analytical laboratory techniques such as Raman spectroscopy or SEM-EDS. Regarding the study of materials, the analyses showed the presence of graphite as black pigment, instead of the more common carbon black, probably related to the presence of graphite deposits in Valle d'Aosta.

1.3.3 Unusual findings

Although in most cases there was not a large variation in the palette of medieval painters, diagnostic techniques have proved to be extremely useful to identify the use of uncommon pigments and peculiar processes of realization in the wall paintings.

An interesting example of medieval repointings was identified on the walls of Miravet Castle [82] in Spain thanks to the use of X-ray diffraction, SEM-EDS and FT-IR. The repointing, based on a lime-rich mortar, was made not only for waterproofing the wall but it had a decorative function too. The decoration, obtained with engraving and with the use of red and black pigments, enhances the visual aspect of the joints.

In the work by Kakoulli *et al.* [83] the earliest evidence for asbestos composites connected to the production of Byzantine wall painting in Cyprus was found. In particular, the use of secondary electron images showed the fibrous nature of the particles in the finish coating at the interface between the red cinnabar paint layer and the plaster. The fibrous nature of the particles supported the presence of an asbestiform mineral, identified as chrysotile. The discovery suggests that asbestos was discovered and used in Cyprus since ancient times for its good physical properties.

Concerning the use of rare pigments, the study of fragments from the 13th century wall paintings discovered under the Cathedral of Siena [84] (Italy), shown, through the joint use of XRD, SEM-EDS and micro-Raman spectroscopy, the discovery of crocoite ($PbCrO_4$) and chrysocolla, whose use in medieval European paintings was not previously reported (Figure 1.2). Besides, thanks to microstratigraphy, it was possible to know that three painting techniques, fresco, tempera and lime paint, even with organic vegetable fibres, were combined according to the desired effects or the characteristics of the pigments. In addition, the use of gold leaf applied on a ground preparation together with white lead, red lead and verdigris with an organic binder was found. Yellow crocoite was also found in Northern Bohemia [85], after non-invasive (XRF) and microdestructive laboratory analyses (micro-Raman and powder X-ray micro-diffraction).

The presence of glushinskite, a magnesium oxalate, was reported by Chiari and Scott [86]. It was used as white pigment in the wall paintings of the Church of Saint Fiorenzo in Bastia, Mondovì (Italy). In the same publication another peculiarity was found in frescoes preserved in an Italian church. Lead sulphate anglesite, generally identified as a lead-based pigment degradation product, appeared to be present as a pigment willingly used by artists in the Saint Andrea Church in Vercelli, (Italy).

In the work of Švarcová *et al.* [76] for the first time, cumengeite, ($Pb_{21}Cu_{20}Cl_{42}(OH)_{40}$), was identified as a blue pigment in Bohemian Gothic murals paintings using micro-XRD. Rare copper pigments are also described in the literature linked to their use in medieval art. In the study of a thirteenth-century wall painting in the Gozzoburg city palace in Krems, Austria [87], thanks to the use of SEM-EDS and XRD copper trihydroxy-chloride (clinoatacamite) was identified as a pigment probably synthesized specifically for these painting. Other green copper pigments, such as conichalcite ($CaCuAsO_4(OH)$) and dolerophanite ($Cu_2(SO_4)O$) were found by using

Raman spectroscopy in the wall paintings of the Voronet Monastery (Romania) [88]. Aceto *et al.* [89] reported the use of a mixture of rare green copper arsenate, such as olivenite ($Cu_2(AsO_4)(OH)$), cornwallite ($Cu_5(AsO_4)_2(OH)_4$) and conichalcite ($CaCu(AsO_4)(OH)$) on mural paintings of Ala di Stura (Piedmont, Italy). In addition, in the same study it was suggested the presence of skutterudite mineral, $(Co,Ni)_xAs_{3-x}$, used for the production of smalt. This mineral could have probably been excavated from Punta Corna mine, in the nearby valley of Viù.

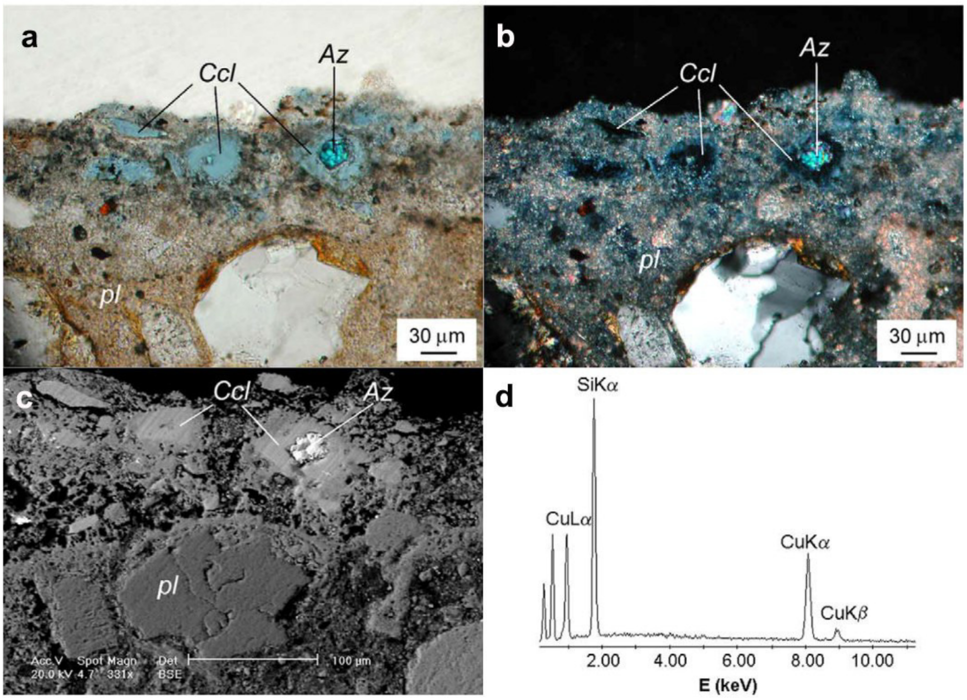

Figure 1.2: The pigment chrysocolla (Ccl) is plunge in lime binder; the layer is secco-applied on the underlying plaster (pl). An azurite (Az) inclusion is highlighted. Transmitted plane polarized light (a), crossed polarizers (b), BSE image obtained at SEM-EDS (c) and compositional spectrum of chrysocolla (d) (source: Mugnaini et al.2006 [84]).

1.4 The study of the state of conservation

In the last few years the number of researches focused on the use of portable techniques, used alone or together with other laboratory techniques for the study of the state of conservation of paintings, is increasing since their reliability has been extensively tested not only for the identification of original materials but, above all, for the recognition of secondary products with the aim of identifying the factors that generated them.

Some materials used to create the wall paintings, such as binders and pigments, have proved to be particularly unstable over time under certain environmental conditions as described in the work by Vandenabeele *et al.* [66] on the *in situ* analysis, with Raman spectroscopy, of mediaeval wall paintings. Some degradation products, such as the metacinnabar (HgS), were responsible for a localized darkening that had a strong impact on the visual appreciation of the paintings. Besides, the clinoatacamite ($Cu_2Cl(OH)_3$) was observed in the laboratory due to the degradation of both malachite and azurite under the influence of moisture.

In the study of bohemian gothic mural paintings [76], *in situ* X-ray fluorescence analyses were applied in some areas that had undergone a colour change from blue to green colour. The analyses showed the presence of copper pigments. Further laboratory analysis of micro samples using optical microscopy, scanning electron microscopy and micro-diffraction of X-ray microscopy verified the transformation of natural azurite into atacamite and paratacamite due to the action of salts and moisture in the fragments selected from the wall paintings.

Although malachite is a quite stable pigment to saline attack, its degradation can be accelerated by the presence of oxalic acid, as it has been reported, produced by the activity of microorganisms and evidenced by the presence of calcium oxalate weddellite [76]. The same hypothesis about the degradation of malachite was proposed in the *in situ* totally non-destructive study of a wall painting in Santa María de Lemoniz [90] (Basque Country, Spain) using a portable Raman spectrometer. For the first time, the mechanism for the transformation of malachite into basic copper sulphates was proposed by integrating Raman data with thermodynamic speciation studies. The study showed the presence of calcium oxalate, which favoured the degradation of the pigment because it provided the acid medium necessary to reduce the pH.

The degradation of copper-based pigments was also found in the investigation of the Madonna and Child Enthroned with Saints of Ambrogio Lorenzetti [91], where some areas painted with azurite showed numerous colour changes that were attributed to the presence of copper chloride. Mugnaini *et al.* [84] found that the environmental factors, such as the presence of strong humidity, caused the transformation of azurite into paratacamite and malachite, as well as the presence of salt efflorescence and biological patinas. In this case the combined use of non-invasive diagnostic imaging techniques and laboratory techniques was proposed in the study where the digital mapping Geographic Information System (GIS) was applied for the study of the state of conservation of the paintings. The increase in humidity in the walls and the high activity of chloride ions were also the causes of the transformation of copper carbonate pigments (azurite and/or malachite) to green copper chlorides, as atacamite ($Cu_2Cl(OH)_3$) [85].

Lead pigments also suffer chemical transformations that can be studied. In the research by Domínguez Vidal *et al.* [92] by using *in situ* Raman spectroscopy for the study of one of the main halls of the Palace of the Lions in the Alhambra (Spain) it was possible to identify calomel $(HgCl)_2$ as a secondary product of cinnabar, and anglesite ($PbSO_4$) as the last stage of degradation of minium after plattnerite (PbO_2) formation.

The presence of light yellow mimetite ($Pb_5(AsO_4)_3Cl$) was found by Hradil *et al.* [85] as a degradation product caused by the alteration of the orpiment and the minium used in the mixture. In the absence of arsenic, the minium decomposed into brown-black plattnerite easily identified by the micro-XRD, but not by the micro-Raman, as the lead dioxide has a weak Raman spectrum difficult to be registered because of its thermal decomposition under the effect of the laser [93]. Together with mimetite, laurionite ($PbCl(OH)$) whose formation is linked to a white lead saline corrosion process, was also found.

Minium degradation, together with azurite degradation was also identified during a multi-analytical approach through the use of non-destructive techniques proposed for the material characterization of the 16th century wall paintings from Ribeira Sacra (Galicia, Spain) [94]. *In situ* non-invasive XRF and Visible reflectance spectroscopy (Vis-RS) analyses were generally effective. However, laboratory analyses were necessary to identify the transformations of red lead and azurite into lead dioxide and paratacamite respectively.

The analytical study published by Daniilia *et al.* [95] was focused on the study of the conservation state of the 15th century wall paintings in the monastery of Christ Antiphonite in Cyprus. Degradation phenomena were studied in relation to the surrounding environmental characteristics, through optical microscopy (OM), scanning electron microscopy (SEM-EDS), micro-Raman and FT-IR spectroscopy. It was assumed that the transformation of red lead from orange to black plattnerite may have been induced not only by the effect of temperature, light and humidity but also by the presence of chlorine salts due to the proximity of the monastery to the sea. On the other hand, in areas where an alteration of the blue pigment was evident, a leaching phenomenon of alkali from smalt particles was concluded, because the decreasing in the potassium oxide content confirmed thanks to electron microscopy measurements.

A similar case study was reported in the work by Nevin *et al*. [96] about the original technique of one of a series of post-Byzantine wall paintings in Galata, Cyprus. Micro-FT-IR and Raman were successfully employed for the characterization of alteration products, such as the alteration of red lead, and the discoloration and the loss of smalt pigment. In particular, hydrated copper oxalate, analogous to the naturally occurring blue-green mineral moolooite (CuC_2O_4), and calcium oxalates were identified by point by point and imaging analyses (FT-IR reflectance imaging) on cross sections, assuming the influence of the organic binder in the formation of those products.

In the research on Pre-Romanesque murals at Kostol’any pod Tríbečom, Slovakia [97], an interesting aspect was discovered by *in situ* measurements with portable X-ray fluorescence. In this case, copper compounds were identified although no green or blue hues were visible. The hypothesis that an organic binder had been used to stabilize copper-based pigments in an alkaline environment was confirmed by the MALDI-TOF-MS technique. However, organic binders proved to be less stable over time. Therefore, the explanation of the loss of colour was attributed to different intrinsic and extrinsic factors to the work of art: firstly, to the corrosive action exerted by the salts and consequently the secondary products were washed by the wall moisture. Furthermore, the X-ray microdiffraction technique also confirmed the presence of blackening of the minium, which was transformed, probably due to a natural degradation process, into brown-black plattnerite.

The chemical transformation of red lead into plattnerite was also detected by Raman spectroscopy in the study of wall painting on Protaton Church [78]. On the contrary, in the study of wall paintings in Thessaloniki cathedral [79] there was no evidence of lead dioxide but the Raman analyses showed the presence of lead sulphate and lead carbonate as decay products of red lead. This degradation could be attributed to a series of environmental factors such as changes in temperature and humidity and atmospheric contamination. The colours of the Carolingian and Romanesque paintings have also changed considerably over time [98], specially areas where red lead, massicot or red lake were used, producing blackening and the red lead conversion into plattnerite.

The study by Kotulanova *et al.* [99] carried out on fragments from wall painting in Kostol’any pod Tríběcom, (Slovakia) - where different products due to the degradation of red lead were found - and on reference sample, showed the influence of natural inorganic salts and synthetic salts in the darkening of lead based pigments.

1.4.1 Degradation due to anthropic factors

In the last 30-40 years the increase of atmospheric contaminants released by industrial activities and the use of fossil fuels has affected the integrity of the Cultural Heritage conserved in the open air. Thus, the efforts of scientists have focused on understanding the chemical reactions that transform the materials and make them more vulnerable. This is the case of the acid gases that can react with the materials of cultural heritage, forming in many cases soluble salts, efflorescences and black crusts. In all cases, sulphates, carbonates, chlorides and nitrates are involved.

Among the sulphate salt, the calcium sulphate dihydrate ($CaSO_4 \cdot 2H_2O$), gypsum, is certainly one of the compounds that are most frequently found in wall paintings due to the reaction of calcium carbonate with atmospheric sulphur dioxide as reported by Edwards *et al.* [100] in the study of medieval mortar and plaster fragments.

The research presented by Amato *et al.* [101] on the analyses on three decorative phases of the presbytery of the church of Santa Maria Antiqua at the Roman Forum in Rome was conducted by the *in situ* video microscope investigation that helped in the selection of the best sampling points for the laboratory analysis. The calcium sulphate, detected in the superficial layers of many samples, could have a dual nature. It can derive from the treatment of the paintings with consolidating cement used during restoration treatments, or from the urban atmosphere of Rome rich in sulphuric acid aerosols to which the church is constantly exposed.

Following with the gypsum, some studies carried out on Islamic and Christian mural paintings (from the tenth to the twelfth century) recovered after reconstruction work in the Alcazar of Seville [102] showed the importance of using different techniques, both portable and in the laboratory for the identification of materials and execution techniques. In this case, the presence of gypsum was attributed to both the environmental contamination and to gypsum residues left after the removal of a gypsum-containing mortar.

Unfortunately, the presence of gypsum is recurrent. In the research by Daniilia *et al.* [103] about wall paintings from St Stephen's monastery at the Meteora (Greece), some conservation problems were found. Beyond the vandalism that they suffered during the World War II and the Civil War, the study showed the presence of a whitish layer of gypsum on the painted surface that affected significantly the aesthetic impact of the mural paintings. Calcium carbonate sulphatation process was also seen *in situ* without sampling in the study of 15th century wall paintings in a chapel of St. Orso Priory palace (Aosta, Italy) [104]. Besides the main inorganic pigments, the collected Raman spectra also enabled the identification of some decay products, such as calcium sulphate.

Gypsum is not the only compound that can form crusts on the surface of the wall paintings. Analyses of crust formations on Byzantine wall paintings in some churches from Mani Peninsula (Greece) [105] revealed that they were made of hydromagnesite ($Mg(CO_3)_4(OH)\cdot 4(H_2O)$), calcite and small amounts of gypsum, the latter present as a product of calcium carbonate degradation. Consequently, hydromagnesite should have been the result of the degradation of a magnesium product, favoured by the presence of moisture. The wall paintings of all the churches under study had been probably covered in the same period with a superficial layer of magnesium lime. In addition, the presence of hydromagnesite also in the preparatory layer was due to its higher solubility than calcite and it was easily dissolved and diffused within the mortar. This was an interesting result, as dolomitic or magnesian limes did not appear often in the Greek area and their use was usually related to the mineralogy and geology of raw materials available in different areas.

Unfortunately, together with gypsum, other salts can cause damages. Analyses carried out with the salts found in the Assumption’s church of Alaiza (Basque Country, Spain) [106] demonstrated the connection between the deterioration of the wall paintings and the agricultural activity in the area surrounding the church. The use of fertilizers such as NH_4NO_3 and $(NH_4)_2SO_4$, generates cations and anions that rise from the ground to the walls through infiltration water causing the decarbonation of the calcite and the subsequent disintegration of the plaster of the wall paintings.

Another anthropic degradation factor often identified in the studies of wall paintings is represented by the use of candles inside places of worship, such as churches and monasteries. An example is the study of the thirteenth century wall paintings discovered under the Siena Cathedral [84]. Darkening of colours as well as dehydration of yellow ochre was attributed to soot deposits from lighted candles or oil lamps and from the heat given off by the candles.

Similarly, the carbon particles identified on the surface of all samples from a post-medieval wall painting [64] could be ascribed to the soot by candles or oil lamps that provided illumination inside the church as well as the carbon particles, identified by Raman spectroscopy, in an Italian crypt [107].

The evidence of the burning of substance such as wax or oil can be demonstrated also by the chemical transformation of some pigments, as hypothesized in the research by Damiani *et al.* [90], in which the transformation of azurite into copper oxide tenorite was probably provoked by the heat from the candles. The thermal degradation of the azurite converted into tenorite was found also on the mural paintings preserved inside the cathedral of Thessaloniki [78], due to the high temperatures released by a fire. Moreover, this incident has caused a total absence of yellow tones in some areas affected by the fire. On the contrary, the presence of red iron oxides was due to the dehydration of yellow ochre during the fire.

In the research by Andreotti *et al.* [108] in which was proposed a laser cleaning method on the wall paintings from the monumental cemetery of Pisa, the study of the surface deposits shown the presence of materials of anthropic origin. Indeed, nitrocellulose used in a past restoration and contamination of pure lead were identified. The presence of lead on the surface of the fragments is due to the fires resulting from the bombardment of the Second World War, when the lead roof melted and the fused lead fell on the wall paintings. The removal of lead deposits was difficult because of the strong adhesion of lead drops. Furthermore, the interactions between the painted surface and the high temperatures had probably caused the alteration of the underlying pigment consisting of iron oxides.

1.4.2 Natural degradation

Particular attention, in recent publications, has been paid to the study of salt naturally formed efflorescences, composed mainly of sulphate, nitrates and carbonates, since they represent one of the natural degradation products that most endanger the integrity of the masonry and consequently also the substrate of the wall paintings. Generally, the study of the composition of soluble salts is useful to identify a specific marker that indicates the cause that generated them.

For this purpose, spectroscopic techniques, especially Raman spectroscopy, are particularly useful since are able to differentiate degradation products that can coexist in construction materials and on pictorial surfaces. An example of the reliability of the use of diagnostic techniques in the characterization of degradation products is the work published by Iordanidis *et al.* [109] where Raman spectroscopy and ESEM-EDS were successful employed for the characterization of salt efflorescence on fragments from mural paintings in three different churches belonging to post-byzantine period. The compounds responsible for the decay were calcite, dolomite, gypsum, alite, nitratine ($NaNO_3$), natron ($Na_2CO_3 \cdot 10H_2O$) and mirabilite ($Na_2SO_4 \cdot 10H_2O$), all caused by temperature and humidity variations.

Although in many studies gypsum is present as a product of sulphuric anhydride contamination, it has been identified as a component of medieval mortars as documented in the research of Damiani *et al*. [91] where it was macroscopically visible in the surface of wall paintings along fractures and detachments in areas where the humidity found preferential flow paths showing that the original materials of the masonry were the sources of sulphates (Figure 1.3).

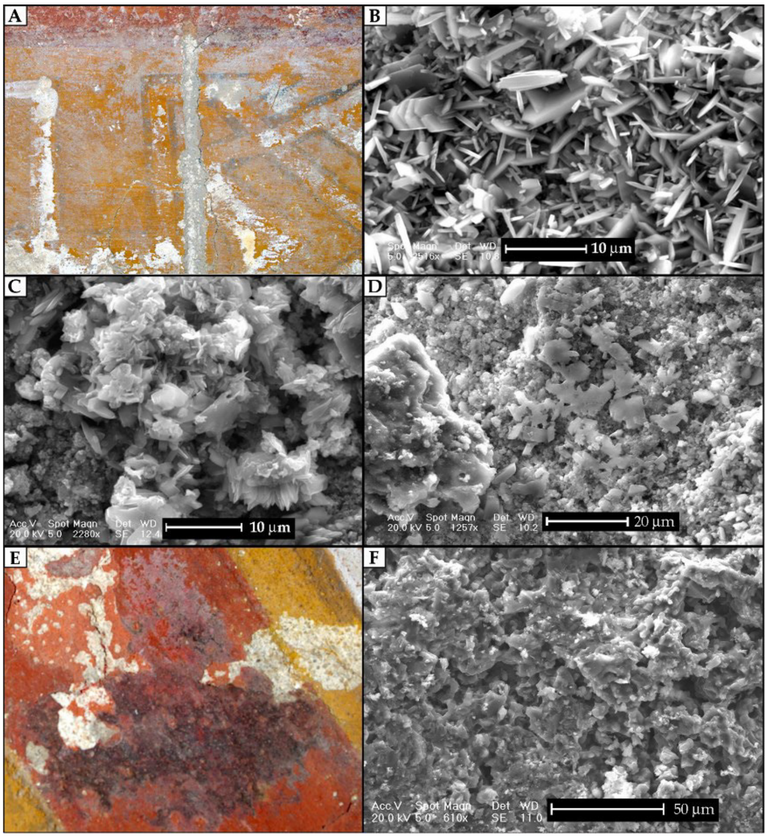

Figure 1.3: evidences of gypsum cristallization (a) Backscattered images of the Ca sulphates showing different shapes and textures (b–d). The darkening of the red pigment (e) and backscattered image of coalescent Ca sulphates present in the darkening area e (f) (source: Damiani et al. 2014 [91]).

Non-destructive image techniques were also used even to evaluate the conservation status of the wall painting "Madonna con Bambino" (XIII-XV century) (Fontecchio - L'Aquila, Italy) [110]. Electronic speckle pattern interferometry (ESPI), ultraviolet (UV) imaging and infrared vision allowed to recognize different degradation products including the action of soluble salts and the leaching of the surface that caused the loss of clay pigments. In this case, it is very important to highlight that the combined use of the integration between ESPI, SEM and thermographic techniques was useful to establish the cause of a superficial cleavage within a sample. In fact, a "sandwich structure" with an interstitial full of moisture was clearly identified.

The same analytical approach was employed in the study of Giovannetti's wall paintings in the Chartreuse (Villeneuve-les-Avignon, France) [111] in which *in situ* digital images (Fluorescence under UV light, IR thermography and photogrammetry) provided information about the original and new materials used during past restoration work and structural aspects. The mural paintings were affected mainly by erosion and chromatic alteration. *In situ* and in laboratory analysed samples shown that in some areas the surface deformations were caused by the presence of hygroscopic salts composed of calcium and sodium sulphate.

Most of the studies on the state of conservation of building materials have highlighted the danger of the presence of nitrate salts on carbonaceous materials that are the main component of brick mortar and wall paintings. In consequence, it is very important to identify these compounds in order to limit the presence of the factors that caused their formation, when possible. For example, in the research by Pérez-Alonso *et al.* [112] on the study of mortars and wall paintings of Santa María de Hermo (Spain), carried out by the use of portable Raman instrumentation, extensive decay of the carbonaceous materials caused by the absorption of nitrates from the ground was found. Their presence was explained by the migration of nitrates from the old cemetery attached to the church wall.

Portable techniques (visible reflectance and Raman spectroscopies) and in the laboratory (attenuated total reflectance-Fourier transform infrared spectroscopy (ATR-FT-IR) and micro-Raman spectroscopies) were applied for the study of the conservation state of medieval wall paintings preserved in a crypt in Puglia region (Italy) [107]. The study was focused on the characterization of degradation products caused mainly by moisture problems due primarily to the fact that the crypt was excavated in the tuff, a highly porous and hygroscopic material. On-site Raman spectroscopy allowed the identification of sulphates, nitrates and calcium oxalates (whewellite and weddellite) that were also quantified together with chlorides, fluorides, nitrites and acetates by ion chromatography, thus, obtaining a clearer picture of the poor state of conservation caused by physical factors (water infiltration), chemical (reactions of materials with atmospheric particulate) and biological ones favoured by the high humidity.

In the study of wall paintings located in two church in the Basque Country [113], the origin of the nitrate salts (potassium nitrate and calcium nitrate) and the presence of ammonium sulphate was ascertained. Their presence could be related to the reaction between calcium carbonate and gypsum, present in the mortar, with the ammonium nitrate from the soil and transported by infiltration waters through capillary rising towards the paintings.

In the study of medieval wall paintings from the Basque Country presented by Veneranda *et al.* [114], *in situ* analyses allowed the characterization of different types of nitrate salts, such as nitrocalcite ($Ca(NO_3)_2{\cdot}4H_2O$) and natron, in a high hydration state suggesting that they were formed due to high humidity.

Another study in which conservation problems were presented, but in this case in a low-contamination rural environment, is the work presented by Madariaga *et al.* [115], in which it was highlighted how the degradation processes generated by natural factors can be dangerous as much as the impact of industrial atmospheres without a conservation plan. Using *in situ* analyses it was possible to demonstrate that the greatest damage was caused by the presence of salt efflorescence, which thanks to Raman spectroscopy were characterized in the laboratory. An extensive presence of nitrates (potassium and sodium nitrate) was confirmed both on the wall paintings and on the building materials. The source of the nitrate salts was the nitrogen compounds from the ground (mainly ammonium nitrate from the plant and grass decomposition) that were absorbed by the porous materials due to capillary rise of water infiltration favoured by a very damaged masonry and that lost cohesion over the years.

Another detailed study in which different environmental factors have accelerated the degradation of wall paintings is shown in the study concerning the Carolingian wall paintings and Romanesque in the Müstair convent [116, 117] (Switzerland), influenced by a saline system originated by rising damp and percolation. Thanks to the use of complementary diagnostic techniques, the study showed that the decay was produced by the presence of soluble salts, nitrates and sulphates, whose formation was influenced by seasonal variations in air humidity.

As the nitrate salts are the most responsible for the degradation of porous materials, the research of Maguregui *et al.* [12] presented a protocol to assess its impact on construction materials using non-invasive and microdestructive analytical techniques with chemometric and thermodynamic data analysis. The church under study showed evidence of problems deriving from the infiltration of soluble salts from natural sources represented by the level of the ground above the zero level of the church and which represents the main entry point for the nitrate salts from the outside. Subsequently, they spread by capillarity involving both the masonry and the wall painting.

In the work published by Martínez-Arkarazo *et al.* [47] portable Raman monitoring was performed to follow the progress in two cleaning operations based on new technologies: a wall painting affected by the impact of nitrate and a black crusted stone altarpiece. Nitrate and gypsum Raman bands decreased after treatment, which allowed the restorers to make decisions *in situ* and suggested when to stop the cleaning operation.

1.4.3 Biodeterioration processes

In certain environmental conditions building materials may be subjected to biodeterioration processes, visible in the form of patinas or encrustations, generated by the colonization of microorganisms such as algae, moss, lichens or fungi. Besides the aesthetic damage, that is the most evident and the first that can be identified over pictorial surfaces, the penetration of fungal hyphae and lichen thallus can cause serious structural damage such as the deterioration of plasters and the consequent loss of the paint layer in the case of wall paintings.

One of the first works in which a degradation due to biological attack was identified by the use of Raman spectroscopy was published in 1999 by Edwards and Rull [118]. Although the characteristic vibrational spectra of calcium oxalate monohydrate, β-carotene, chlorophyll, and para-depside phenolic acids were obtained from fragments of the outer wall of the convent, the degradation was so strong that the damage was extended to the medieval wall paintings in the interior. Indeed, the presence of calcium oxalate dihydrate weddellite was confirmed on fragments of wall paintings, while was evident a chromatic damage due to the leaching of red ochre caused by lichenic acids.

The complementary use of different laboratory analytical techniques (optical microscopy, scanning electron microscopy, micro-infrared spectroscopy and micro-X-ray diffraction with synchrotron light and gas chromatography-mass spectrometry) was essential to identify the nature of black spots visible on the surface of micro samples taken in the Saint Michael's Chapel from the Royal Monastery of Pedralbes (Barcelona) [119]. Complex mixtures of calcium salts of low molecular weight organic acids (LMWOA) were determined and their presence was explained by the reaction between the acids produced by the filamentous fungi and the deposited aerial calcium compounds on the surface of paintings. The analyses shown that these substances did not have a strong ability to penetrate the painted layers and that the dark tone was probably given by the presence of a colorant or pigment produced by fungi, of a polar nature as being soluble in water, and therefore easily removable.

A mechanical and aesthetic damage was identified during the study of the frescoes of the Chapel of the Holy nail, Siena [120] (Italy), in which the scanning (SEM) and transmission electron microscopy (TEM) together with a molecular study allowed to confirm that the cause of the chromatic alteration of the paintings was the presence of a fungus. It accumulated in its hyphae large concentrations of copper, which generally inhibits the colonization of bacteria, taken from the azurite, which was transformed into malachite due to the dissolution of carbonates by organic acids occurred, promoting the leaching of copper.

The same medieval frescoes were studied a few years later in order to clarify the cause of the presence of some blackened areas [121]. The analyses conducted (scanning microscopy with X-ray scattering microanalysis) attested that the blackening of the paints was closely linked to the use of Paraloid B72 acrylic resin during some restoration interventions carried out in the 60s. Thanks to some laboratory tests on fragments, it was noticed that the presence of the resin film inhibited the interaction of the painting with the environment, including transpiration and gaseous exchange. Paraloid-treated and untreated samples showed potential deleterious species on the surface in quiescent state while Bacteria of the genus *Bacillus* were isolated only from untreated samples, proving the fact that the Paraloid resin is resistant to the colonization of bacteria. Moisture combined with different chemical compounds accelerated chemical oxidation and blackening. The hypothesis stated was that the *Firmicutes* bacteria presumably produced extracellular material, which retains water and provides a carbon source available to other bacteria. Numerous alteration products linked to biodegradation, such as oxalates (calcium dihydrate weddellite and monohydrate whewellite) have been detected in Italian wall paintings [91].

In the research by Tortora *et al.* [122] the analysis by non-destructive and micro-invasive techniques were extremely useful for the chemical and structural studies of medieval wall paintings in Ocre (L’Aquila, Italy) and for the development of a detailed plan for the restoration work. The *in situ* techniques allowed to identify structural problems caused by rising damp together with biodegradation and calcium oxalate formation.

The identification of whewellite by using XRD [94] showed that the degradation of the organic binder used to mix copper pigments was probably accelerated by the presence of microorganisms in a high humidity environment. However, in the wall paintings located in the Thessaloniki cathedral [78], the formation of calcium oxalates was probably originated from the yellowing of a protein material, employed by restorers to consolidate the surface during the restoration works after a fire.

In the *in situ* study of gothic wall paintings preserved inside the Church of Valderejo [115] (Basque Country, Spain) in addition to the presence of hydrated calcium oxalate weddellite, it was possible to identify carotenoid pigments on biological patinas that were sampled and characterized by micro-Raman in the laboratory. In this way it was possible better distinguish different organic pigments such as zeaxanthin, β-carotene and astaxanthin.

1.5. Why is it important to apply diagnostic techniques?

Among the anthropic factors that may endanger the conservation of a work of art, some restoration interventions that were carried out in the past must also be considered because in some cases they have proved to be inappropriate or even harmful due mainly to the use of aggressive and non-compatible (from the chemical point of view) products. In these cases, rather than restraining the damage, the chemical reactions between new and ancient materials have caused the formation of even more harmful decaying products. Therefore, knowledge of the chemical behaviour of the materials and degradation products to be treated is essential before applying any restoration method.

A suitable example is the study by Dei *et al.* [123] on the case of the restoration of the painting of San Antonio Abate in the church of San Pietro at Quaracchi (Italy). The green paratacamite, present as a result of a degradation process, was treated by applying ammonium carbonate followed by barium hydroxide. But the subsequent measurements revealed that paratacamite was transformed into copper hydroxide and not into azurite, as it was thought. This incorrect procedure created further instability in materials, as documented by colour changes.

Another example of an invasive restoration is the study of the unique surviving fresco paintings of Manuel Panselinos (13th century AD), one of the most celebrated Greek iconographers of the Byzantine era, located in the Protaton Church [78] (10th century

AD) on Mount Athos (Greece). Thanks to the use of *in situ* ultraviolet fluorescence images, superficial salts deposits, flaking and detachments were identified as the main decaying products/processes. They were formed due to the addition of a cement coating during a restoration intervention in modern times, that prevented the transpiration of moisture from the surface, with the subsequent formation of new salt deposits.

Unfortunately, modern cements are behind many described degradations in cultural heritage. For example, the use of alkaline materials such as Portland cement in the Müstair convent [117] influenced the compositions of the salts already present in the walls and increased their quantity. Moreover, another cause of the decay was represented by the installation of a heating system, which caused strong seasonal variations in relative humidity.

In the study carried out by Irazola *et al.* [113] by using portable instrumentation (Figure 1.4) it was possible to characterize some decaying compounds in two wall paintings in churches of the Basque Country region (Spain). To better characterize the degradation processes, some microsamples were analysed in the laboratory. The superimposing Raman images on the SEM-EDS images of the cross-sections were used to explain the spatial distribution of anhydrite ($CaSO_4$), caused by a phenomenon of dehydration of gypsum in the mortar due to the application of Paraloid resin during past restoration work, which prevented the transpiration of water from the surface. A similar case was studied by Veneranda *et al.* [114] where bassanite ($CaSO_4 \cdot 0.5H_2O$) was identified as a consequence of the gypsum dehydration due to the use of an acrylic resin, and its distribution in the sample was established by Raman imaging in a cross section sample.

In other cases, the lack of a scientific approach to the study of materials before carrying out restorations has led to the application of not compatible procedures and colours with the original appearance of the paintings, as described in the research on late Gothic paintings in the church of Ribera de Valderejo (see chapter 6). For example, analyses conducted *in situ* and in the laboratory revealed the presence of a modern green pigment, phthalocyanine green, in areas where originally any green pigment was used; restorers probably took a wrong decision due to the lack of knowledge about the original raw materials used in the wall paintings.

Figure 1.4: *In situ* Raman analysis of the medieval wall paintings located in the Saint Andrew Church (Biañez, Basque Country).

Other important aspect in this research (see chapter 6) was the identification of a biocide product based on arsenic. Arsenic was first identified by portable XRF and subsequently its molecular composition was identified by micro Raman spectroscopy. The discovery of this product, used in modern times for the removal of biological patinas, proved to be particularly important for restoration interventions in the future in order to warn the restorers of the presence of a highly toxic substance for their health and take adequate precautions.

Another detailed study conducted on medieval wall paintings in Hermo (Spain) [124] demonstrated the importance of a scientific study of the conservation state of wall paintings. The study confirmed the absence of an organic binder unlike the opinion of the restorers. In addition, some biodeterioration process were suggested based on visual inspections; however, the hypothesis was rejected after the spectroscopic analyses revealed the formation of soluble salts (sulphate and above all nitrates) as the main deterioration cause.

1.6 Final remarks

This introduction gives an overview of the results obtained in the study of medieval wall paintings and emphasizes the usefulness of different analytical techniques for the study of the materials. In particular, portable analytical techniques have proved to be reliable in the characterization of ancient and modern pigments and binder media, and in particular in the investigation of the conservation state of wall paintings. The advantages for the preservation of works of art in the use of portable tools are evident above all because they are completely non-invasive, a fundamental requirement for the study of immovable objects especially medieval wall paintings, many of which are already strongly damaged due to neglect and too invasive restoration interventions.

Since the mediaeval era was characterized by a stagnation of economy, the use of poor materials of natural origin and local origin for the realization of mural paintings was widespread. Because of the limited access to pigments, new techniques and unusual pigments were used to make up for the lack of raw materials.

Almost all the studies related to the identification of degradation products have shown a close connection between the conservation status of paintings and the characteristics of the environment in which they were found. In fact, wall paintings, after their realization, must be considered as objects in continuous evolution because new compounds, according to environmental changes, can be formed in a continuous exchange with the surrounding environment. At the same time, it is not possible to attribute to just one agent a certain secondary product because different factors, both natural and anthropic, contribute to the degradation of materials. For this reason, studies concerning the conservation of cultural heritage should focus not only on the work of art itself but also on the environmental study with the aim of identifying the environmental stressors that limit the durability of the materials, in an exchange of knowledge that involves scientists, biologists, conservators and art historians.

This chapter highlights that the spread in the use of diagnostic techniques has developed at the same time a change in sensitivity in the study of cultural heritage for which each artwork is unique and must be preserved for future generations. Some researches showed that the application of unsuitable restoration interventions or the use of products incompatible with the original materials, applied without a thorough knowledge of the materials, can lead to dangerous choices for the preservation of the artworks. Therefore, this introduction underlines the importance of using a scientific approach for the study of the original materials before carrying out restoration operations and for the development of innovative procedures for cleaning, restoration and conservation previously tested in the laboratory in order to suggest to restorers the best method to apply. It is precisely the concept that will be the leitmotif of this PhD project as demonstrated through the case studies and the experimental researches in the following chapters.

References

[1] M. Sablier, P. Garrigue (2014) Cultural heritage and its environment: an issue of interest for Environmental Science and Pollution Research, *Environmental Science and Pollution Research*, 21, 5769-5773.

[2] Air Pollution and Cultural Heritage, Ed. Saiz Jimenez © 2004 Taylor & Francis Group, London, ISBN 90 5809 682 3.

[3] G. D. Smith, Robin J. H. Clark (2002) The role of H_2S in pigment blackening, *Journal of Cultural Heritage*,3, 101-105.

[4] S. Aze, J. M. Vallet, A. Baronnet, O. Grauby (2006) The fading of red lead pigment in wall paintings: tracking the physico-chemical transformations by means of complementary micro-analysis techniques, *European Journal of Mineralogy*, 18, 835-843.

[5] K. Castro, A. Sarmiento, I. Martínez-Arkarazo, J. M. Madariaga, L. A. Fernández (2008) Green Copper Pigments Biodegradation in Cultural Heritage: From Malachite to Moolooite, Thermodynamic Modeling, X-ray Fluorescence, and Raman Evidence, *Analytical Chemistry*, 80, 4103-4110.

[6] M. Cotte, J. Susini, N. Metrich, A. Moscato, C. Gratziu, A. Bertagnini, M. Pagano (2006) Blackening of Pompeian Cinnabar Paintings: X-ray Microspectroscopy Analysis, *Analytical Chemistry*, 78, 7484-7492.

[7] M. Maguregui, U. Knuutinen, I. Martínez-Arkarazo, K. Castro, J. M. Madariaga (2011) Thermodynamic and Spectroscopic Speciation to Explain the Blackening Process of Hematite Formed by Atmospheric SO_2 Impact: The Case of Marcus Lucretius House (Pompeii), *Analytical Chemistry*, 83, 3319-3326.

[8] A. Coccato, L. Moens, P. Vandenabeele (2017) On the stability of mediaeval inorganic pigments: a literature review of the effect of climate, material selection, biological activity, analysis and conservation treatments, *Heritage Science*, 5, 12. https://doi.org/10.1186/s40494-017-0125-6.

[9] R. A. J. Wüst, C. Schlüchter (2000) The Origin of Soluble Salts in Rocks of the Thebes Mountains, Egypt: The Damage Potential to Ancient Egyptian Wall Art, *Journal of Archaeological Science*, 27, 1161-1172.

[10] R. Rossi-Manaresi, A. Tucci (1991) Pore structure and the disruptive or cementing effect of salt crystallization in various types of stone, *Studies in Conservation*, 36, 53-58.

[11] A. Arnold, K, Zehnder, Monitoring Wall Paintings Affected by Soluble Salts, The Conservation of Wall Paintings pp103-136, Proceedings of a symposium organized by the Courtauld Institute of Art and the Getty Conservation Institute, London, July 13-16, 1987, Sharon Cather Editor.

[12] M. Maguregui, A. Sarmiento, I. Martínez-Arkarazo, M. Angulo, K. Castro, G. Arana, N. Etxebarria, J. M. Madariaga (2008) Analytical diagnosis methodology to

evaluate nitrate impact on historical building materials, *Analytical and Bioanalytical Chemistry*, 391, 1361-370.

[13] J. Aramendia, L. Gómez-Nubla, I. Arrizabalaga, N. Prieto-Taboada, K. Castro, J. M. Madariaga (2013) Multianalytical approach to study the dissolution process of weathering steel: The role of urban pollution, *Corrosion Science*, 76, 154-162.

[14] S. J. Haneef, J. B. Johnson, C. Dickinson, G. E. Thompson, G. C. Wood (1992) Effect of dry deposition of NO_x and SO_2 gaseous pollutants on the degradation of calcareous building stones, *Atmospheric Environment. Part A. General Topics*, 26, 2963-2974.

[15] O. Gómez-Laserna, N. Prieto-Taboada, H. Morillas, I. Arrizabalaga, M. A. Olazabal, G. Arana, J. M. Madariaga (2015) Analytical study to evaluate the origin and severity of damage caused by salt weathering in a historical Palace House: the attack of infiltration water, *Analytical Methods*, 7, 4608-4615.

[16] P. Pouli, E. Papakonstantinou, K. Frantzikinaki, A. Panou, G. Frantzi, C. Vasiliadis, C. Fotakis (2016) The two-wavelength laser cleaning methodology; theoretical background and examples from its application on CH objects and monuments with emphasis to the Athens Acropolis sculptures, *Heritage Science*, 4, 1-11.

[17] M. Maguregui, U. Knuutinen, I. Martínez-Arkarazo, A. Giakoumaki, K. Castro, J. M. Madariaga (2012) Field Raman analysis to diagnose the conservation state of excavated walls and wall paintings in the archaeological site of Pompeii (Italy), *Journal of Raman Spectroscopy*, 43, 1747-1753.

[18] M. Veneranda, N. Prieto-Taboada, S. Fdez-Ortiz de Vallejuelo, M. Maguregui, H. Morillas, I. Marcaida, K. Castro, J. M Madariaga, M. Osanna (2017) Biodeterioration of Pompeian mural paintings: fungal colonization favoured by the presence of volcanic material residues, *Environmental Science and Pollution Research*, 24, 19599-19608.

[19] C. Schabereiter-Gurtner, C. Saiz-Jimenez, G. Piñar, W. Lubitz, S. Rolleke (2002) Altamira cave Paleolithic paintings harbor partly unknown bacterial communities, *Microbiology Letters*, 211, 7-11.

[20] O. Pepe, L. Sannino, S. Palomba, M. Anastasio, G. Blaiotta, F. Villani, G. Moschetti (2010) Heterotrophic microorganisms in deteriorated medieval wall paintings in southern Italian churches, *Microbiological Research*, 165, 21-32.

[21] K. Sterflinger, G. Piñar (2013) Microbial deterioration of cultural heritage and works of art — tilting at windmills?, *Applied Microbiology and Biotechnology*, 97, 9637-9646.

[22] T. Rosado, A. Reis, J. Mirão, A. Candeias, P. Vandenabeele, A. T. Caldeira (2014) Pink! Why not? On the unusual colour of Évora Cathedral, *International Biodeterioration & Biodegradation*, 94, 121-127.

[23] O. Ciferri (2002) The role of microorganisms in the degradation of cultural heritage, *Studies in Conservation*, 47, 35-45.

[24] M. Maguregui, U. Knuutinen, J. Trebolazabala, H. Morillas, K. Castro, I. Martínez-Arkarazo, J. M. Madariaga (2012) Use of in situ and confocal Raman spectroscopy to

study the nature and distribution of carotenoids in brown patinas from a deteriorated wall painting in Marcus Lucretius House (Pompeii), *Analytical and Bioanalytical Chemistry*, 402, 1529-1539.

[25] H. G. M. Edwards, D. W. Farwell, M. R. D. Seaward, C. Giacobini (1991) Preliminary Raman microscopic analyses of a lichen encrustation involved in the biodeterioration of renaissance frescoes in Central Italy, *International Biodeterioration*, 27, 1-9.

[26] H. G. M. Edwards, D. W. Farwell, R. Jenkins, M. R. D. Seaward (1992) Vibrational Raman spectroscopic studies of calcium oxalate monohydrate and dihydrate in lichen encrustations on renaissance frescoes, *Journal of Raman Spectrosc*opy, 23, 185-189.

[27] M. Singha, B. R. Arbad (2015) Characterization of 4^{th}–5^{th} century A.D. earthen plaster support layers of Ajanta mural paintings, *Construction and Building Material*, 82, 142-154.

[28] M. Matteini, A. Moles, The reconversion of oxidized white lead in mural paintings: a control after a five years period, ICOM Commetee for Conservation 6^{th} Triennial Meeting Ottawa 1981.

[29] D. Bersani, C. Conti, P. Matousek, F. Pozzi, P. Vandenabeele (2016) Methodological evolutions of Raman spectroscopy in art and archaeology, *Analytical Methods*, 8, 8395-8409.

[30] G. Bitossi, R. Giorgi, M. Mauro, B. Salvadori, L. Dei (2005) Spectroscopic techniques in Cultural Heritage conservation: a survey, *Applied Spectroscopy. Reviews*, 40, 187-228.

[31] D. Bersani, J. M. Madariaga (2012) Applications of Raman spectroscopy in art and archaeology, *Journal of Raman Spectroscopy*, 43, 1523-1528.

[32] B. Guineau (1984) Analyse non-destructive des pigments par microsonde Raman laser: exemples de l'azurite et de la malachite, *Studies in Conservation*, 29, 35-41.

[33] G. Simsek, P. Colomban, F. Casadio, L. Bellot-Gurlet, G. Zelleke, K. T. Faber, V. Milande, L. Tilliard (2015) On-Site Identification of Early Böttger Red Stoneware Using Portable XRF/Raman Instruments: 2, Glaze & Gilding Analysis, *Journal of the American Ceramic Society*, 98, 3006-3013.

[34] A. Rousaki, C. Vázquez, V. Aldazábal, C. Bellelli, M. Carballido Calatayud, A. Hajduk, E. Vargas, O. Palacios, P. Vandenabeele, L. Moens (2017) The first use of portable Raman instrumentation for the in situ study of prehistoric rock paintings in Patagonian sites, *Journal of Raman Spectroscopy*, 48, 1459-146.

[35] G. D. Smith, L. Burgio, S. Firth, R. J. H. Clark (2001) Laser-induced degradation of lead pigments with reference to Botticelli’s Trionfo d’Amore, *Analytica Chimica Acta*, 440, 185-188.

[36] I. M. Bell, R. J. H. Clark, P. J. Gibbs (1997) Raman spectroscopic library of natural and synthetic pigments (pre- ≈ 1850 AD), *Spectrochimica Acta Part A: Molecular and Biomolecular Spectroscopy*, 53, 2159-2179.

[37] P. Ropret, S. A. Centeno, P. Bukovec (2008) Raman identification of yellow synthetic organic pigments in modern and contemporary paintings: Reference spectra and case studies, *Spectrochimica Acta Part A: Molecular and Biomolecular Spectroscopy*, 69, 486-497.

[38] P. Vandenabeele, B. Wehling, L. Moens, H. Edwards, M. De Reu, G. Van Hooydonk (2000) Analysis with micro-Raman spectroscopy of natural organic binding media and varnishes used in art, *Analytica Chimica Acta*, 407, 261-274.

[39] J. M. Madariaga, M. Maguregui, S. Fdez-Ortiz De Vallejuelo, U. Knuutinen, K. Castro, I. Martinez-Arkarazo, A. Giakoumaki, A. Pitarch (2014) In situ analysis with portable Raman and ED-XRF spectrometers for the diagnosis of the formation of efflorescence on walls and wall paintings of the Insula IX 3 (Pompeii, Italy), *Journal of Raman Spectroscopy*, 45, 1059-1067.

[40] N. Prieto-Taboada, O. Gómez-Laserna, I. Martínez-Arkarazo, M. A. Olazabal, J. M. Madariaga (2014), Raman Spectra of the Different Phases in the $CaSO_4$-H_2O System, *Analytical Chemistry*, 86, 10131-10137.

[41] P. Moioli, C. Seccaroni (2000) Analysis of art objects using a portable x-ray fluorescence spectrometer, *X-Ray Spectrometry*, 29, 48-52.

[42] D. Anglos (2001) Laser-Induced Breakdown Spectroscopy in Art and Archaeology, *Applied Spectroscopy*, 55, 186-205.

[43] D. Ajò, U. Casellato, E. Fiorin, P. A. Vigato (2004) Ciro Ferri's frescoes: a study of painting materials and technique by SEM-EDS microscopy, X-ray diffraction, micro FT-IR and photoluminescence spectroscopy, *Journal of Cultural Heritage*, 5, 333-348.

[44] H. Brecoulaki, A. Andreotti, I. Bonaduce, M. P. Colombini, A. Lluveras (2012) Characterization of organic media in the wall-paintings of the “Palace of Nestor” at Pylos, Greece: evidence for a *secco* painting techniques in the Bronze Age, *Journal of Archaeological Science*, 39, 2866-2876.

[45] D. Lau, C. Villis, S. Furman, M. Livet (2008) Multispectral and hyperspectral image analysis of elemental and micro-Raman maps of cross-sections from a 16th century painting, *Analytica Chimica Acta*, 610, 15-24.

[46] N. Prieto-Taboada, O. Gómez-Laserna, I. Martínez-Arkarazo, M. A. Olazabal, J. M. Madariaga (2013) Relevance of cross-section analysis in correct diagnosis of the state of conservation of building materials as evidenced by spectroscopic imaging, *Analytical Chemistry*, 85, 9501-9507.

[47] I. Martínez-Arkarazo, A. Sarmiento, M. Maguregui, K. Castro, J. M. Madariaga (2010) Portable Raman monitoring of modern cleaning and consolidation operations of artworks on mineral supports, *Analytical and Bioanalytical Chemistry*, 2010, 397, 2717-2725.

[48] P. Rydzewski, Medieval Art, Art and Human Experience, Copyright © 1967 Pergamon Press Ltd., pp. 122-137.

[49] H. G. M. Edwards, C. J. Brooke, J. K. F. Tait (1997) Fourier Transform Raman Spectroscopic Study of Pigments from English Mediaeval Wall Paintings, *Journal of Raman Spectroscopy*, 28, 95-98.

[50] H. G. M. Edwards, D. W. Farwell, E. M. Newton, F. Rull Perez (1999) Minium; FT-Raman non-destructive analysis applied to an historical controversy, *Analyst*, 124, 1323-1326.

[51] H. G. M. Edwards, D. W. Farwell, F. Rull Perez, S. Jorge Villar, (1999) Spanish mediaeval frescoes at Basconcillos del Tozo: a Fourier transform Raman spectroscopic study, *Journal of Raman Spectroscopy*, 30, 307-311.

[52] F. Rull Pérez, H. G. M. Edwards, A. Rivas, L. Drummond (1999) Fourier transform Raman spectroscopic characterization of pigments in the mediaeval frescoes at Convento de la Peregrina, Sahagun, Léon, Spain. Part 1-preliminary study, *Journal of Raman Spectroscopy*, 30, 301-305.

[53] H. G. M. Edwards, F. Rull, P. Vandenabeele, E. M. Newton, L. Moens, J. Medina, C. García (2001) Mediaeval Pigments in the Monastery of San Baudelio, Spain: A Raman Spectroscopic Analysis, *Applied Spectroscopy*, 55, 71-76.

[54] S. E. J. Villar, H. G. M. Edwards, J. Medina, F. Rull Pérez (2006), Raman spectroscopic analysis of mediaeval wall paintings in the Palencia region, Spain, *Journal of Raman Spectroscopy*, 37, 1078-1085.

[55] F. Daniel, A. Mounier, P. Ricarrere, Of some blue and bluish grey pigments in medieval mural paintings in the South West of France, Proceedings of the 39th International Symposium for Archaeometry, Leuven 2012, 329-334.

[56] A. Palet Casas, J. D. Andrés Llopis (1992) The identification of aerinite as a blue pigment in the Romanesque frescoes of the Pyrenean Region, *Studies in Conservation*, 37, 132-136.

[57] J. Pérez-Arantegui, C. Pardos, J. L. Abad, J. R. García (2013) Microcharacterization of a Natural Blue Pigment Used in Wall Paintings During the Romanesque Period in Northern Spain, *Microscopy and Microanalysis*, 19, 1645-1652.

[58] L. Lepot, S. Denoe, B. Gilbert (2006) The technique of the mural paintings of the Tournai Cathedral, *Journal of Raman Spectroscopy*, 37, 1098-1103.

[59] M. Marić-Stojanović, D. Bajuk-Bogdanović, S. Uskoković-Marković, I. Holclajtner-Antunović (2018) Spectroscopic analysis of XIV century wall paintings from Patriarchate of Peć Monastery, Serbia, *Spectrochimica Acta Part A: Molecular and Biomolecular Spectroscopy*, 191, 469-477.

[60] R. J. H. Clark, R. R. Hark, N. Salvadó, S. Butí, T. Pradell (2010) Spectroscopy study of mural paintings fromthe Pyrenean Church of Saint Eulàlia of Unha, *Journal of Raman Spectroscopy*, 41, 1418-1424.

[61] A. Zucchiatti, P. Prati, A. Bouquillon, L. Giuntini, M. Massi, A. Migliori, A. Cagnana, S. Roascio (2004) Characterization of early medieval frescoes by µ-PIXE, SEM and Raman spectroscopy, *Nuclear Instruments and Methods in Physics Research Section B: Beam Interactions with Materials and Atoms*, 219-220, 20-25.

[62] I. Holclajtner-Antunović, M. Stojanović-Marić, D. Bajuk-Bogdanović, R. Žikić, S. Uskoković-Marković (2016) Multi-analytical study of techniques and palettes of wall paintings of the monastery of Žiča, Serbia, *Spectrochimica Acta Part A: Molecular and Biomolecular Spectroscopy*, 156, 78-88.

[63] M. Gutman, M. Lesar-Kikelj, A. Mladenovič, V. Čobal-Sedmak, A. Križnarb, S. Kramard (2014) Raman microspectroscopic analysis of pigments of the Gothic wall painting from the Dominican Monastery in Ptuj (Slovenia), *Journal of Raman Spectroscopy*, 45, 1103-1109.

[64] H. G. M. Edwards, D. W. Farwell, C. J. Brooke (2005) Raman spectroscopic study of a post-medieval wall painting in need of conservation, *Analytical and Bioanalytical Chemistry*, 383, 312-321.

[65] B. Minceva-Sukarova, O. Grupce, V. Tanevska, L. Robeva-Cukovska, S. Mamucevska-Miljkovic (2007) Micro-Raman spectroscopic studies of Byzantine cultural heritage in Republic of Macedonia, *Macedonian Journal of Chemistry and Chemical Engineering*, 26, 103-110.

[66] P. Vandenabeele, K. Lambert, S. Matthys, W. Schudel, A. Bergmans, L. Moens (2005) In situ analysis of mediaeval wall paintings: a challenge for mobile Raman spectroscopy, *Analytical and Bioanalytical Chemistry*, 383, 707-712.

[67] J. L. Pérez-Rodríguez, M. D. Robador, M. A. Centeno, B. Siguenza, A. Duran (2014) Wall paintings studied using Raman spectroscopy: A comparative study between various assays of cross sections and external layers, *Spectrochimica Acta Part A: Molecular and Biomolecular Spectroscopy*, 120, 602-609.

[68] A. Deneckere, W. Schudel, M. Van Bos, H. Wouters, A. Bergmans, P. Vandenabeele, L. Moens (2010) In situ investigations of vault paintings in the Antwerp cathedral, *Spectrochimica Acta Part A: Molecular and Biomolecular Spectroscopy*, 75, 511-519.

[69] K. F. Gebremariam, L. Kvittingen, F.G. Banica (2013) Application of a portable XRF analyzer to investigate the medieval wall paintings of Yemrehanna Krestos Church, Ethiopia, *X-Ray Spectrometry*, 42, 462-469.

[70] J. L. Ferrero, C. Roldán, D. Juanes, E. Rollano, C. Morera (2002) Analysis of pigments from Spanish works of art using a portable EDXRF spectrometer, *X-Ray Spectrometry*, 3, 441-447.

[71] M. Sawczak, A. Kamińska, G. Rabczuk, M. Ferretti, R. Jendrzejewski, G. Śliwiński (2009) Complementary use of the Raman and XRF techniques for non-destructive analysis of historical paint layers, *Applied Surface Science*, 255, 5542-5545.

[72] O. Syta, K. Rozum, M. Choińska, D. Zielińska, G. Z. Żukowska, A. Kijowska, B. Wagner (2014) Analytical procedure for characterization of medieval wall-paintings by X-ray fluorescence spectrometry, laser ablation inductively coupled plasma mass spectrometry and Raman spectroscopy, *Spectrochimica Acta Part B: Atomic Spectroscopy*, 101, 140-148.

[73] D. Lampakis, I. Karapanagiotis, O. Katsibiri (2017) Spectroscopic Investigation Leading to the Documentation of Three Post-Byzantine Wall Paintings, *Applied Spectroscopy*, 71, 129-140.

[74] T. Zorba, K.S. Andrikopoulos, K.M. Paraskevopoulos, E. Pavlidou, K. Popkonstantinov, R. Kostova, V. Platnyov, S. Daniilia (2007) Infrared and Raman Vibrational Spectroscopies Reveal the Palette of Frescos Found in the Medieval Monastery of Karaach Teke, *Annali di Chimica, by Società Chimica Italiana*, 97, 491-503.

[75] A. G. Nord, K. Tronner, K. Billström, B. Strandberg Zerpe (2017) Analysis of mediaeval Swedish paintings influenced by Russian-Byzantine art, *Journal of Cultural Heritage*, 23, 162-169.

[76] S. Švarcová, D. Hradil, J. Hradilová, E. Kočí, P. Bezdičk (2009) Micro-analytical evidence of origin and degradation of copper pigments found in Bohemian Gothic murals, *Analytical and Bioanalytical Chemistry*, 395, 2037-2050.

[77] A. Iordanidis, J. García-Guinea, A. Strati, A. Gkimourtzina (2014) A comparative study of pigments from the wall paintings of two Greek Byzantine churches, *Analytical Letters*, 47, 2708-2721.

[78] S. Daniilia, S. Sotiropoulou, D. Bikiaris, C. Salpistis, G. Karagiannis, Y. Chryssoulakis, B. A. Price, J. H. Carlson (2000) Panselinos' Byzantine wall paintings in the Protaton Church, Mount Athos, Greece: a technical examination, *Journal of Cultural Heritage*, 1, 91-110.

[79] S. Sotiropoulou, S Daniilia, C. Miliani, F. Rosi, L. Cartechini, D. Papanikola-Bakirtzis (2008) Microanalytical investigation of degradation issues in Byzantine wall paintings, *Applied Physics A*, 92, 143-150.

[80] E. Cheilakou, M. Troullinos, M. Koui (2014) Identification of pigments on Byzantine wall paintings from Crete (14th century AD) using non-invasive Fiber Optics Diffuse Reflectance Spectroscopy (FORS), *Journal of Archaeological Science*, 41, 541-555.

[81] L. Appolonia, D. Vaudan, V. Chatel, M. Aceto, P. Mirti (2009) Combined use of FORS, XRF and Raman spectroscopy in the study of mural paintings in the Aosta Valley (Italy), *Analytical and Bioanalytical Chemistry*, 395, 2005-2013.

[82] S. Boularand, P. Giráldez, L. Ventolà, M. Vendrell-Saz (2011) Templar joint repointings: materials, techniques and paint decoration in Miravet Castle, Spain, *Archaeometry*, 53, 743-752.

[83] I. Kakoulli, S. V. Prikhodko, A. King, C. Fischer (2014) Earliest evidence for asbestos composites linked to Byzantine wall paintings production, *Journal of Archaeological Science,* 44, 148-153.

[84] S. Mugnaini, A. Bagnoli, P. Bensi, F. Droghini, A. Scala, G. Guasparri (2006) Thirteenth century wall paintings under the Siena Cathedral (Italy). Mineralogical and petrographic study of materials, painting techniques and state of conservation, *Journal of Cultural Heritage*, 7, 171-185.

[85] D. Hradil, J. Hradilová, P. Bezdička, S. Švarcová, Z. Čermáková, V. Košařová, I. Němece (2014) Crocoite $PbCrO_4$ and mimetite $Pb_5(AsO_4)_3Cl$: rare minerals in highly degraded mediaeval murals in Northern Bohemia, *Journal of Raman Spectroscopy*, 45, 848-858.

[86] G. Chiari, D. Scott (2004) Pigment analysis: potentialities and problems, *Periodico di Mineralogia*, 73, 227-237.

[87] E. Bidaud, E. Halwax, E. Pantos, B. Sipek (2008) Analyses of a green copper pigment used in a thirteenth-century wall painting, *Studies in Conservation*, 53, 81-92.

[88] N. Buzgar, A. Buzatu, A. I. Apopei, V. Cotiugăb (2014) In situ Raman spectroscopy at the Voroneţ Monastery (16th century, Romania): New results for green and blue pigments, *Vibrational Spectroscopy*, 72, 142-148.

[89] M. Aceto, G. Gatti, A. Agostino, G. Fenoglio, V. Giordano, M. Varetto, G. Castagneri (2012) The mural paintings of Ala di Stura (Piedmont, Italy): a hidden treasure investigated, *Journal of Raman Spectroscopy*, 43, 1754-1760.

[90] M. Pérez-Alonso, K. Castro, J. M. Madariaga (2006) Investigation of degradation mechanisms by portable Raman spectroscopy and thermodynamic speciation: The wall painting of Santa María de Lemoniz (Basque Country, North of Spain), *Analytica Chimica Acta*, 571, 121-128.

[91] D. Damiani, E. Gliozzo, I. Turbanti Memmi (2014) The 'Madonna and Child Enthroned with Saints' of Ambrogio Lorenzetti in the St. Augustine Church (Siena, Italy): Raman microspectroscopy and SEM-EDS characterisation of the pigments, *Archaeological and Anthropological Sciences*, 6, 363-371.

[92] A. Domínguez-Vidal, M. J. de la Torre-Lopez, R. Rubio-Domenec, M. J. Ayora-Cañada (2012) In situ non-invasive Raman microspectroscopic investigation of polychrome plasterworks in the Alhambra, *Analyst*, 137, 5763-5769.

[93] L. Burgio, R. J. H. Clark, S. Firth (2001) Raman spectroscopy as a means for the identification of plattnerite (PbO_2), of lead pigments and of their degradation products, *Analyst*, 126, 222-227.

[94] L. Pereira-Pardo, M. Gil, B. Prieto, B. Silva (2016) Multi-analytical approach to the material characterization of 16th century wall paintings from Ribeira Sacra (Galicia, NWSpain): Pictorial palette, technique and alterations, *COLOR research and application*, 41, 263-269.

[95] S. Daniilia, E. Minopoulou (2009) A study of smalt and red lead discolouration in Antiphonitis wall paintings in Cyprus, *Applied Physics A*, 96, 701-711.

[96] A. Nevin, J. Loring Melia, I. Osticioli, G. Gautier, M. P. Colombini (2008) The identification of copper oxalates in a 16th century Cypriot exterior wall painting using micro FTIR, micro Raman spectroscopy and Gas Chromatography-Mass Spectrometry, *Journal of Cultural Heritage*, 9, 154-161.

[97] D. Hradil, J. Hradilová, E. Kocí, S. Švarcová, P. Bezdička, J. Maříková-Kubková (2013) Unique pre-romanesque murals in Kostoľany Pod Tríbečom, Slovakia: the painting technique and causes of damage, *Archaeometry*, 55, 691-706.

[98] O. Emmenegger (1986) Deterioration and preservation of Carolingian and mediaeval mural paintings in the Müstair Convent (Switzerland) Part III: Techniques and materials used and past restorations, *Studies in Conservation*, 31, 197-199.

[99] E. Kotulanová, P. Bezdička, D. Hradila, J. Hradilová, S. Švarcová, T. Grygara (2009) Degradation of lead-based pigments by salt solutions, *Journal of Cultural Heritage*, 10, 367-378.

[100] H. G. M. Edwards, D. W. Farwell (2008) The conservational heritage of wall paintings and buildings: an FT-Raman spectroscopic study of prehistoric, Roman, mediaeval and Renaissance lime substrates and mortars, *Journal of Raman Spectroscopy*, 39, 985-992.

[101] S. R. Amato, D. Bersani, P. P. Lottici, P. Pogliani, C. Pelosi (2017) A multi-analytical approach to the study of the mural paintings in the presbytery of Santa Maria Antiqua al Foro Romano in Rome, *Archaeometry*, 59, 1-15.

[102] M. D. Robador, L. De Viguerie, J. L. Pérez-Rodríguez, H. Rousselière, P. Walter, J. Castaing (2016) The Structure and Chemical Composition of Wall Paintings From Islamic and Christian Times in the Seville Alcazar, *Archaeometry*, 58, 255-270.

[103] S. Daniilia, E. Minopoulou, K. S. Andrikopoulos, A. Tsakalof, K. Bairachtari (2008) From Byzantine to post-Byzantine art: the painting technique of St Stephen's wall paintings at Meteora, Greece, *Journal of Archaeological Science*, 35, 2474-2485.

[104] A. Perardi, L. Appolonia, P. Mirti (2003) Non-destructive in situ determination of pigments in 15th century wall paintings by Raman microscopy, *Analytica Chimica Acta*, 480, 317-325.

[105] A. Hein, I, Karatasios, D. Mourelatos (2009), Byzantine wall paintings from Mani (Greece): microanalytical investigation of pigments and plasters, *Analytical and Bioanalytical Chemistry*, 395, 2061-2071.

[106] M. Veneranda, M. Irazola, M. Díez, A. Iturregui, J. Aramendia, K. Castro, J. M. Madariaga (2014) Raman spectroscopic study of the degradation of a middle age mural painting: the role of agricultural activities, *Journal of Raman Spectroscopy*, 45, 1110-1118.

[107] D. Fico, A. Pennetta, G. Rella, A. Savino, V. Terlizzi, G. Egidio De Benedetto (2016) A combined analytical approach applied to Medieval wall paintings from Puglia (Italy): The study of painting techniques and its conservation state, *Journal of Raman Spectroscopy*, 47, 321-328

[108] A. Andreotti, M. P. Colombini, A. Nevin, K. Melessanaki, P. Pouli, C. Fotakis (2006) Multianalytical Study of Laser Pulse Duration Effects in the IR Laser Cleaning of Wall Paintings from the Monumental Cemetery of Pisa, *Laser Chemistry*, 39046, 1-11.

[109] A. Iordanidis, J. García-Guinea, A. Strati, A. Gkimourtzina, A. Papoulidou (2011) Byzantine wall paintings from Kastoria, northern Greece: Spectroscopic study of pigments and efflorescing salts, *Spectrochimica Acta Part A: Molecular and Biomolecular Spectroscopy*, 78, 874-887.

[110] S. Sfarra, C. Ibarra-Castanedo, M. Tortora, L. Arrizza, G. Cerichelli, I. Nardi, X. Maldague (2016), Diagnostics of wall paintings: A smart and reliable approach, *Journal of Cultural Heritage*, 18, 229-241.

[111] J. M. Vallet, D. Syvilay, V. Detalle, D. Giovannacci, L. De Luca, C. Stefani, J. L. Bodnar, G. Walker, O. Guillon, M, Feillou, B. Trichereau, D. Martos-Le Vif, K. Mouhoubi, P. Marron, N. Martin-Beaumont, F. De Banes Gardonne, Development of a NDT toolbox dedicated to the conservation of wall paintings: application to the frescoes chapel in the Chartreuse Villeneuve-les-Avignon (Francia), Digital Heritage 2013, Marseille.

[112] M. Pérez-Alonso, K. Castro, I. Martínez-Arkarazo, M. Angulo, M. A. Olazabal, J. M. Madariaga (2004) Analysis of bulk and inorganic degradation products of stones, mortars and wall paintings by portable Raman microprobe spectroscopy, *Analytical and Bioanalytical Chemistry*, 379, 42-50.

[113] M. Irazola, M. Olivares, K. Castro, M. Maguregui, I. Martínez-Arkarazo, J. M. Madariaga (2012) In situ Raman spectroscopy analysis combined with Raman and SEM-EDS imaging to assess the conservation state of 16th century wall paintings, *Journal of Raman Spectroscopy*, 43, 1676-1684.

[114] M. Veneranda, M. Irazola, A. Pitarch, M. Olivares, A. Iturregui, K. Castro, J. M. Madariaga (2014) In-situ and laboratory Raman analysis in the field of cultural heritage: the case of a mural painting, *Journal of Raman Spectroscopy,* 45, 228-237.

[115] J. M. Madariaga, I. Costantini, K. Castro (2019) Analysis of natural degradation of medieval mural paintings in the open air abandoned church of Ribera, North of Spain, *Raman Spectroscopy in Art and Archaeology*, Volume 2, 213-233.

[116] A. Arnold, A. Kung, K. Zehnder (1986) Deterioration and preservation of Carolingian and mediaeval mural paintings in the Müstair Convent (Switzerland) Part I: Decay mechanisms and preservation, *Studies in Conservation*, 31, 190-194.

[117] F. Mairinger, M. Schreiner (1986) Deterioration and preservation of Carolingian and mediaeval mural paintings in the Müstair Convent (Switzerland) Part I: Decay mechanisms and preservation, *Studies in Conservation*, 31, 195-196.

[118] H. G. M. Edwards, F. Rull Pérez (1999) Lichen Biodeterioration of the Convento de la Peregrina, Sahagun, Spain, *Biospectroscopy*, 5, 47-52.

[119] N. Salvadó, S. Butí, T. Pradell, V. Beltran, G. Cinque, J. Juanhuix, L. Font, R. Senserrich (2016) Low molecular weight organic acid salts, markers of old fungi activity in wall paintings, *Analytical Methods*, 8, 1637-1645.

[120] C. Milanesi, F. Baldi, R. Vignani, F. Ciampolini, C. Faleria, M. Cresti (2006) Fungal deterioration of medieval wall fresco determined by analysing small fragments containing copper, *International Biodeterioration & Biodegradation*, 57, 7-13.

[121] C. Milanesi, F. Baldi, S. Borin, L. Brusetti, F. Ciampolini, F. Iacopini, M. Cresti (2009) Fungal deterioration of medieval wall fresco determined by analysing small fragments containing copper, *International Biodeterioration & Biodegradation*, 63, 844-850.

[122] M. Tortora, S. Sfarra, M. Chiarini, V. Daniele, G. Taglieri, G. Cerichelli (2016) Non-destructive and micro-invasive testing techniques for characterizing materials, structures and restoration problems in mural paintings, *Applied Surface Science*, 387, 971-985.

[123] L. Dei, A. Ahle, P. Baglioni, D. Dini, E. Ferroni (1998) Green degradation products of azurite in wall paintings: identification and conservation treatment, *Studies in Conservation*, 43, 80-88.

[124] M. Pérez-Alonso, K. Castro, M. Álvarez, J.M. Madariaga (2004) Scientific analysis versus restorer's expertise for diagnosis prior to a restoration process: the case of Santa Maria Church (Hermo, Asturias, North of Spain), *Analytica Chimica Acta*, 524, 379-389.

CHAPTER 2

Objectives

This PhD thesis concerns the study of some late Gothic mural paintings, belonging to Basque and Italian territory, using non destructive and micro-destructive analytical techniques. The main objective is to retrace the history of these artworks through the characterization of original materials and new materials employed in the past restauration works carried out in modern era. In addition, it will pay a particular attention to the conservation state of the murals and to the study of degradation products with the aim to understand the factors that have caused the observed damages.

The study of the murals paintings of the Basque territory is part of the Research Projects CTP09-P04 and CTP12-P10, founded by the Basque Country Government, thanks to which medieval mural paintings, located in the north of Spain, have been studied by the IBeA research group.

One of the last example of gothic mural paintings in the Basque Country is located in the Saint Stephen’s church in the abandoned village of Ribera de Valderejo (Álava), in a rural area outside of direct sources of pollution.

The murals have an unusual aspect since some portions of wall paintings are characterized by a grey colour. Thus, our objective was to check if the area is really uncontaminated and understand the degradation phenomena that caused the degradation of the materials over the years and, understand if the appearance of murals paintings was the result of a process of degradation of a pigment used or if it was a choice of painters in medieval times.

Another research project developed in collaboration with the Department of Physics and Earth Science "Macedonio Melloni" of University of Parma (Italy) was about the study of late Gothic wall paintings preserved in the Saint Stephen’s church in Montani (Bolzano, Italy) where a phenomenon of blackening is visible on the surface of the wall paintings.

In order to answer the numerous questions, an research program was planned with the following particular objectives:

- elemental and molecular analysis of original materials used for the creation of wall paintings such as buildings materials, mortars and pigments (chapters 5 and 6).
- recognition and characterization of materials used during past restorations works in the modern era, to verify the compatibility with the original materials, the danger for the work of art and for the surrounding environment (chapters 5 and 6).
- study of the conservation state by means of characterization of new mineral phases generated from the interaction of materials with the surrounding environment. Indeed, it has been studied the influence of the surrounding environment in triggering the reactions that cause or accelerate the degradation of raw materials (chapters 5 and 7).
- Propose new methodological approach to the determination of degradation products and the impact agents that degrade the studied wall paintings (chapters 8 and 9).

CHAPTER 3

Emplacement and samples

The wall paintings analysed in this PhD work belong to the Saint Stephen’s church in Ribera de Valderejo (Álava) and to the Saint Stephen’s chapel in Montani (Bolzano) located in the Basque and Italian territory (Figure 3.1) and belonging to the Gothic and Late-Gothic period respectively.

The study campaigns were mainly carried out using portable non-destructive diagnostic techniques. However, as will be discussed later, it was necessary to take micro samples only in selected areas in order to complete the analysis in the laboratory.

The state of conservation of the buildings and consequently of the wall paintings conserved inside them is very different due mainly to the state of abandonment in which the church of Ribera de Valderejo stands, contrary to that of Montani. However, in both cases the pictorial surfaces present some problems that will be discussed below.

Different diagnostic techniques were used in order to identify the original materials used for the realization of wall paintings, for the study of products used in modern times during restoration interventions and to verify the suitability of these treatments. Thus, a conservation status study was carried out through the characterization of secondary products and assessing the environmental impact in the formation of degradation products and the influence that the environment may have in favouring or accelerating their formation.

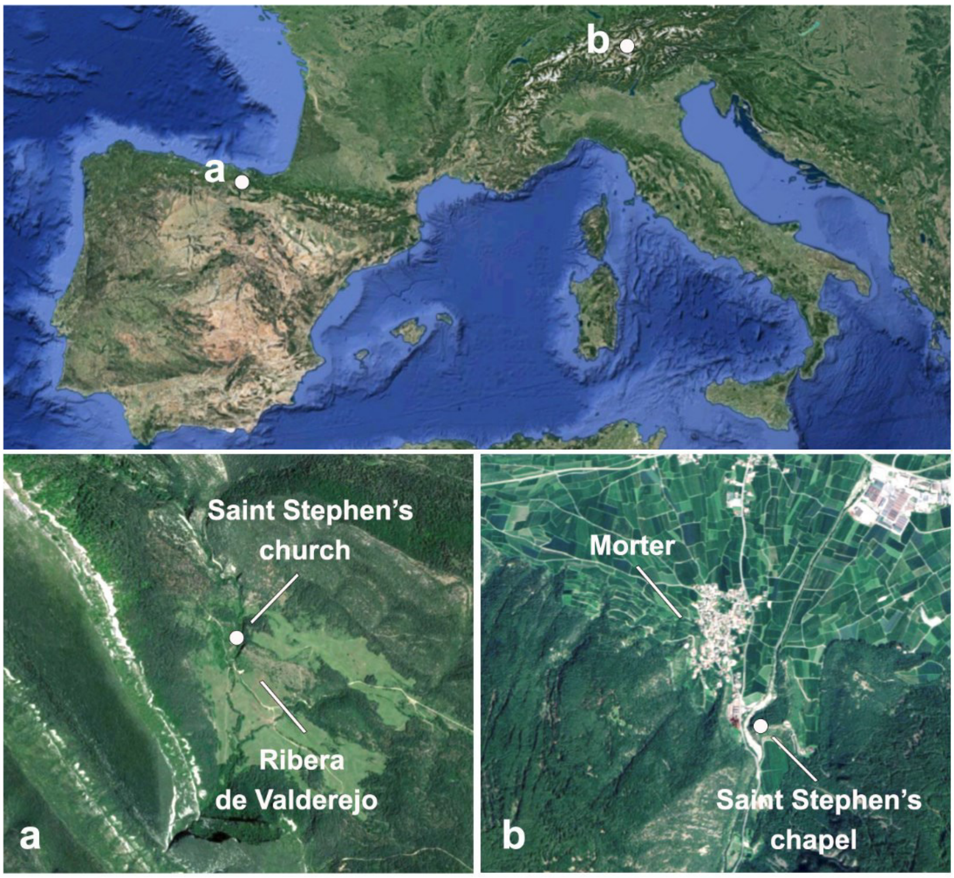

Figure 3.1: Localization of the studied wall paintings in Ribera de Valderejo (Álava, Spain) (a) and in Montani (Bozen, Italy) (b).

3.1 Saint Stephen's church in Ribera de Valderejo (Álava, Spain)

The church of Saint Stephen is the only still standing building in the abandoned village of Ribera de Valderejo (Figure 3.2). In this northern area of Spain, the depopulation of rural areas in the twentieth century caused the desertion of small villages that are currently facing ruin. Unfortunately, the Cultural Heritage preserved in these places has paid a high price.

Figure 3.2: Church of Saint Stephen (Ribera de Valderejo, Álava, Spain).

The structure has a single nave covered with a pointed barrel vault like most of the churches in the Basque territory. It has undergone many renovations over the years. However, the remains of the Romanesque temple are still visible, including the entrance portal of great value decorated with columns and capitals carved with human and fantastic themes (Figure 3.3).

Figure 3.3: Romanic portal and particular of carved capitals.

In the early 80's, below a thick gypsum plaster, some mural paintings, traced back to the end of the 15th century or the beginning of the 16th century [1], were partially discovered in the apse wall and some in the lateral naves after the relocation of the Renaissance altarpiece in the Fine Arts Museum of Álava.

The scenes that are well preserved are located in the apse wall divided in two groups by the proto Gothic window and represent several religious subjects: *the Apostolate*, *the Temptation of Adam and Eve* and the *Expulsion from Paradise* and images of *Saints* (Figure 3.4). The paintings are one of the few examples of Gothic painting present in the Basque territory and require special attention in order to be preserved since their conservation is at risk.

Figure 3.4: Painted apse wall of Saint Stephen's church.

3.1.1 Wall paintings description

Currently, only the paintings in the apse wall and some of the lateral naves were discovered (Figure 3.5). The cycle of paintings shows different religious themes: above the proto Gothic window, which divides the apse wall, a badly damaged scene was attributed to a *Deesis*, below the *Apostolate* divided into two groups of six people by the window. On the left, in the lower part of the wall, a particular scene from an iconographic point of view is found: the depiction of the *Original Sin*. On the left side a snake with a human head is twisted around the tree of life, and on the right side the figures of Adam and Eve. On the right, in the same scene, it is possible to see a figure covered with feathers, except the face, that represents an angel. The painter wanted to represent in the same scene three different moments: *the Temptation of the Snake*, *Adam and Eve that Realize their Sin and Try to Cover Themselves up*, and, finally, the *Expulsion from the Paradise* by an angel.

At the bottom on the right, we find the representation of Saint Lawrence, who holds in his right hand the grill, symbol of his martyrdom. This is the only example of this saint preserved in the late medieval painting in Álava. Further below, on the left, there are two figures representing Saint Sebastian pierced by arrows, and Saint Michael, more deteriorated, with a spear while he strikes a snake.

Figure 3.5: Wall paintings discovered and investigated in the Saint Stephen’s church.

On the top of the right side wall, the representation of the *Tetramorph* can be observed, but it is unfortunately damaged due to a further construction of a window. However, it is possible to recognize the symbols of the evangelists: the winged bull corresponding to Saint Luke, the angel of Saint Mark and in the centre the moon with human features. On the left side, there are more deteriorated figures, and only the representation of Saint Christopher can be recognized.

3.1.2 Conservation state

The church of Ribera de Valderejo is in critical condition and actually it is closed to visitors for security reasons. The church is located in a natural park and there is not industrial activity in its surroundings. Thus, the damages must be considered mainly as the result of the natural decay. Due to the state of abandon of the church, the infiltrations of the rainwater and snow are causing the partial collapse of the roof and this makes a particular scenario for the formation of saline efflorescence products inside and outside the masonry. Moreover, the building is almost completely surrounded by vegetation. Therefore, there are visible aesthetic, chemical and structural damages caused by both, microorganisms and macroorganisms (plant roots) that are stifling and destroying this interesting building (Figure 3.6).

Figure 3.6: Degradation process caused by infiltration water and presence of biological patinas.

The murals are in bad conditions because of the state of decay of the entire building, which has not windows or a door. Therefore, the paintings are continuously exposed to the atmospheric agents. Moreover, the infiltration of water inside the masonry in some areas is causing the detachment of the plaster with the consequent loss of the paint layer.

In these paintings there are extensive areas of grey colour especially in places that should be green (representing the grass in the scenes). In contrast, the only green part seems to be a repainting made in modern times. From existing documents, we know that over the years some restoration works have been carried out, but they still do not clarify why the grass is grey in the paintings. A first intervention was done in 1983. In 1992 it was suggested to move the murals at the Museum of Fine Arts to prevent their loss because the building was already in a complete state of disrepair. This proposal that could have definitively secured the wall paintings was rejected and it was decided to make an *in situ* restoration treatment.

3.1.3 Sampling

During the mural painting studies, it was not possible to clarify some important aspects only with the portable instruments, thus, micrometric wall painting samples were taken with a scalpel in areas of already deteriorated frescoes, in order to not cause further damage to the artwork. Some samples were collected in the *Original Sin* representation, which is the most interesting area for research. They were embedded in resin in the laboratory to study the stratigraphy (Figure 3.7) and additional analyses were conducted using benchtop techniques able to provide complementary information.

In addition, in order to study the composition of some salts efflorescence, some samples were collected to be analyzed in the laboratory to understand the effects of the surrounding natural environment on the onset of these secondary products. These samples were collected using a scalpel and stored in a plastic sample bag (Figure 3.8). The analysis in the laboratory was carried out both on efflorescence as it is and in the form of pellets.

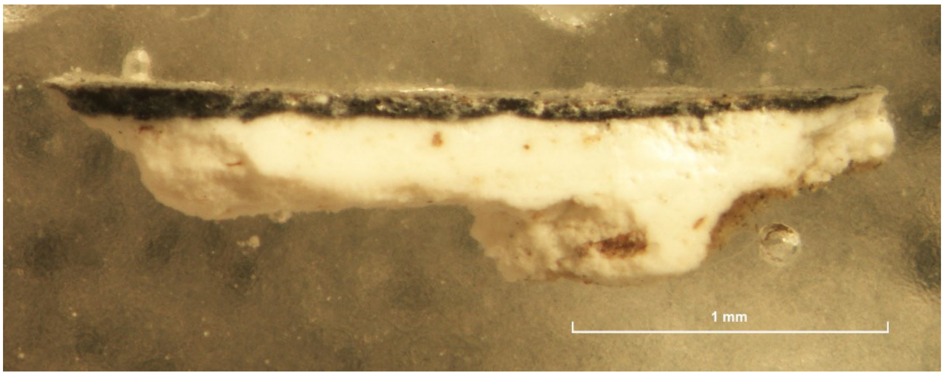

Figure 3.7: Optical image of cross section of a sample collected in the *Original Sin* representation.

Figure 3.8: Sampling of salt efflorescences present in the structural walls.

Besides, some samples of biological patinas were collected in an attempt to better characterize them using laboratory diagnostic techniques. All collected samples are summarizing in the table 1.

Table 3.1: Samples taken from the wall paintings and walls of Saint Stephen of Ribera de Valderejo.

Sample	Acronym	Analytical technique
Grey paint fragment	1-G	Micro-Raman, SEM-EDX
Grey paint fragment	2-G	Micro-Raman, SEM-EDX
Grey paint fragment	3-G	Micro-Raman, SEM-EDX
Green paint fragment	4-GR	Micro-Raman

Salt efflorescence	1- SALT	Micro-Raman
Salt efflorescence	2- SALT	Micro-Raman
Salt efflorescence	3-SALT	Micro-Raman
Salt efflorescence	4-SALT	Micro-Raman
Salt crust	5- SALT	Micro-Raman
Salt crust	6- SALT	Micro-Raman
Structural stone	1-ST	Micro-Raman and XRD
Biological patina	1-BIO	Micro-Raman, DNA extraction
Biological patina	2-BIO	Micro-Raman, DNA extraction
Biological patina	3-BIO	Micro-Raman, DNA extraction
Biological patina	4-BIO	Micro-Raman, DNA extraction
Biological patina	5-BIO	Micro-Raman, DNA extraction

3.2 Saint Stephen’s chapel of Montani (Bolzano, Italy)

The chapel of Saint Stephen’s is a splendid example of preservation of late medieval artistic heritage. It is perched in a rock spur above the open barrier between the Val Martello and the village of Montani (Figure 3.9).

The structure consists of a single nave with a wooden ceiling, divided by profiled cornices in narrow squares, with the exception of the spaces previously covered by five painted wooden tables dating back to 1430, which were removed for security reasons and are now preserved in the civic museum of Bolzano.

Figure 3.9: Saint Stephen’s chapel of Montani (Bolzano, Italy).

The nave culminates in the choir, with a cross vault, in whose center there is the high altar enriched by crosses incised in the plaster. The building, in its simplicity, retains some details, such as the rectangular shape of the choir, not found in other Gothic buildings of worship in Val Venosta. The eastern wall has a round-arched wall, which bears witness to the presence of a previous construction. The shapes of the windows and the use of tufa cornices suggest that the building was built in the early decades of the fifteenth century: the openings in the southern wall are wider than the lancet window, with fish bladder, located on the wall at the conclusion of the choir, while the north wall has no opening.

3.2.1 Wall paintings description

The interior of the chapel of Saint Stephen is completely covered with paintings, realized with the fresco technique, belonging to two different periods: the north wall, the presbytery and the triumphal arch are of Lombard origin (Figure 3.10), belonging to a period between 1430-1440, while the walls to the south and west were painted by a Swabian shop: next to the Montani coat of arms, on the west wall, there is the date of the cycle of frescoes, 1487 (the same year in which the church was consecrated) [2].

In the north wall the life of Saint Stephen is depicted. The narration is divided into two registers and the scenes unfold within rectangular backgrounds: the upper area houses the *Election of Saint Stephen as a Deacon*, *the Dispute Between the Saint and the Elders of the People,* the scene of *the Stripping* and that where *the Jews Collect Stones and lay their cloaks at the Feet of a Man Called Saul*. They follow in the lower register: *the Stoning, the Funeral, the Burial, Gamaliele Appears in Rome to the Priest Luciano* and *the Finding of the Mortal Remains in 365 near Jerusalem.*

Figure 3.10: Interior of Saint Stephen's chapel of Montani.

The representations of the triumphal arch are not part of the Saint Stephen cycle; it is occupied by the representations of Saint Anthony the Great and the *Martyrdom of Saint Ursula* while the intrados are occupied by various figures of saints: Dorothy, Michael, Pantaleon, Sebastian, George and Mary Magdalene. Above the altar in the pendentives we find the scene of the *Annunciation*, on the left the Virgin is represented, on the right the angel Gabriel; in the part to the left of the altar a Crucifixion is painted and above we see a group of three saints: Christopher, Erasmus and Acacius. Part of this iconographic program is the two images of Saint Eustace and Saint Alexis under the staircase.

In the vault, the *Triumph of the Virgin* is depicted in the genre of the garden of paradise, opposed to a half-length image of *Christ Blessing* in almond that occupies a rather important space; near the figure of God there are the *Four Evangelists* and their symbols, the angel, the lion, the ox and the eagle. In the back wall of the choir, the *Apostles* are represented in groups of two in a sitting position within an architecture that gives depth to the representation.

In 1487 the decoration of the walls was completed by a painter from the Swabian school, although it is not possible to trace the name of the artist. In the south wall is shown the cycle of the *Passion of Christ* divided into nine scenes beginning with the *Entrance to Jerusalem*; followed by the *Last Supper*, the scene in the *Garden of Olives*, the *kiss of Judas* combined with the *Healing of Malchus's Severed Ear*, *the Presentation to Pilate*, *the Flagellation with Two Tormentors, the Crowning of Thorns.* The iconographic program completes the scene by *Simon of Cyrene who Carries the Cross and the Crucifixion.*

Most of the west wall houses the representation of the *Last Judgment*: the figure of Christ in almond and placed above the entrance door, with a cornice in tufa and a round arch on the sides of the Judge, Christ kneeling Mary and John the Baptist. On the side where the blessed are placed, stands the crest of the Montani Family with the date of construction of the pictorial cycle. In the intrados of the windows there are four figures of saints: Stephen and Sebastian, Leonard and Ursula, painted, like statues, on shelves in false tabernacles.

3.2.2 Conservation state

The state of conservation of the cycle of frescoes in the complex is good, except for the lower part of the north wall. In this area, some pictorial film leaks have occurred and quite large plaster has fallen due to the presence of strong humidity, which, due to capillarity, creeps into the wall. This is due to the fact that the outer wall of the church is in contact, for about 50 cm in height, with an embankment that surrounds it. This deterioration process has irreparably damaged the lower part of the narration of *Saint Stephen's life* and the representation of the *Epiphany* in the presbyter.

The state of conservation of the cycle of murals from the Swabian period is not particularly critical and it is, therefore, still possible to admire the minuteness of details and the plasticity in the rendering of the bodies; the colours also seem to have retained their original vivacity. Even in the south wall the loss of colour concerns the masonry areas in correspondence of the floor slab.

Regarding the murals located in the presbyter and in the triumphal arch, painting surfaces show a phenomenon of blackening probably caused by the degradation of a lead-based pigment used originally (lead white according to restorers). This phenomenon is sometimes circumscribed in small areas where the pigment was used in order to create chromatic contrasts, such as *chiaroscuro* effects. In other areas, instead, its layout concerns larger coloured areas. The chromatic alteration strongly influences the correct usability of the work because it drastically distorts the true effect sought by the artists (Figure 3.11).

Some delimited areas in the east wall were treated with preliminary cleaning tests carried out with the traditional method of reconverting the lead, using a solution of acetic acid and hydrogen peroxide in cellulose pulp [3]. Since the results obtained were not considered satisfactory, we made a complete analysis to understand this blackening phenomenon as well as the suitability of the used treatment. Indeed, although there is not much evidence of the use of this treatment in the scientific literature, it is nevertheless used by restorers as confirmed by this case study [4, 5].

Figure 3.11: Vault of chapel where the blackening of paintings is evident.

3.2.3 Sampling

In this work, portable instruments were applied for a first screening of the painting surfaces allowed identifying the areas of interest where the blackening appeared and micro-sampling was then necessary to perform further analyses to better understand the degradation phenomena. The samples taken from the wall paintings come from blackened areas and areas subjected to reconversion treatment, yellow (Figure 3.12) and green, of lead white in order to verify the affective suitability of the treatment not only visually but also through an analytical study.

In addition to these fragments, some powdered samples composed only of the degradation material were taken from blue, yellow and red areas not subjected to cleaning tests, scraping the surface with a scalpel. In this way it was possible to obtain a more accurate characterization of the degradation material and to characterize the pigments used by the painters. All the collected samples are listed in table 3.2.

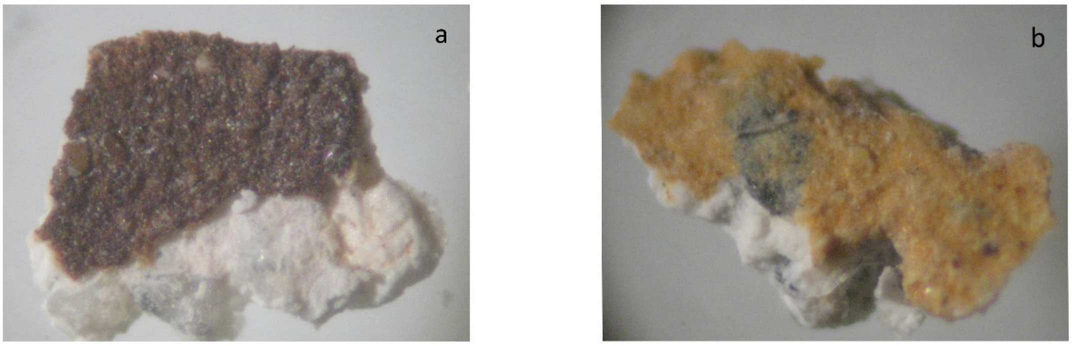

Figure 3.12: Microsamples taken in a darkened area (a) and in a cleaned area after the reconversion treatment (b) (magnification 40X).

Table 3.2: Samples taken from the wall paintings preserved inside the Saint Stephen’s chapel of Montani.

Sample colour	Type	Acronym	Analytical technique
(Cleaned) green	Fragment	1-CYF	Micro Raman
Blackened green	Fragment	2-BYF	Micro Raman
(Cleaned) yellow	Fragment	3-CGF	Micro Raman
Blackened yellow	Fragment	4-BGF	Micro Raman
Blackened red	Powder	5-BRP	Micro Raman
Blackened red	Powder	6-BRP	Micro Raman and XRD
Blackened blue	Powder	7-BBP	Micro Raman and XRD

References

[1] R. Saenz Pascual, La pintura gotica en Álava. Una contribución a su estudio, ed: Vitoria-Gasteiz: Diputación Foral de Álava, Departamento de Cultura y Euskera,1997.

[2] L. Andergassen, Montani, la cappella di Santo Stefano. Montani di Sopra, Montani di Sotto, Schnell & Steiner GmbH (2001), Leibnizstraße13, D-93055 Regensburg.

[3] M. Matteini, Ossidazione della biacca in pitture murali- Metodi proposti per la riconversione del pigmento ossidato nelle pitture di A. Baldovinetti della chiesa di S. Miniato (Firenze), *In Atti del Convegno sul Restauro delle Opere d'Arte*, Florence, 2-6 November, 1976, 257-269.

[4] M. Matteini, A. Moles, The reconversion of oxidized white lead in mural paintings: a control after a five year period, ICOM Committee for Conservation, 6th Triennial Meeting, Ottawa, 1981 81/15/1.

[5] M. Koller, H. Leitner, H. Paschinger (1990) Reconversion of altered lead pigments in alpine mural paintings, *Studies of Conservation,* 35, 15-20.

CHAPTER 4

Experimental techniques

As documented in the chapter 1, different diagnostic techniques have been used since the 1990s for the characterization of wall paintings. Undoubtedly, portable non-destructive techniques are the most used ones for works of art that represent the immovable cultural heritage, thanks to which it was possible to obtain *in situ* information without affecting the pictorial surfaces and without sampling. Moreover, as demonstrated in the following chapters, portable techniques are extremely useful for selecting areas of particular interest from a diagnostic point of view and identify an area where take samples in order to complete the investigations using benchtop instruments.

This chapter summarizes the diagnostic techniques used both *in situ* and in the laboratory, the laboratory instruments used for treatment of samples and the commercial products employed to develop this PhD project.

4.1 General purpose instruments and tools

Loading analytical balance

To know the exact weight of the samples, powder samples were weighed using an AS 200 analytical balance (Mettler Toledo, USA) with a precision of ± 0.0001 g.

Stereoscopic microscope

The analytical study of mural paintings samples was often assisted by their visual assessment at microscopic scale. Thanks to the support of Dr. X. Murelaga Bereicua from the Department of Stratigraphy and Paleontology (UPV/EHU), high quality images of the fragments under analysis were acquired by means of the SMZ-U microscope (Nikon, Japan) coupled to the Nikon Digital Sight DS-L1 camera (Figure 4.1).

Figure 4.1 SMZ-U microscope.

Metallographic polisher

With the aim of collect elemental (SEM-EDS) and molecular (Raman spectroscopy) chemical images, mural painting fragments were prepared as cross sections. The fragments were first embedded into acrylic resin. Once the resin polymerization process was completed, embedded samples were treated with the Forcipol®1 metallographic polisher (Metkon, Turkey). In the first step the fragments were ground with finer and finer sandpapers (P320-2000). Afterwards, the roughed samples were polished with a diamond suspension on a synthetic napless cloth to produce a scratch-free mirror finish.

Agate mortar

In order to ensure reliable results, the particle size of some efflorescence salts samples needed to be reduced and homogenized. To achieve this purpose, the grinding procedure was carried out manually by means of an agate mortar. The commercial products used for the realization of pellets were calcium carbonate ($CaCO_3$, Merck, 99.95 Suprapur®), gypsum ($CaSO_4.2H_2O$, Fluka, ≥ 99.0%) and potassium nitrate (KNO_3, Merck, ≥ 99.0%).

Digital hydraulic press

In order to perform semi quantitative analyses with Raman spectroscopy, salt samples were mixed thoroughly in an agate mortar. Some salt pellets were prepared using a CrushIR hydraulic press (Pike technologies, USA, Figure 4.2). The press, specifically designed for making high quality KBr pellets, ensures excellent reproducibility thanks to the combination of digital pressure reading and adjustable pressure setting (maximum value: 13.6 tons/cm^2). The instrument is equipped with a PIKE Evacuable Pellet Press having a pellet holder with a diameter of 13 mm.

Figure 4.2: CrushIR hydraulic press.

Cutting plotter, laser ablation system-excimer/CO_2 laser, and Thermal roller laminator

After AutoCAD design of the 3D structure the COP and PSA polymer layers were cut using a cutter plotter (Graphtec CE5000-40 Craft Robo Pro, Tokyo, Japan). On the other hand, PMMA layers were cut using a CO_2 laser ablation system (Optec Laser Micromachining Systems, Belgium). A thermal roller laminator (Titan-110, GBC Films, USA, Figure 4.3) was employed to assemble the microfluidic devices (see chapter 9).

Zeonor COP sheets of 100 µm thickness were purchased by Zeonex (Düsseldorf, Germany). ArCare®8939 PSA of 127 µm double side roll was provided by Adhesive Research (Limerick, Ireland). Poly(methyl-methacrylate) (PMMA) 50 µm slides were purchased from Goodfellow, UK.

Figure 4.3: Cutter plotter Graphtec CE5000-40 Craft Robo Pro.

For the realization of microfluidic sensors, described in the chapter 9, two types of ionogel were prepared, for the ILs: (IO-1) 1-ethyl-3-methylimidazolium ethyl sulfate (Sigma-Aldrich, ≥ 95%, opaque) and (IO-2) trihexyltetradecyl-phosphonium dicyanamide (Sigma-Aldrich, ≥ 95%, transparent). The ionogel was obtained by mixing two monomers, one linear (N-isopropylacrylamide, Sigma-Aldrich, 97%), and the other for giving the three-dimensional structure (N,N'-methylene-bis acrylamide, Sigma-Aldrich, 99%). In addition, a photoinitiator was added (2,2- Dimethoxy-2-phenylacetophenone, Sigma-Aldrich, 99%) to induce photopolymerization.

Copper chloride ($CuCl_2$, Sigma-Aldrich, ≥ 99%) was chosen as a reagent substance and was placed over the ionogel for its ability to form a stable metal complex with ammonia.

In order to simulate the formation of ammonium nitrate in the laboratory ammonium chloride (NH_4Cl, Sigma-Aldrich, 99.99 Suprapur®) and potassium nitrate (KNO_3, Merck, ≥ 99.0%) were dissolved in milli Q water at different concentrations.

4.2 Hand-held and portable analytical techniques for *in situ* analyses

4.2.1 X-Ray Fluorescence Spectroscopy

Energy Dispersive - X-Ray Fluorescence (ED-XRF) XMET5100 ED-XRF spectrometer (Oxford Instruments, UK)

Figure 4.4: Use of portable ED-XRF instrumentation on the structural walls of Saint Stephen’s church (Ribera de Valderejo, Álava).

The hand-held XMET5100 ED-XRF spectrometer (Oxford Instruments, UK, Figure 4.4), used for elemental analysis in the Saint Stephen’s church of Ribera de Valderejo (Álava, Spain, see chapter 6), makes use of an X-Ray tube excitation source composed of a rhodium anode (maximum voltage of 45 keV). The analyser has a silicon drift detector that provides an energy resolution of 150 eV (calculated for the Mn Kα line at -20° C) and a spectral resolution of 20 eV. Data acquisition is carried out thanks to a personal digital assistant (PDA) integrated into the instrument, which also provides semi-quantitative information of the detected elements. With regards to mural paintings characterization, *in situ* ED-XRF data were collected by putting in contact the head of the system with the paint surface.

Thermo Scientific Niton XL3t GOLDD+ XRF Analyzer

The elemental analyses within Saint Stephen's church of Montani (Bozen, Italy) were carried out by a portable spectrophotometer Niton™ XL3t GOLDD+, Thermo Fisher Scientific Inc. (Waltham, Massachusetts, USA) equipped with a multi-channel silicon Peltier-cooled detector, a beryllium window, silver anode working at a maximum voltage of 50 kV, tube current of 40 µA, measuring areas of 3 mm in diameter and applying acquisition time of 60 second.

4.2.2 Raman Spectroscopy

InnoRam™-785S Raman spectrometer (B&WTEK Inc., USA)

The portable InnoRam™ spectrometer (B&WTEK, Inc., USA, Figure 4.5) is equipped with a diode 785 nm laser. The spectrometer works in a spectral range 65 - 2980 cm^{-1}. The maximum nominal laser power of the system is 300 mW. Spectra acquisition was carried out with the software BWSpec™ 3.26. The spectra were acquired with a measurement time varying from 0.5 to 10 s, in a spectral range from 100 to 2200 cm^{-1} and with a number of accumulations varying between 20 and 200 (depending on the case of analysis, the presence of fluorescence and the signal-to-noise ratio). The laser power was reduced to 10% in order to avoid any thermal photodecomposition or laser induced chemical transformation of the materials. The obtained Raman spectra were processed by Nicolet Omnic 7.2 software (Madison, USA).

Figure 4.5: Use of portable InnoRam^{TM}-785S spectrometer (785nm) spectrometer within the Saint Stephen's church in Ribera de Valderejo (Álava, Spain).

BWS5445-532S Raman spectrometer (B&WTEK Inc., USA)

The BWS5445-532S portable Raman system is equipped with a 532 nm green laser (maximum power of 45 mW) and a CCD detector. The system works in a range between 62 and 3750 cm^{-1} and with a mean spectral resolution of 4.2 cm^{-1}.

On the one hand, mural paintings were analyzed by putting in contact the hand-held probe with the wall surface. However, the portable instrument can be coupled to a BAC151B video-microscope (BWTECK, USA). The benefits provided by the use of this tool are manifold. For example, the integrated camera and objectives (20x and 50x) allows to better focus on the sample, improving the Raman signal. Furthermore, its unique dual laser wavelength port provides flexibility because it allows collecting two molecular spectra from the same spot of analysis by sequentially using the green and the red lasers. Considering the different power of the excitation sources, specific measurement conditions were adopted for each Raman system. Raman spectra were acquired with the BWSpec™ 4 (B&WTEK Inc., USA) software.

ASD High Resolution FieldSpec4 spectroradiometer (Analytical Spectral Devices Inc., Boulder, USA)

Figure 4.6: ASD High Resolution FieldSpec4 spectroradiometer

Reflectance measurements of all samples were carried out using the ASD High Resolution FieldSpec4 spectroradiometer (Analytical Spectral Devices Inc., Boulder, USA, Figure 4.6) equipped with a bare optic fibre for remote mode operations. The light source consisted of a halogen lamp (ASD Iluminator) placed at 30 cm of distance from the samples. The angle between the incident light and the sample, and that between the sample and the detector fibre was 45° in both cases. The fibre has an acceptance cone with an angle of 25° and was placed to a minimum distance of the sample to minimize the measurement surface. This device works in the 350-2500 nm wavelength range and uses three detectors for the different spectroscopic ranges: 350-1000 nm (silicon photo-diode array for Vis-NIR), 1001-1800 nm (InGaAs photo-diode for SWIR1) and 1801-2500 nm (InGaAs photo-diode for SWIR2). The spectral resolution is 3 nm in the visible region and 6 nm in the near infrared region. Sensor optimization and calibration was set with a Spectralon® white reference scanned once before each sample, and each spectrum is the result of the average of 10 scans. Spectra were collected with RS3 software (ASD Inc.), analysed with ViewSpecPro software (ASD Inc.) and compared with those found in the bibliography.

4.3 Bench top analytical techniques for non-destructive laboratory analyses

4.3.1 Scanning Electron Microscopy (SEM) Energy Dispersive X-Ray Spectrometer (EDS)

EVO40 Scanning Electron Microscope (Carl Zeiss STS, Germany)

Elemental images of selected samples were performed using an EVO40 scanning electron microscope (Carl Zeiss STS, Germany) coupled to an X-Max Energy-Dispersive X-Ray Spectrometer (Oxford Instruments, UK). Previous to SEM-EDS analyses, the selected samples were fixed in specific aluminium sample holders (pin) with carbon type. Furthermore, with the aim of improving the quality of SEM images, a thin gold film (<20 µm) was applied on the surface of the sample using a Emitech K550X sputter coater vacuum chamber (Quorum Technologies, UK). EDS analyses were carried out using a working distance of 8–10 mm, an I Probe of 180 pA, a 35º take-off angle, an acceleration potential of 30 kV, an integration time of 50 s and a number of scans between 6 and 10. The INCA Microanalysis Suite 4.3 (Oxford Instruments, UK) software was used to collect and manage the collected data.

4.3.2 Raman Spectroscopy

InVia Confocal Raman spectrometer (Renishaw, UK)

The inVia Confocal Raman microscope (Figure 4.7) is equipped with a 514 nm (maximum power of 50 mW) and a 785 nm (maximum power of 350 mW) excitation laser, a DMLM Leica microscope (Bradford, UK) and a CCD detector. The spectrometer works in a spectral range between 65 and 3800 cm^{-1} with a mean spectral resolution of 1.2 cm^{-1}. On the one side, StreamLine technology was employed to generate high definition molecular images of specific samples. Briefly, the motorized stage of the microscope coupled to the Raman spectrometer moves the sample beneath the lens so that the line of laser-light is rastered across the area under analysis. Afterwards, from the collected spectra, chemical images are generated by taking into account the position of main band of the compound of interest. In both cases, the Renishaw Wire 3.2 (Renishaw, UK) software was used for data collection and analysis.

Some powered samples of pure commercial plattnerite (PbO_2, Sigma Aldrich, 99%) was analysed with InVia Confocal Raman spectrometer in order to compare the spectrum with those obtained during the Raman analyses of wall paintings fragments taken in the Saint Stephen's chapel of Montani (Bozen, Italy) (See chapter 5).

Figure 4.7: InVia Confocal Raman spectrometer.

Renishaw RA100 spectrometer (Renishaw, UK)

The RA100 Raman system (Renishaw, UK) is equipped with a 785 nm red laser (maximum power of 150 mW) and a CCD detector. The system works in a spectral range from 200 to 3200 cm^{-1} and with a mean spectral resolution of 2 cm^{-1}. The spectrometer is coupled to a X-Y motorized tripod which mounts a microprobe implementing a video-camera (which allows focusing the laser beam on the sample) and long range objectives (4x, 10x, 20x and 50x). Spectra acquisition was performed with the WIRE^{TM} 2.0 software (Renishaw, UK), and data interpretation was carried out by comparison with the reference spectra.

Horiba - Jobin Yvon LabRam micro-spectrometer

The micro-Raman measurements were carried out with a 632.8 nm laser in a nearly backscattered geometry by using a Horiba - Jobin Yvon LabRam micro-spectrometer (300 mm focal length) equipped with an integrated Olympus BX40 microscope. The spectral resolution was about 1.5 cm^{-1}. The Rayleigh radiation was blocked by a holographic edge filter and the backscattered Raman light was dispersed by an 1800 grooves/mm holographic grating on a Peltier cooled CCD, consisting of an array of 1024/256 pixels. The entrance slit width was fixed at 100 µm. The laser power on the samples was adjusted by means of density filters. Raman spectra were collected at very low laser power (< 0.1 mW) in order to avoid photo-thermal effects on the samples induced by the laser excitation as well as at varying power to check the thermal behaviour of the pigments. The spectra were collected using a 50x ultra long working distance (ULWD) microscope objective. Typical exposures were 10-20 s, with 3-5 accumulations. The system was regularly calibrated using the 520.6 cm^{-1} Raman band of silicon. The data analysis was performed by LABSPEC 5.78.24, Horiba - Jobin Yvon LabRam, built-in software package. All collected spectra were compared with reference spectra.

4.3.4 X-Ray Diffraction (XRD)

PRO PANalytical Xpert X-Ray Diffractometer (PANalytical, Netherlands)

The used X-Ray Diffractometer is equipped with a copper tube, a vertical goniometer (Bragg-Brentano geometry), a programmable divergence slit, a secondary graphite monochromator and a Pixcel detector. The condition of all measurements were set at 40 KV, 40 mA and a scan ranging between 5 and 70º 2theta.

Bruker D2 PHASER diffractometer

Powder XRD analysis of mural paintings samples were carried out with a Bruker D2 PHASER diffractometer operating in Bragg-Brentano geometry, equipped with a LYNXEYE detector (based on silicon strip technology) and copper anode (CuKα). The powdered samples (few milligrams) were analysed on a zero-background sample holder (ZBH) and measurements were taken in steps of 0.02° over 2θ range from 10 to 60°.

4.4 Isolation and characterization of biodeteriogens genomic DNA sequences via PCR amplification

To genomically characterize the main biodeteriogens the biological strains, collected in Ribera de Valderejo, sterile swabs and PDA petri dishes were sent to the BAT laboratory (CIAL institute, Madrid) for their characterization.

Starting from the genomic characterisation of green patinas, the biological strains contained in the PDA Petri dishes were cultured for seven days at room temperature (25 °C). Then, metagenomic DNA was isolated in a biological safety cabinet (BIO II Advance, Telstar, Spain) using the soil DNA isolation commercial kit. All the steps in the isolation procedure were carried out following the manufacturer's instructions. In order to amplify the region of internal transcribed spacer (ITS), a polymerase chain reaction (PCR) and secondary PCR procedures were performed as described by Leake *et al.* [1]. To verify the success of the extraction, the metagenomic DNA was checked by using 0.8% w/v agarose gel electrophoresis. A Inc PTC-100 (MJ Research, USA) thermal cycler was used to amplify segments of DNA via the PCR. For the characterisation of the fungi and bacteria species, the 18S and 16S ribosomal RNA gene region was amplified, respectively. An output file containing ITS sequences with a partial 18S and 16S ribosomal RNA genes' sequence were then analysed by using Bioedit software. Finally, ITS sequences' identification was carried out by comparison with the National Centre for Biotechnology Information (NCBI) database [2].

References

[1] J. L. Leake, S. E. Dowd, R. D. Wolcott, A. M. Zischkau and Y. Sun (2009) Identification of yeast in chronic wounds using new pathogen – detection technologies, *Journal of Wound Care*, 18, 103-108.

[2] D. L. Wheeler, T. Barrett, D. A. Benson, S. H. Bryant, K. Canese, V. Chetvernin, D. M. Church, M. DiCuccio, R. Edgar, S. Federhen, L. Y. Geer, Y. Kapustin, O. Khovayko, D. Landsman, D. J. Lipman, T. L. Madden, D. R. Maglott, J. Ostell, V. Miller, K. D. Pruitt, G. D. Schuler, E. Sequeira, S. T. Sherry, K. Sirotkin, A. Souvorov, G. Starchenko, R. L. Tatusov, T. A. Tatusova, L. Wagner, E. Yaschenko, Database resources of the National Center for Biotechnology Information, *Nucleic Acids Research*, 2007, 35, D5–D12.

CHAPTER 5

Investigation of mural paintings blackening in the chapel of Saint Stephen’s in Montani (Italy)

As reported in chapter 3, a part of the doctoral project was carried out through a collaboration with the Department of Mathematical, Physical and Computer Sciences of the University of Parma (Italy) and involved the study of wall paintings preserved inside the Saint Stephen’s chapel in Montani (Val Venosta, Bolzano, Italy) in order to characterize the alteration products that cause the blackening of paintings.

Chemical alterations of raw materials, like pigments and organic binders, can cause chromatic changes with a negative aesthetic effect, preventing a full appreciation of the artwork. Blackening phenomena or alteration of pigments are widely described in the literature [1]: the most known examples are the darkening of vermilion [2], haematite [3], azurite [4] and of lead-based pigments, in particular white and red lead [5-9]. Since these processes endanger the preservation of the wall paintings, it is essential to understand the chemical alteration processes that occur during the ageing of the pigments.

The lead-based pigments (the most used are white lead, $2PbCO_3{\cdot}Pb(OH)_2$, and red lead, Pb_3O_4) have been widely employed in the production of artworks since ancient times [10]. The formation of their secondary products are well known to conservators and scientists as well as their instability and their tendency to blacken, especially when using the fresco technique [11]. However recent research has shown the presence of blackening of lead white even in secco mural paintings [7].

The natural ageing of lead-based compounds can manifest in the form of different chromatic alterations from light pink to dark brown depending on the type of decay products. The factors that cause the degradation of lead-based pigments are different and interrelated, and over the past years several studies have been conducted to clarify which conditions may give rise to the different decay compounds [12].

The blackening of white lead and red lead can occur in the form of lead sulphide PbS (galena mineral) in the presence of atmospheric hydrogen sulphide (H_2S). This degradation path has been observed especially on manuscripts [13-15]. The formation of lead sulphide could be caused also by the interaction of the lead pigments with sulphur-based pigments, even if in the literature there is, however, no clear evidence of this effect [16, 17].

The formation of black lead dioxide β-PbO_2 (plattnerite mineral) as a degradation product is a rarer phenomenon than the development of lead sulphide. Plattnerite has been identified in mural paintings as a decay product of both white lead and red lead [18]. It is worth mentioning that recent studies claimed that plattnerite was intentionally used as pigment in some mural paintings in Iran, after the discovery of this mineral in a nearby mine [19], but this is a very particular case.

The darkening of lead white in the fresco technique has been attributed to oxidation processes favoured by the alkaline environment before the lime is transformed into calcium carbonate and in the presence of moisture [11]. However, the use of a hydrophobic binder such as egg or oil can inhibit the process of degradation despite the alkaline environment [20]. Chemical tests conducted on white lead in a NaOH alkaline solution have shown the transformation of the white pigment in a mixture of massicot (β-PbO), as the main product of reaction, together with red lead and plattnerite [20].

Other studies have suggested that the presence of microorganisms such as bacteria (*Arthobacter* genus [22] or *Flavobacterium* species [23]) can favour the degradation of white and red lead into plattnerite. As stated by Matteini and Moles [11], the blackening of red lead can occur in presence of hydrogen peroxide (H_2O_2) produced by the metabolic activity of microorganisms. Furthermore, some bacteria can transform lead white, red lead and massicot into PbS. This phenomenon is caused by the interaction of hydrogen sulphide, produced by bacteria utilizing sulphur-containing amino acids, with lead-based pigments [15].

Tests performed in laboratory on reference samples of lead based pigments have highlighted the influence on the degradation of natural inorganic salts and synthetic salts that may be present on wall paintings after cleaning interventions [24]. The results showed that blackening of white lead occurred only in the presence of a strong oxidizing agent, such as NaClO, used as fungicide agent, with formation of plattnerite, scrutinyite (α-PbO_2) and cerussite ($PbCO_3$). On the contrary, the blackening did not occur in the presence of hydrogen peroxide. However, red lead tends to darken in all salt solutions containing dissolved atmospheric CO_2 in the form of hydrogen carbonate anions, forming a mixture of plattnerite and cerussite [24]. Thus, relatively drastic conditions seem to be needed for the darkening of lead white in wall paintings.

Moreover, studies on naturally aged wall paintings and physical-chemical tests on raw materials in sulphuric acid solution, proved the presence of a mixture of plattnerite (β-PbO_2) and anglesite ($PbSO_4$) as decay product of red lead pigment [12]. This degradation of the red lead, proposed by Aze *et al.* [12], has been explained by a process of sulphation or carbonation of β-PbO, a highly reactive specie, which can be found as impurity in the red pigment. β-PbO is transformed into anglesite, and subsequently a solvolytic disproportionation process of Pb_3O_4 takes place with the formation of plattnerite.

The whitening of the red lead, converted into lead carbonates cerussite and hydrocerussite ($Pb_3(CO_3)_2(OH)_2$), or in lead sulphate anglesite, is a less known phenomenon although it has been observed over pictorial surfaces. It occurs when the pigment reacts with atmospheric pollutants such as SO_2, CO and CO_2 in specific temperature and moisture conditions [12, 25]. Other authors suggest that the alteration of minium gives initially a dark colour, with formation of plattnerite, which then turns into a more stable anglesite, causing the total loss of the colour [26].

Other lead compounds such as lead monoxides, massicot (β-PbO-orthorhombic) and litharge (α-PbO-tetragonal), have been frequently identified in wall paintings together with red lead. They may be present either as pigments, or as impurities of the same red lead. In fact, α-PbO and β-PbO are intermediate products generating from the calcination of the white lead at high temperatures during the manufacturing process of red lead [27]. Lead monoxides are instable in the presence of moisture and in an alkaline environment. In fact, the carbonation processes cause the formation of lead carbonates cerussite, hydrocerussite and plumbonacrite ($Pb_5O(OH)_2(CO_3)_3$) [28].

The present work concerns the study of wall paintings preserved in the Saint Stephen’s chapel located in Montani (Bolzano) in Val Venosta (Italy). They are affected by a degradation phenomenon, which is clearly visible as an extended darkening, especially on the apse and on the vault.

Preliminary cleaning tests on yellow and green areas were carried out, according to the method of white-lead reconversion, using hydrogen peroxide in a solution of acetic acid, at very low concentration, and distilled water [29]. The darkening, supposed to be due to transformation of white lead into lead dioxide (plattnerite), has been explained by Matteini *et al.* [30] as an oxidation reaction where the lead changes its oxidation number from +2 to + 4. The proposed treatment consists in the reverse process, a chemical reduction through hydrogen peroxide: the use of acetic acid at low concentration gives lead acetate and subsequently, after hydration and carbonation, basic lead carbonate. This procedure has been, in some cases, successfully applied for the reconversion of oxidized white lead pigment found in wall paintings [31, 32]. Although the conversion of the pigments is still debated, the method of reconversion to white lead has been studied in the last years also for different substrates. [33-35].

Since the darkening of the wall paintings in the Saint Stephen's chapel was initially attributed to a degradation process of lead-based pigments without a prior analytical exploration, the aim of the research conducted in this PhD project was initially to support this hypothesis and consequently verify the sustainability of the cleaning tests. First, X-ray fluorescence spectroscopy analysis was carried out *in situ* in the areas of interest with the aim to select the areas to be sampled. Then, on a limited quantity of micro-samples collected from the painting surface, it was possible to complete the study thanks to additional laboratory analyses by micro-Raman spectroscopy and powder X-ray diffraction.

5.1 Results

5.1.1 *In situ* analysis

X-ray fluorescence spectroscopy

X-ray fluorescence spectroscopy analysis was first carried out *in situ* in order to check the presence of lead in all black alterations and confirm in this way the initial hypothesis of restorers.

Lead was systematically detected in all chromatic alterations. An important example was the case of two angels on the vault, one painted in white and the other apparently painted in brown black. In the white angel, XRF analysis shown the presence of calcium (probably $CaCO_3$, *Saint Giovanni white*), whereas in the dark one lead was found (Figure 5.1).

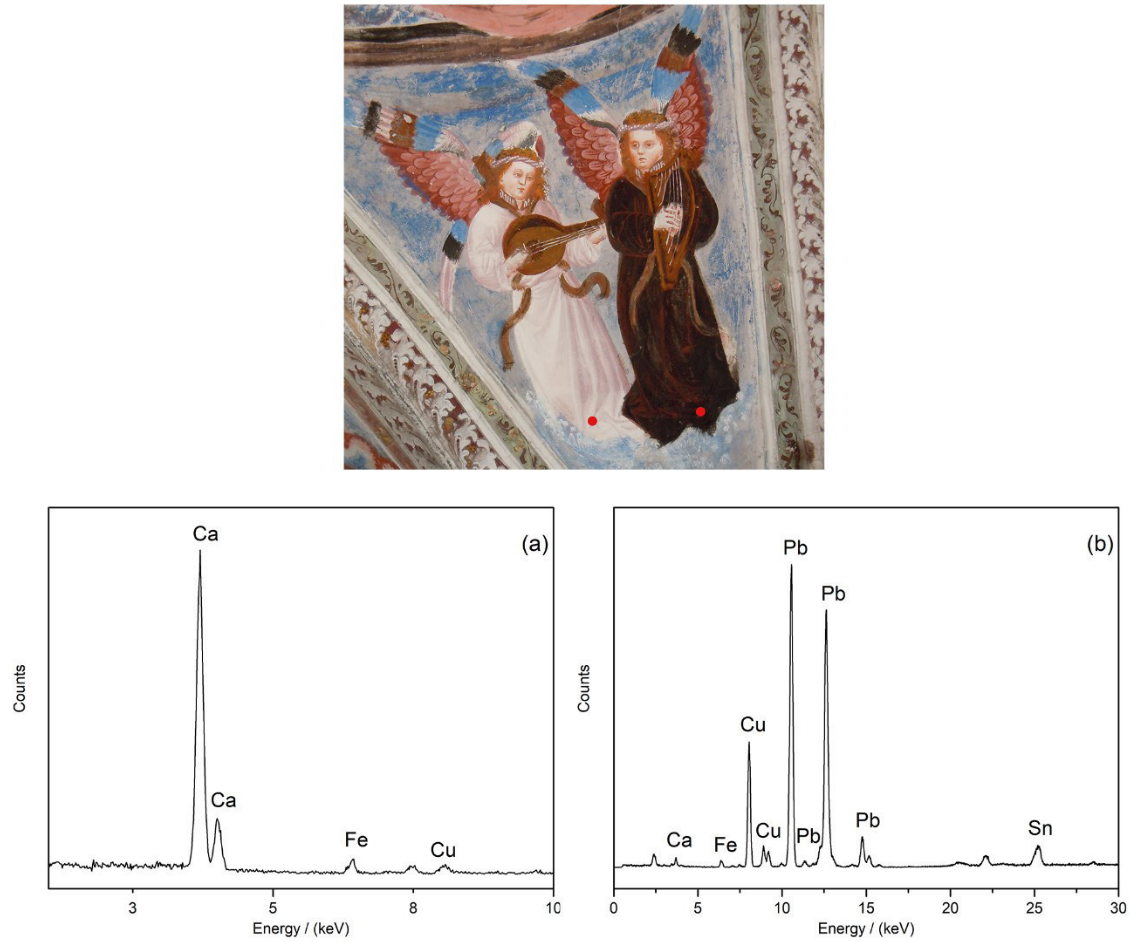

Figure 5.1: (Top) Detail of the vault and points (in red) of XRF analysis. (a) The spectrum collected in a white robe point gives evidence mainly for calcium. In the black robe, the XRF spectrum shows the presence of lead-based compounds probably mixed with copper-based pigments (b).

The same phenomenon was seen in one of the three wise men (Figure 5.2), whose slave was partially darkened. In the dark part lead was found whereas in the light part it was not detected. Some millimetre size samples were taken for further micro-Raman and XRD analysis.

Figure 5.2: Detail of the sleeve of one of the three Wise Men, where different blue colours are observed.

5.1.2 Laboratory analyses

Micro-Raman spectroscopy

Analysis of plattnerite standards

Since the hypothesis formulated by the restorers was that the blackening of paintings was caused by the presence of plattnerite (PbO_2), Raman analysis were carried out in order to confirm this assumption.

As attested by previous studies, plattnerite has a very weak Raman scattering, and it can degrade if the excitation laser power is not kept sufficiently low [36]. The problem of laser induced degradation of lead pigments is indeed a well-known phenomenon, even if some aspects have still to be better understood [37,38]. It has been repeatedly shown that if the laser power is higher than some threshold, depending on the laser wavelength and the nature of the analysed sample, degradation phenomena may be triggered during Raman analyses and secondary products, as red lead, massicot and litharge, are formed. [39-41]. Thus, we decided to perform Raman measurements first on plattnerite standards, both on mineral plattnerite and on powdered synthetic plattnerite (with excitation lines 633 and 532 nm), with the aim to choose the suitable analysis parameters and to avoid any thermal degradation on the real mural painting samples.

Previous study assigned the observed features of synthetic plattnerite at 424, 515 and 653 cm^{-1} to E_g, A_{1g}, and B_{2g} modes, respectively, by analogy with the corresponding modes of isostructural SnO_2 [36]. As the few published Raman spectra [42] of plattnerite are reported starting from 200 cm^{-1}, our Raman analysis on the standard samples were carried out to verify also the possible presence of other features at lower wavenumbers.

In mineral plattnerite (Figure 5.3a) we observed a Raman feature at 159 cm^{-1} that has never been reported belonging to plattnerite together with other bands at 380 and 515 cm^{-1} and a shoulder at 540 cm^{-1}. Raman spectra obtained in commercial plattnerite powder showed the same features together with a weak peak at 653 cm^{-1} (Figure 5.3b). Finally, the features at 159, 380 and 653 cm^{-1} were visible with the characteristic band at 515 cm^{-1} also in the spectra of synthetic plattnerite collected with the 532 nm excitation laser (Figure 5.3c). Our Raman analyses that allowed obtaining defined spectra, without inducing degradation due to the laser power, were carried out at laser powers lower than 1.0 mW on the sample, with 50x ULWD objective, using attenuation filters D1-D2 (Horiba).

Previous studies carried out on synthetic plattnerite powder attributed the presence of the peak at 380 cm^{-1} and the shoulder at about 540 cm^{-1} to residues of red lead which has a very intense Raman scattering [36]. However, our XRD analyses performed on the commercial plattnerite showed that only a crystalline phase was present in the sample (Figure 5.3). Thus, we propose to ascribe such bands to plattnerite.

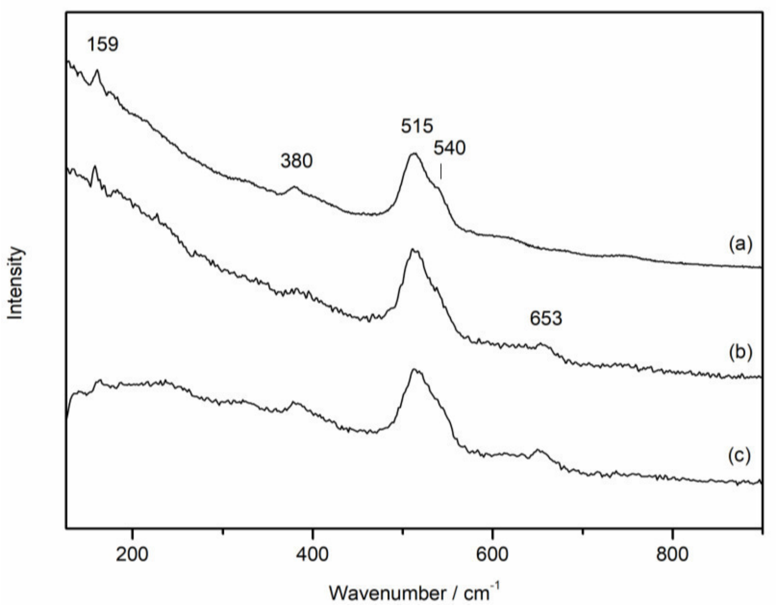

Figure 5.3: Unpolarised Raman spectrum of mineral plattnerite (a) and powdered synthetic plattnerite analysed with 633 nm (b) and 532 nm (c).

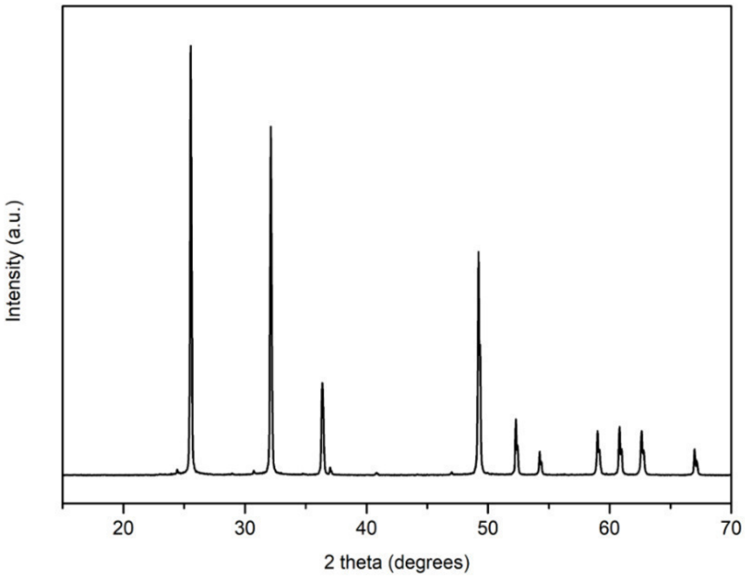

Figure 5.4: X-ray diffraction pattern of pure plattnerite in the commercial compound.

Study of pigment degradations in the wall paintings

As previously mentioned, the restorer’s hypothesis was that plattnerite was present in the mural paintings as decay product of white lead. Thus, the Raman analysis were carried out for the identification of this pigment first on fragments of wall paintings belonging to cleaned areas, green and yellow, where the reconversion method of white lead was applied.

The analysis performed on a green sample showed that the colour was provided by natural green earth celadonite ($K(Mg,Fe^{2+})(Fe^{3+},Al)[Si_4O_{10}](OH)_2$), identified by the features [43] at 178, 275, 394, 553,701 cm^{-1} (Figure 5.5a) mixed with lead-tin yellow type I and II. The bands at 78, 126, 193, 273, 289, 377, 454, 522 cm^{-1} were assigned to lead-tin yellow type I (Pb_2SnO_4) pigment (Figure 5.5d) and those at 65, 88, 136, 324, 450 cm^{-1} to lead-tin yellow type II ($PbSn_{1-x}Si_xO_3$) (Figure 5.5e) [44].

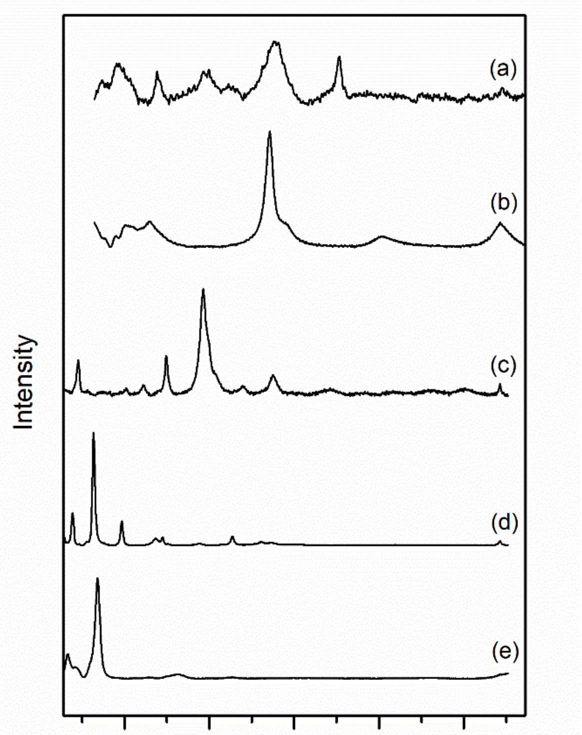

Figure 5.5: Raman spectra of pigments identified on the yellow and green fragments taken from cleaned areas: celadonite (a), lazurite (b), goethite (c), lead-tin yellow type I (d) and lead-tin yellow type II (e).

The Raman spectra taken from the surface of yellow sample suggested the use of yellow earth, mainly goethite (α-FeOOH), evidenced by the features [45] at 91, 245, 298, 384, 479, 550 cm^{-1} (Figure 5.5c). Moreover, lead tin yellow type I and II were also detected. Some blue grains were also found and the spectra (Figure 5.5b) showed the characteristics bands at 259, 542, 579, 804, 1089 cm^{-1} of lazurite ($Na_8(Al_6Si_6O_{24})S_n$), main component of lapis lazuli [46].

Although a treatment for white lead conversion was used, no spectrum of this compound was collected during Raman analysis on fragments of wall paintings taken from cleaned zones (Figure 5.6). The only lead-based pigments identified were lead tin yellow pigments type I and II. The same situation was found in the green and yellow fragments coming from blackened areas where plattnerite was identified. No evidence of the use of white lead in the past was found.

Figure 5.6: Detail of yellow area partially cleaned with the traditional method of white-lead reconversion and points (in red) of XRF analysis where lead was detected and where Raman spectroscopy only found lead tin yellow.

Raman spectra obtained analysing a powdered sample of degradation material, scraped by a scalpel from the surface of the wall paintings, showed a structured wide band centred at 515 cm^{-1} that confirmed the presence of lead dioxide PbO_2 (plattnerite mineral, tetragonal symmetry) [36].

The main Raman band in our samples has never been identified at wavenumbers higher than 515-516 cm^{-1}. Additionally, all spectra collected in brownish samples showed additional features, at 165 and 228 cm^{-1} (Figure 5.7), which did not appear neither in the Raman spectra of pure plattnerite, nor of mineral plattnerite. These features have not been reported, according to the existing references, to any known phase of the lead oxides family and they remained unassigned, although we though they belong to stannate, the side product of the decomposition of lead tin yellow pigments.

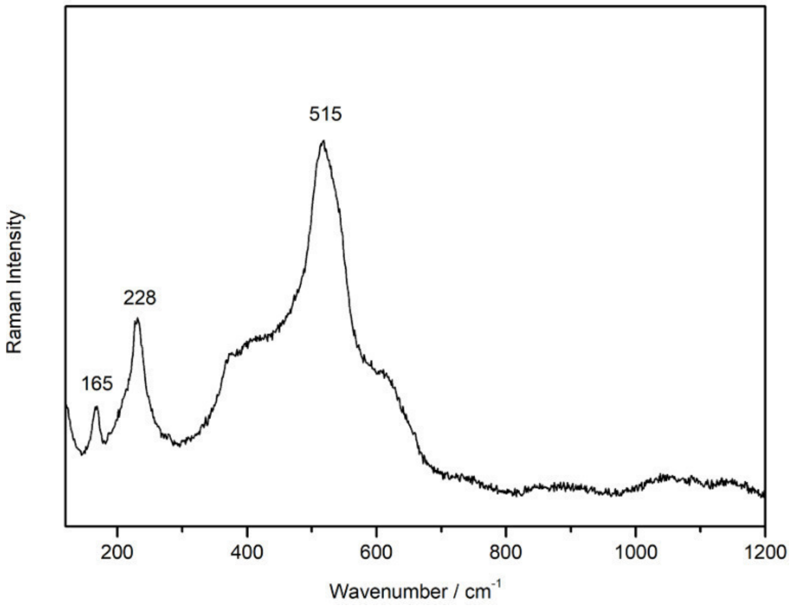

Figure 5.7: Spectrum of black alteration product presents on the wall painting.

Recently, Gutman *et al.* [47] reported the darkening of the red lead in a wall painting into black or brown plattnerite. The characteristic Raman band of plattnerite claimed at 521 cm^{-1}, was, however, too sharp and did not correspond to the plattnerite Raman spectrum as reported by Burgio *et al.* [36].

The Raman features of plattnerite identified in this work and in literature are listed in the Table 5.1. The last row of table collects our proposed Raman features of plattnerite.

Table 5.1: Main features in the Raman spectra of plattnerite found in this research and in the known literature.

Samples	Wavenumbers of the main features observed (cm^{-1})
PbO_2 mural paintings	165, 228, 515
PbO_2 crystalline	159, 380, 515
PbO_2 synthetic (632 nm)	159, 515, 540 (sh), 653
PbO_2 synthetic (532 nm)	159, 380, 515, 540 (sh), 653
PbO_2 synthetic [36]	515, 653
PbO_2 mural paintings ("altered minium") [50]	515, 545
PbO_2 from minium alteration [48]	520
PbO_2 from minium alteration [12]	518
PbO_2 from minium alteration [8]	226, 512
PbO_2 from lead white alteration [7]	515
PbO_2 from lead white alteration [9]	515
Proposed Raman bands for PbO_2	159(m), 380(s), 515(vs), 540(sh), 653(m)

The Raman spectra collected in a brownish red sample showed not only the plattnerite features but also the peaks of red lead (Pb_3O_4) at 62, 86, 121, 221, 386, 479 and 548 cm^{-1} and of massicot (β-PbO) at 70, 142 and 287 cm^{-1} (Figure 5.8a). In addition, Raman spectra collected in another reddish area of the same sample revealed the presence of haematite (Fe_2O_3) with features at 222, 242, 291, 409, 494, 608, 659 cm^{-1} (Figure 5.8b) and of vermilion (HgS) with Raman bands at 252, 283 and 342 cm^{-1} [49] (Figure 5.8c).

As the measurements were performed at very low laser power, it was possible to hypothesize that red lead and massicot were used as pigments. Although massicot has been often identified as a yellow pigment [50], it may be present as an impurity, formed during the production of red lead [51].

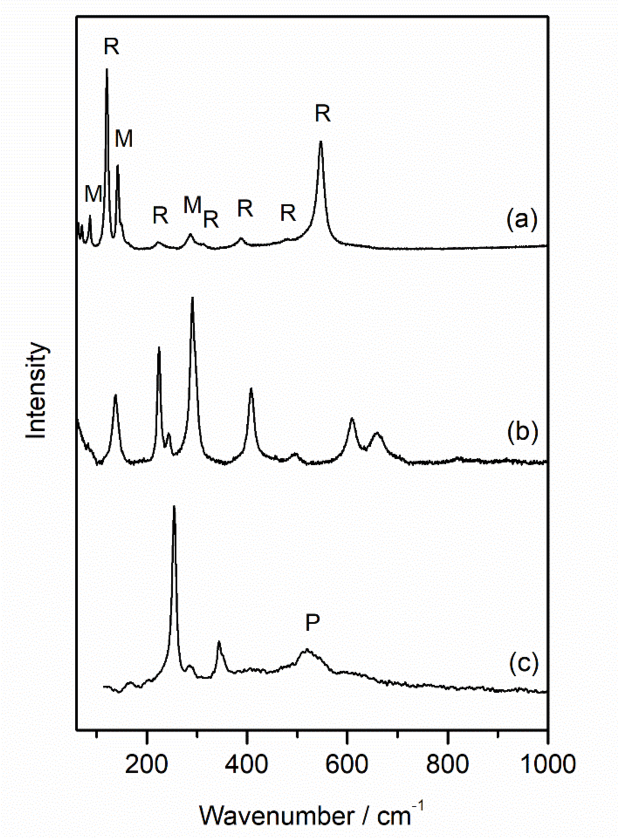

Figure 5.8: Raman spectra of pigments identified on a red blackened sample: massicot (M) and red lead (R) (a), haematite (b), vermilion with the main feature of plattnerite (P) (c).

The Raman spectrum reported in Figure 5.9, collected from another blackened reddish sample, shows low frequency features at 80, 128 cm^{-1} that can be attributed to lead tin yellow type I (Pb_2SnO_4) and haematite (main Raman bands at 222, 291, 608 cm^{-1}), whereas a well-defined band at 978 cm^{-1} can be attributed to lead sulphate ($PbSO_4$, mineral anglesite). The characteristic large band of plattnerite at 515 cm^{-1} is present as well. Red lead was identified also in this sample. This pigment was probably used in a mixture with lead tin yellow and haematite. The distribution of these pigments was shown in the Raman maps collected in the surface of the sample and reported in Figure 5.10.

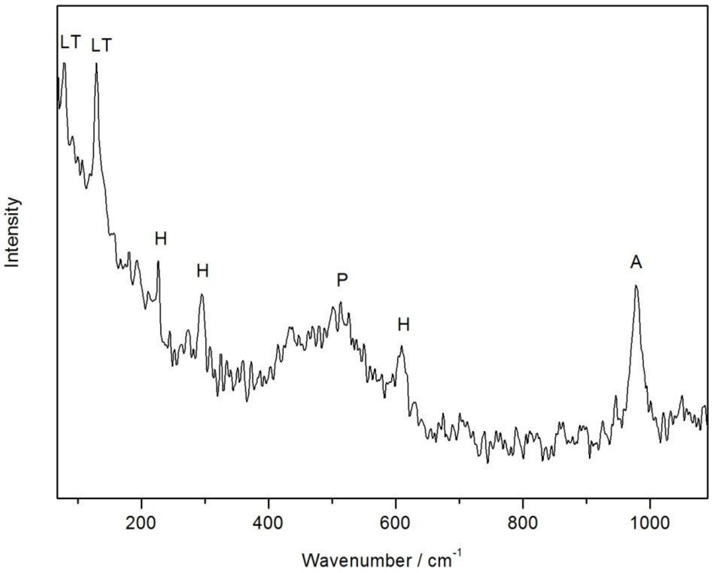

Figure 5.9: Raman spectrum collected in a blackened red sample, showing the presence of lead tin yellow type I (LT), haematite (H), plattnerite (P) and anglesite (A).

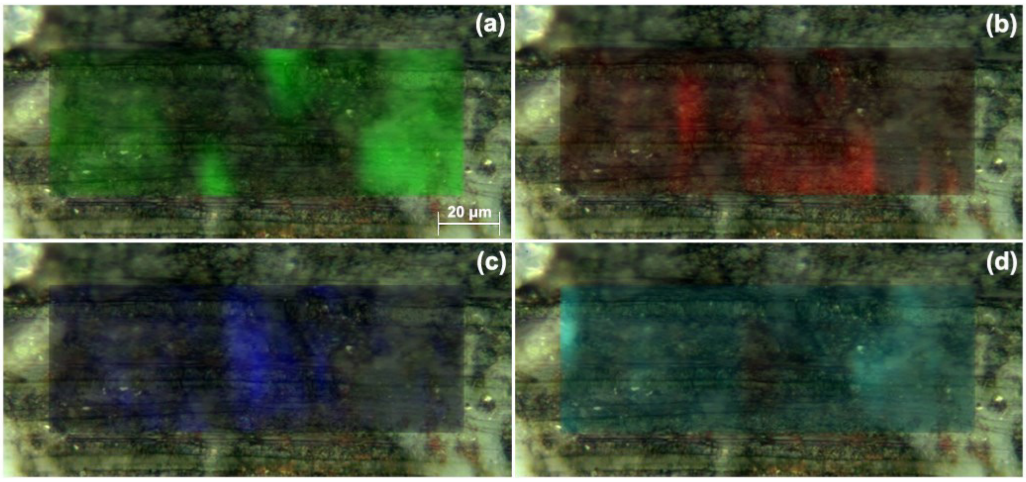

Figure 5.10: Raman imaging analysis of the blackened reddish sample shows the distribution of calcium carbonate (a), haematite (b), red lead (c) and lead tin yellow type I (d).

The presence of both plattnerite and lead sulphate confirms the results of a recent investigation about the natural ageing of red lead [11] suggesting the sulphation of lead monoxide, present as a manufacturing residue of red lead. The formation of plattnerite can results by further interaction of Pb_3O_4 with acidic environmental pollutants, such as sulphuric acid [11]. However, as other authors argued, the blackening of the lead red may have been caused by a natural aging process favoured by the presence of sunlight and moisture [52].

Raman spectra collected in a darkened blue-green sample showed the main feature of plattnerite at 515 cm^{-1} together with the aforementioned Raman bands at 165 and 228 cm^{-1}. Azurite, a basic copper carbonate ($Cu_3(CO_3)_2{\cdot}(OH)_2$) is the mineral pigment that determines the blue colour. Its Raman bands are located at 111, 137, 153, 177, 193, 236, 246, 280, 330, 400, 764, 838, 1095 cm^{-1} (Figure 5.11a).

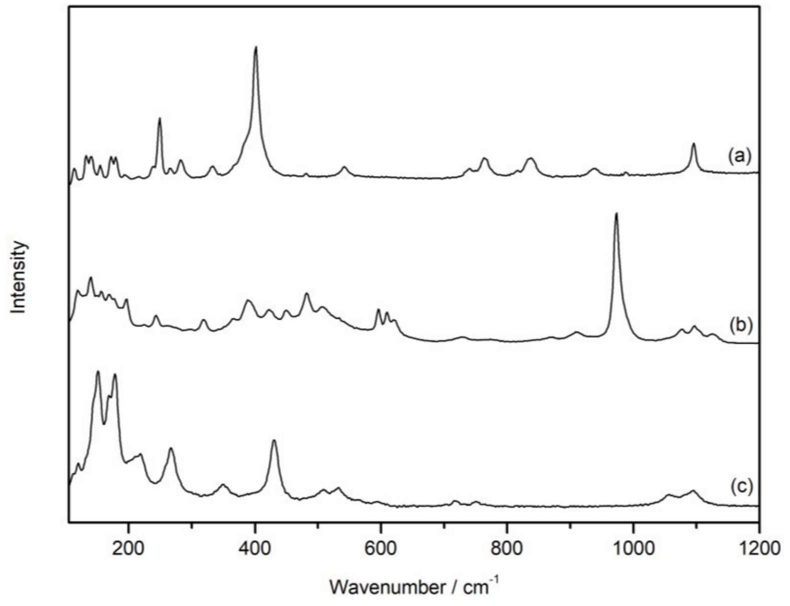

Figure 5.11: Raman spectra collected in dark/blue sample show the presence of azurite (a), brochantite (b) and malachite (c).

Moreover, in this sample the presence of three different yellow pigments was determined, such as goethite, lead tin yellow type I and II. In addition, the green copper pigment malachite ($Cu_2(CO_3)(OH)_2$) with Raman features at 120, 151, 168, 177, 218, 266, 350, 430, 508, 532, 717, 750, 1056, 1092, cm^{-1} was also identified (Figure 5.11c).

Although the degradation of azurite used in mural paintings into greenish-brown pigments is a known phenomenon [53], Raman analysis carried out in this sample shown that the colour change was caused by the degradation of a lead-based pigment used in a mixture with azurite and malachite. Among the lead-based pigments only lead tin yellow (I and II) were identified and any traces of red lead nor lead white were found, as initially hypothesized, from which the plattnerite could originate according to known literature. Thus, another decaying pathway must be established.

In the samples with azurite and plattnerite we never detected lead white although it has a very intense Raman scattering. Thus, the presence of lead white should have been detected even if present at trace levels. A similar situation was found in other samples in which plattnerite is present, such as in the samples from yellow and green areas, both blackened and subjected to cleaning tests. In all these samples lead tin yellow type I and II were the only lead-based pigments identified and, although the white lead conversion method was applied, any trace of this pigment was identified in the original nor in the treated samples.

Therefore, an involvement of the lead tin yellows, in particular of type I, in the darkening process cannot be excluded. From a thermodynamic point of view (values of the stability constants and redox potentials), lead stannate could be transformed (degrade) under the influence of SO_2 gas into anglesite ($PbSO_4$) and plattnerite. This hypothesis could justify the presence of the Raman bands at 165 and 228 cm^{-1} that have never been identified in lead pigment decay products and that could belong to a tin compound that was formed together with plattnerite.

Furthermore, the process of synthesis of lead tin yellow pigments, according to ancient recipes found in Bolognese Manuscript (recipes 272 and 273) [54], involved calcination of mixtures of compounds in various stoichiometric ratios between lead oxides, generally PbO and Pb_3O_4 and tin oxide (IV) (SnO_2). The complete formation of lead tin yellow type I occurs at 800° C while for the type II higher temperatures are necessary and also a 10% weight percentage in silica. [55] Although the stoichiometric ratios between the components during the calcination were respected, residual phases or mixtures of compounds coexisting in the final product could be formed. Therefore, even an involvement of possible intermediate residual phases, in particular of red lead, should be considered in order to understand the degradation of lead tin pigments.

Raman analysis carried out on three black-brown samples showed that blackening is not caused only by the presence of plattnerite. Indeed, the Raman analysis performed on black grains showed a further degradation process, the darkening of haematite. In addition to the bands of haematite and goethite, used in mixture, the spectra showed the characteristic band at 660 cm^{-1} of the iron oxide magnetite (Fe_3O_4) (Figure 5.12).

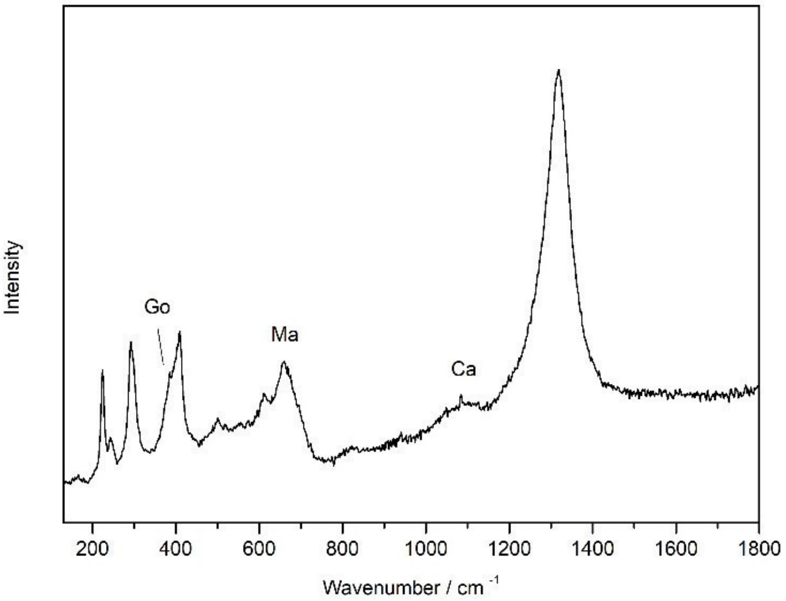

Figure 5.12: Raman spectrum collected in the black grains show the features of haematite with the main bands of goethite (Go), magnetite (Ma) and calcite (Ca).

Besides, the presence of coquimbite or paracoquimbite, iron (III) sulphate nonahydrate ($Fe_2(SO_4)_3{\cdot}9H_2O$), with the most intense Raman band at 1025 cm^{-1} was detected. The two polymorphic compounds present the main band in the same position, the only one visible in the spectrum collected in the wall paintings (Figure 5.13).

The degradation process of haematite was studied for the first time by Maguregui *et al.* [56] following the identification of magnetite and coquimbite on wall paintings in the archaeological site of Pompeii (Italy). These decay products were caused by a phenomenon of sulphation due to the presence of SO_2 gas released by the eruption of Vesuvius, but also present in the modern atmospheres around Pompeii. The study of the chemical reactions was carried out by laboratory experiments exposing haematite to SO_2 vapours [57]. At first, haematite pigment, in the presence of sulphur dioxide, is reduced to magnetite whose formation causes the blackening of the paints. On the other hand, the SO_2 is oxidized to SO_3, which is mixed with the water present as atmospheric humidity giving H_2SO_4. In the Pompeii mural paintings, the formation of coquimbite on the surface is generated by the interaction of iron (III) oxide with carbonate and sulphate anions of the plaster generated by cycles of wet deposition of acid aerosol (SO_3 or H_2SO_4) of the environment.

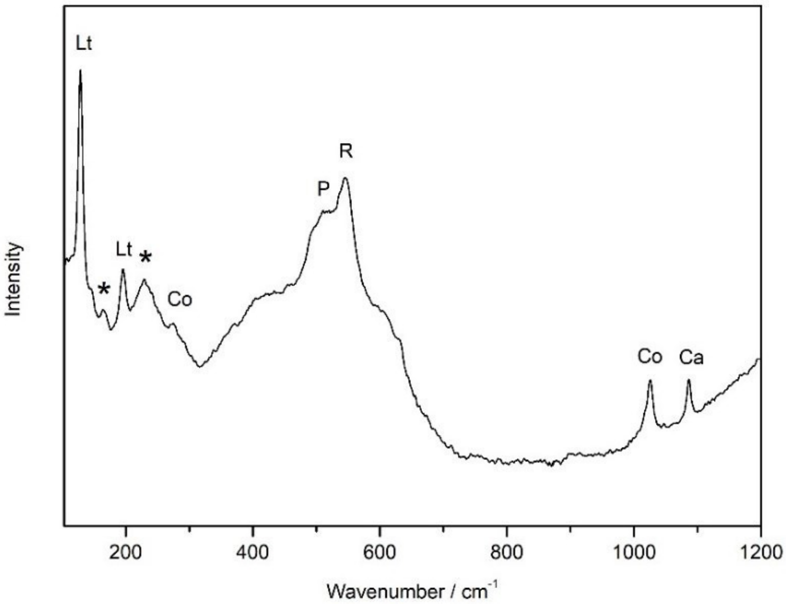

Figure 5.13: Raman spectrum collected in a red blackening sample show the features of lead tin yellow type I, plattnerite (P), red lead (R), coquimbite (Co) and calcite (Ca) and the features at 165 cm^{-1} and 228 cm^{-1} (∗).

As attested by Gómez *et al*. [58] the formation of iron sulphate in the pore stones can occur at pH values lower than 4.5, as occurs in the presence of acid pollutants. Subsequently coquimbite is produced by hydration processes.

Thus, the presence of magnetite in the chapel of Saint Stephen could indicate an impact of SO_x gases, degrading the haematite. The presence of coquimbite could also be a consequence of such degradation favoured by the presence of gypsum in the mortar and the rain water infiltration.

Another issue that would support the role of SO_x in the darkening phenomena inside the chapel could be the presence of basic copper sulphates. Together with malachite, the copper sulphate brochantite ($Cu_4(SO_4)(OH)_6$) was found in a sample. The identification was possible, thanks to literature [59], taking into account the position of minor bands that are different from other compounds with different hydration state such as posnjakite ($Cu_4(SO_4)(OH)_6 \cdot H_2O$) or langite ($Cu_4(SO_4)(OH)_6 \cdot 2H_2O$). The Raman features were located at 118, 140, 156, 169, 195, 243, 298, 319, 365, 390, 420, 448, 482, 506, 596, 608, 620, 769, 870, 909, 972, 1076, 1096, 1125 cm^{-1} (Figure 5.11b). Previous studies showed brochantite as an alteration product from the sulphation of malachite by SO_2 in wall paintings [60], but also in nature mixed with malachite [61]. However, an intentional use of brochantite as a green pigment has been also demonstrated [62].

The state of conservation of the wall paintings of the Saint Stephen's chapel is good, except for the wall exposed to the north that shows a particularly severe degradation phenomenon, being covered for about half of its height of the ground in the outer part and this favours the infiltration of water into the walls. This process and continuous rainwater infiltration may have created favourable conditions for pigment degradation.

In addition, although the area in which the chapel is located seems an uncontaminated mountain area, the contribution of anthropological factors must be considered in the study of the degradation phenomena affecting the wall paintings.

Indeed, studies on air quality in the district of Bolzano showed that the collected data in the detection station of Laces, adjacent to the town of Montani, represented an anomaly compared with other stations due to the high values of PM10. The atmospheric pollution in Val Venosta is increased by the orographic layout of the valley and by the cold currents which, due to thermal inversion phenomena, drain the air masses full in contaminants into the plains zones where then they tend to be stagnant. The use of wood heating in rural areas have contributed significantly over the years to the increase in concentrations of pollutants in this area, especially in winter.

With regards to sulphur dioxide, values above the norm were not recorded in the studies carried out over the past ten years. However, the values of SO_2 have decreased significantly in Europe thanks to new environmental policies that have promoted the use of biomass fuels, which have a lower environmental impact instead of coal fuels widely used in past decades. This means that SO_2 values in the past were much higher than present.

X-ray diffraction

X-ray powder diffraction analyses were also carried out in order to characterize the decay products of lead-based pigments on painting's surface. The following results were obtained by powdered samples taken from red and blue areas, analysed also by Raman spectroscopy. The diffraction pattern representative of a red darkened area (Figure 5.14) confirmed the presence of plattnerite at $2\theta = 25.4°$, 31.9°, 36.1°, 49°, 52.1°, 58.8°, massicot (29.1°) and red lead (26.3°, 30.8°). The most intense peak at 26.7° is likely due to quartz of the mortar, corresponding to its most intense reflection.

Figure 5.15 reports the diffraction pattern collected in a darkened blue sample. Azurite was the main component in the powder and it was identified by the features at $2\theta = 17.1°$, 17.4°, 17.7°, 23.3°, 24.2°, 25.1°, 28.6°, 30.5°, 34.5°, 35.2°, 35.6°, 39.3°, 40.4°, 41.5°, 47.7°. Malachite ($CuCO_3 \cdot Cu(OH)_2$), was identified by peaks at 14.7°, 29.4°, 31.2°. Also in this case the diffraction pattern showed the features of plattnerite (P), confirming that the darkening was caused by a lead base pigment.

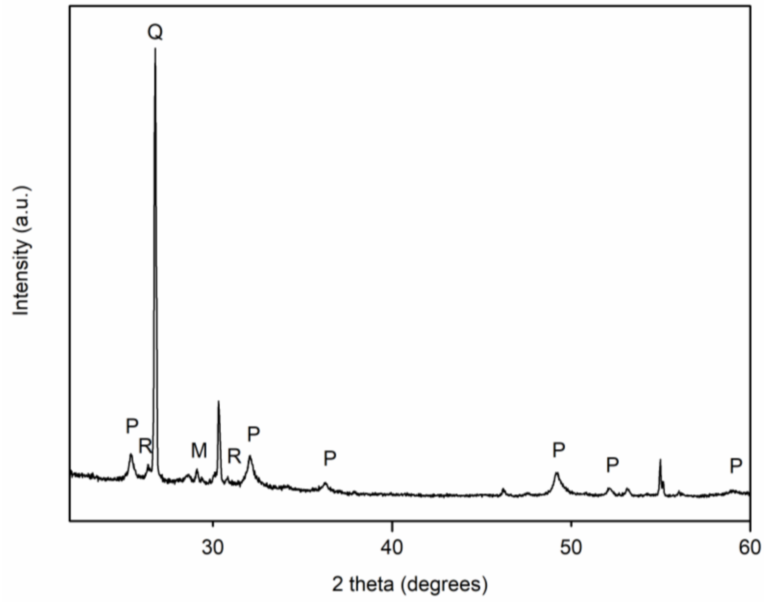

Figure 5.14: X-ray diffraction pattern of a powdered darkened red sample 7-BRP. Peaks assigned to plattnerite (P), massicot (M) and red lead (R) and quartz (Q) are indicated.

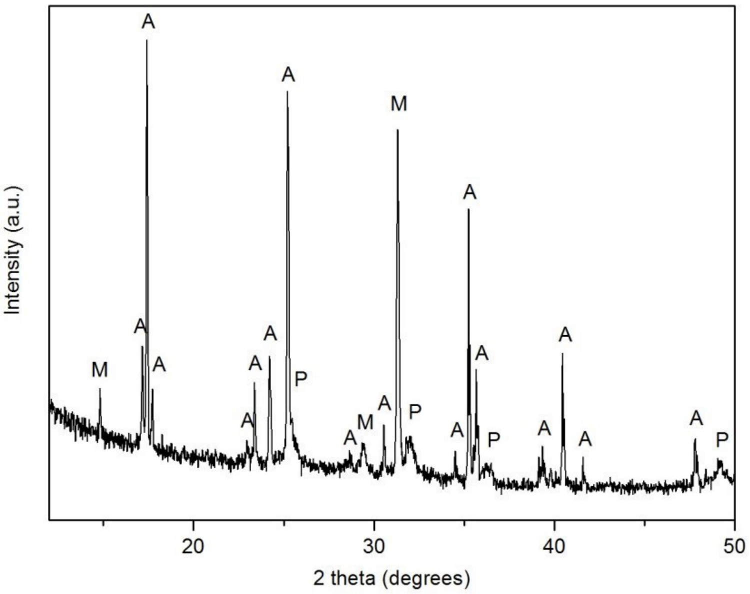

Figure 5.15: X-ray diffraction pattern of the darkened blue sample. Peaks assigned to plattnerite (P), azurite (A) and malachite (M) are indicated.

Final remarks

This research concerning the study of late - Gothic wall paintings preserved inside the Saint Stephen's chapel in Montani (Val Venosta, Bolzano, Italy) confirms the presence of lead, either in the darkened area, or in cleaned areas treated according to the method of reconversion of lead white.

Thanks to the use of laboratory techniques, especially of Raman instrumentation, it was possible to identify the nature of mortar and pigments (Table 5.2 summarizes the different compounds detected during this research) belonging to the Gothic period.

Samples of commercial pure plattnerite and in mineral form were analysed and all the Raman features at 159 (m), 380 (s), 515(vs), 540 (sh) and 653 (m) cm^{-1} were reported for the first time belonging to the β form of lead dioxide.

Raman spectra obtained at low laser excitation power (≈ 1.0 mW) and powder XRD evidenced the presence of plattnerite (PbO_2) on all blackened samples and, in minor amount, of anglesite as alteration products of lead-based pigments. The aging process occurs in the presence of a basic substrate, humidity and sunlight (dry and wet cycles) and was favoured by the presence of acidic pollutants (SO_x) in the atmosphere, which stagnate in the area where the chapel is located, due to the particular orographic characteristic of the valley.

Red lead was clearly identified on the samples belonging to red painted areas originally. Actually, we have no evidence that the darkening of wall paintings could be attributed to the use of white lead because its Raman spectrum has never been collected on the samples.

A cleaning test using the method of reconversion of white lead was applied in a very limited area of the paints, unfortunately before verifying the composition of the black patina to prove the actual presence of lead white. The Raman spectra collected on the cleaned areas gave no evidence of plattnerite, confirming apparently the effectiveness of the conversion treatment but no traces of lead white were identified. However, it was decided not to proceed with the cleaning of larger areas because the method was considered too aggressive and the treated areas showed a pulverization of the pigments. This work represents another example of the importance of the use of non-destructive diagnostic techniques with the aim to identify the secondary products and to give indications to restorers and conservators on the suitable method to be used.

All the Raman spectra collected in brownish samples taken from the mural paintings showed unassigned features at 165 and 228 cm^{-1} that cannot be attributed to known lead oxide phases. The constant presence of lead tin yellow pigments on all the analysed blackened samples suggested that these bands, always visible together with the main plattnerite band, could prove the presence of tin and lead based compounds as secondary products not yet mentioned in the literature. To verify this new decaying process, laboratory tests in which lead tin pigments are subjected to aging with SO_2 vapours, in the presence of moisture, should be conducted in order to verify the blackening of the pigments, the possible formation of plattnerite, and the formation of side tin and/or lead based compounds.

The spectroscopic results obtained after applying all these techniques allowed us to identify another degradation process other than the initially expected one. Indeed, the blackening process of haematite was also demonstrated by using Raman spectroscopy, and the presence of magnetite caused, together with the plattnerite, the chromatic change of the painted surfaces. Among the sulphate compounds identified in the samples, coquimbite was also identified as a haematite decay product, which confirmed that a strong sulphation process has been produced.

Table 5.2: Compounds identified in wall paintings with Raman spectroscopy.

Assigned species	Chemical formula	Wavenumbers of the main features observed (cm^{-1})	Sample
Haematite	α-Fe_2O_3	222 (s), 242 (w), 291 (s), 409 (m), 494 (w), 608 (w), 659 (w)	5-BPR, 6-BPR
Goethite	α-FeOOH	91 (m), 245 (w), 298 (m), 384 (s), 479 (w), 550 (w)	1-CYF, 4-BYF, 6-BPR, 7-BBP
Celadonite	$K(Mg,Fe^{2+})(Fe^{3+},Al)[Si_4O_{10}](OH)_2$	178 (w), 275 (w), 394 (w), 553 (m), 701 (w)	1-CGF, 2-BGF
Lazurite	$Na_8(Al_6Si_6O_{24})S_n$	259 (w), 542 (s), 579 (sh), 804 (w), 1089 (w)	1-CGF
Azurite	$Cu_3(CO_3)_2 \cdot (OH)_2$	82 (m), 111 (vw), 137 (m), 153 (m), 177 (w), 193 (vw), 236 (w), 246 (w), 280 (vw), 330 (w), 400 (vs), 764 (w), 838 (w), 1095 (m)	7-BBP
Malachite	$Cu_2(CO_3)(OH)_2$	120 (m), 151 (vs), 168 (s), 177 (vs), 218, 266 (s), 350 (m), 430 (s), 508 (m), 532 (m), 717 (w), 750 (w), 1056 (m), 1092 (m), 1365 (w), 1490 (m)	7-BBP
Brochantite	$Cu_4(SO_4)(OH)_6$	118 (w), 140 (m), 156 (w), 169 (w), 195 (m), 243 (m), 298 (vw), 319 (m), 365 (vw), 390 (m), 420 (w), 448 (w), 482 (m), 506 (w), 596 (m), 608 (m), 620 (w), 769 (vw), 870 (vw), 909 (w), 972 (vs), 1076 (w), 1096 (m), 1125 (w)	7-BBP
Vermilion	HgS	252 (vs), 283 (w), 342 (m)	6-BRP
Lead tin yellow type I	Pb_2SnO_4	78 (m), 126 (vs), 193 (m), 273 (w), 289 (w), 377 (vw), 454 (w), 522 (vw)	1-CYF, 2-BGF, 3-CGF, 4- BYF, 5-BRP, 6-BRP, 7-BBP
Lead tin yellow type II	$PbSn_{1-x}Si_xO_3$	65 (m), 88 (sh), 136 (vs), 324 (w), 450 (vw)	1-CYF, 2-BGF, 3-CGF, 4- BYF, 5-

			BRP, 6-BRP, 7-BBP
Red lead	Pb_3O_4	52 (w), 62 (w), 85 (vw), 120 (vs), 222 (vw), 390 (w), 478 (w), 549 (s)	5-BRP, 6-BRP
Massicot	β-PbO	70 (w), 86 (m),142 (vs), 287 (m), 388 (w)	5-BRP
Plattnerite	$\beta\text{-}PbO_2$	515 (m) 540 (w)	2-BGF, 4-BYF, 5-BRP, 6-BRP, 7-BBP
Anglesite	$PbSO_4$	978 (s)	6-BRP
Magnetite	Fe_3O_4	660 (m)	5-BPR, 6-BPR
Coquimbite	$Fe_2(SO_4)_3 \cdot 9H_2O$	280(w), 1025 (m)	6-BPR

References

[1] K. Castro, A. Sarmiento, I. Martínez-Arkarazo, J. M. Madariaga, L. A. Fernández (2008) Green Copper Pigments Biodegradation in Cultural Heritage: From Malachite to Moolooite, Thermodynamic Modeling, X-ray Fluorescence, and Raman Evidence, Analytical Chemistry, 80, 4103-4110.

[2] K. Keune, J. J. Boon (2005) Analytical Imaging Studies Clarifying the Process of the Darkening of Vermilion in Paintings, *Analytical Chemistry*, 77, 4742-4750.

[3] M. Maguregui, U. Knuutinen, I. Martínez-Arkarazo, K. Castro, J. M. Madariaga (2011) Thermodynamic and Spectroscopic Speciation to Explain the Blackening Process of Hematite Formed by Atmospheric SO2 Impact: The Case of Marcus Lucretius House (Pompeii), *Analytical Chemistry*, 83, 3319-3326.

[4] E. Mattei, G. de Vivo, A. De Santis, C. Gaetani, C. Pelosi, U. Santamaria (2008) Raman spectroscopic analysis of azurite blackening, *Journal of Raman Spectrosc*opy, 39, 302-306.

[5] V. S. F. Muralha, C. Miguel, M. João Melo (2012) Micro-Raman study of Medieval Cistercian 12–13th century manuscripts: Santa Maria de Alcobaça, Portugal, *Journal of Raman Spectrosc*opy, 43, 1737-1746.

[6] D. Hradil, J. Hradilová, E. Koč, S. Švarcová, P. Bezdička, J. Mař Íková-Kubková (2013) Unique Pre-Romanesque murals in Kostoľany pod Tríbečom, Slovakia: the painting technique and causes of damage, *Archaeometry*, 55, 691-706.

[7] M. Vagnini, R. Vivani, E. Viscuso, M. Favazza, B.G. Brunetti, A. Sgamellotti, C. Miliani (2018) Investigation on the process of lead white blackening by Raman spectroscopy, XRD and other methods: Study of Cimabue's paintings in Assisi, *Vibrational Spectroscopy*, 98, 41-49.

[8] S. Daniilia, S. Sotiropoulou, D. Bikiaris, C. Salpistis, G. Karagiannis, Y. Chryssoulakis, B. A. Priced, J. H. Carlsone (2000) Panselinos' Byzantine wall paintings in the Protaton Church, Mount Athos, Greece: a technical examination, *Journal of Cultural Heritage,* 1, 91–110.

[9] L. de Ferri, F. Mazzini, D, Vallotto, G. Pojana (2017) In situ non-invasive characterization of pigments and alteration products on the masonry altar of S. Maria ad Undas (Idro, Italy), *Archaeological and Anthropological Sciences,* 1-17.

[10] C. Cennini, *Il libro dell'arte*, F. Frezzato, Neri Pozza Editore, 2009.

[11] S. Giovannoni, M. Matteini, A. Moles (1990) Studies and developments concerning the problem of altered lead pigments in wall painting, *Studies in Conservation*, 35, 21-25.

[12] S. Aze, J. M. Vallet, M. Pomey, A. Baronnet, O. Grauby (2007) Red lead darkening in wall paintings: natural ageing of experimental wall paintings versus artificial ageing tests, *European Journal of Mineralogy*, 19, 883-890.

[13] G. D. Smith, A. Derbyshire, R.J. H. Clark (2002) In Situ Spectroscopic Detection of Lead Sulphide on a Blackened Manuscript Illumination by Raman Microscopy, *Studies in Conservation*, 47, 250-256.

[14] C. L. Hoevel (1985) A Study of the Discoloration Products Found in White Lead Paint Films, *The American Institute for Conservation: Book and Paper Group Annual*, Vol. 4.

[15] G. D. Smith, R. J.H. Clark (2002) The role of H_2S in pigment blackening, *Journal of Cultural Heritage,* 3, 101-105.

[16] H. G. M. Edwards, D. W. Farwell, E. M. Newton, F. Rull (1999) *Minium;* FT-Raman non-destructive analysis applied to an historical controversy*, Analyst*, 124, 1323-1326.

[17] S. Bruni, F. Cariati, F. Casadio, V. Guglielmi (2001) Micro-Raman identification of the palette of a precious XVI century illuminated Persian codex, *Journal of Cultural Heritage*, 4, 291-296.

[18] C. Pelosi, G. Agresti, M. Andaloro, P. Baraldi, P. Pogliani, U. Santamaria (2013) The rock hewn wall paintings in Cappadocia (Turkey). characterization of the constituent materials and a chronological overview, *E-Preservation Science*, 10, 99-108.

[19] P. Holakooei, A.H. Karimy (2015) Early Islamic pigments used at the Masjid-i Jame of Fahraj, Iran: a possible use of black plattnerite*, Journal of Archaeological Science,* 54, 217-227.

[20] M. Matteini, A. Moles (1979) A preliminary investigation of the unusual technique of Leonardo’s mural ‘The last supper’, *Studies in Conservation*, 24, 125-133.

[21] N. N. Brandt, N. L. Rebrikova, A. Yu. Chikishev (2009) Raman spectroscopy of the components of 18th-century icon painting, *Moscow University Physics Bulletin,* 64, 600-*604.*

[22] J.P. Petushkova, N. Lyalinova (1986) Microbiological degradation of lead-containing pigments in mural paintings, *Studies in Conservation*, 31, 65-69.

[23] F. Qingping, Z. Xiaojun, M. Xiaojun (1999) Effects of microbes on color changes of red lead in murals, *The Journal of General and Applied Microbiology*, 45, 85-88.

[24] E. Kotulanová, P. Bezdička, D. Hradil, J. Hradilová, S. Švarcová, T. Grygar (2009) Degradation of lead-based pigments by salt solutions, *Journal of Cultural Heritage*, 10, 367-378.

[25] S. Sotiropoulou, S. Daniilia, C. Miliani, F. Rosi, L. Cartechini, D. Papanikola-Bakirtzis (2008) Microanalytical investigation of degradation issues in Byzantine wall paintings, *Applied Physics A*, 92, 143-150

[26] A. Domínguez-Vidal, M. J. de la Torre-López, R. Rubio-Domenec, M. J. Ayora-Cañada (2012) In situ noninvasive Raman microspectroscopic investigation of polychrome plasterworks in the Alhambra, *Analyst,* 137, 5763-5769.

[27] M. San Andrés, J.M. De la Roja, S.D. Dornheim, V.G. Baonza, 2008, Litharge and massicot: thermal decomposition synthetic route for basic lead(II) carbonate and Raman microscopy analysis, In Castillejo et al. (eds) *Lasers in the Conservation of Artworks* Proceedings of the International Conference Lacona VII, Madrid, Spain, 17-21 september 2007.

[28] S. Aze, J.M. Vallet, V. Detalle, O. Grauby, A. Baronnet (2008) Chromatic alterations of red lead pigments in artworks: a review, *Phase Transitions,* 81, 145-154.

[29] M. Matteini, A. Moles, S. Giovannoni, Scientific Methodologies Applied to Works of Art, Florence 2-5 May, 1984, 113.

[30] M. Matteini, Ossidazione della biacca in pitture murali- Metodi proposti per la riconversione del pigmento ossidato nelle pitture di A. Baldovinetti della chiesa di S. Miniato (Firenze), In Atti del Convegno sul Restauro delle Opere d'Arte, Florence, 2-6 November, 1976, 257.

[31] M. Matteini, A. Moles, The reconversion of oxidized white lead in mural paintings: a control after a five-year period, ICOM Committee for Conservation, 6th Triennial Meeting, Ottawa, 1981 81/15/1.

[32] M. Koller, H. Leitner, H. Paschinger (1990) Reconversion of altered lead pigments in alpine mural paintings, *Studies in Conservation*, 35, 15-20.

[33] M. R. McFarland (1997) The whitening effects of peroxide gels on darkened lead white paint, *The book and Paper Group Annual*, Vol. 16.

[34] S. M. Lussier (2006) An Examination of Lead White Discoloration and the Impact of Treatment on Paper Artifacts: A Summary of Experimental Testing, *The Book and Paper Group Annual,* Vol. 25, 9-12.

[35] S. M. Lussier and G. D. Smith (2007) A review of the phenomenon of lead white darkening and its conversion treatment, *Studies in Conservation*, 8, 41-53.

[36] L. Burgio, R. J. H. Clark, S. Firth (2001) Raman spectroscopy as a means for the identification of plattnerite (PbO_2), of lead pigments and of their degradation products, *Analyst*, 126, 222-227.

[37] P. Pouli, D. C. Emmony, C. E. Madden, I. Sutherland (2003) Studies towards a thorough understanding of the laser-induced discoloration mechanisms of medieval pigments, *Journal of Cultural Heritage,* 4, 271-275.

[38] R. Bordalo, P. J. Morais, H. Gouveia, C. Young (2006) Laser Cleaning of Easle Paintings: an overview, *Laser Chemis*try, Article ID 90279, 9 pages http://dx.doi.org/10.1155/2006/90279.

[39] C. Andalò, M. Bicchieri, P. Bocchini, G. Casu, G.C. Galletti, P. A. Mandò, M. Nardone, A. Sodo, M. Plossi Zappalà (2001) The beautiful "Trionfo d'Amore" attributed to Botticelli: a chemical characterisation by proton-induced X-ray emission and micro-Raman spectroscopy *Analytica Chimica Acta*, 429, 279-286.

[40] G. D. Smith, L. Burgio, S. Firth, R. J. H. Clark (2001) Laser-induced degradation of lead pigments with reference to Botticelli's Trionfo d'Amore, *Analytica Chimica Acta*, 440, 185-188.

[41] A. De Santis, E. Mattei, C. Pelosi (2007) Micro-Raman and stratigraphic studies of the paintings on the 'Cembalo' model musical instrument (A.D. 1650) and laser-induced degradation of the detected pigments, *Journal of Raman Spectrosc*opy, 38, 1368-1378.

[42] S. Daniilia, E. Minopoulou, Fr. D. Demosthenous, G. Karagiannis (2008) A comparative study of wall paintings at the Cypriot monastery of Christ Antiphonitis: one artist or two? *Journal of Archeological Science*, 35, 1695 1707.

[43] F. Ospitali, D. Bersani, G. Di Lonardo, P. P. Lottici (2008) 'Green earths': vibrational and elemental characterization of glauconites, celadonites and historical pigments *Journal of Raman Spectrosc*opy*,* 39, 1066-1073.

[44] J. Bagdzevičienė, G. Niaura, E. Garškaitė, J. Senvaitienė, J. Lukšėnienė, S. Tautkus (2011) Spectroscopic analysis of lead tin yellow pigment in medieval necklace beads from Kernavė-Kriveikiškės cemetery in Lithuania, *Chemija,* 22*,* 216-222.

[45] D.L.A. de Faria, F.N. Lopes (2007) Heated goethite and natural hematite: Can Raman spectroscopy be used to differentiate them?, *Vibrational Spectroscopy*, 45, 117-121.

[46] M. Bicchieri, M. Nardone, P.A. Russo, A. Sodo, M. Corsi, G. Cristoforetti, V. Palleschi, A. Salvetti, E. Tognoni (2001) Characterization of azurite and lazurite based pigments by laser induced breakdown spectroscopy and micro-Raman spectroscopy, *Spectrochimica Acta B*, 56, 915-922.

[47] M. Gutman, M. Lesar-Kikelj, A. Mladenovič, V. Čobal-Sedmak, A. Križnarb, S. Kramard (2014) Raman microspectroscopic analysis of pigments of the Gothic wall painting from the Dominican Monastery in Ptuj (Slovenia), *Journal of Raman Spectrosc*opy, 45, 1103-1109.

[48] M. Aceto, G. Gatti, A. Agostino, G. Fenoglio, V. Giordano, M. Varetto, G. Castagner (2012) The mural paintings of Ala di Stura (Piedmont, Italy): a hidden treasure investigated, *Journal of Raman Spectrosc*opy, 43, 1754-1760.

[49] H. G. M. Edwards, D. W. Farwell, S. Rozenberg (1999) Raman spectroscopic study of red pigment and fresco fragments from King Herod's Palace at Jericho, *Journal of Raman Spectrosc*opy, 30, 361-366.

[50] I. Aliatis, D. Bersani, E. Campani, A. Casoli, P. P. Lottici, S. Mantovana, I.G. Marino (2010) Pigments used in Roman wall paintings in the Vesuvian area, *Journal of Raman Spectrosc*opy*,* 41, 1537-1542.

[51] P. Vandenabeele, B. Wehling, L. Moens, B. Dekeyzer, B. Cardon, A. von Bohlen, R. Klockenhämper (1999) Pigment investigation of a late-medieval manuscript with total reflection X-ray fluorescence and micro-Raman spectroscopy, *Analyst,* 124, 169-172.

[52] S. Daniilia, E. Minopoulou (2009) A study of smalt and red lead discolouration in Antiphonitis wall paintings in Cyprus, *Applied Physics A, 96*, 701-711.

[53] A. Lluveras, S. Boularand, A. Andreotti,·M. Vendrell-Saz (2010) Degradation of azurite in mural paintings: distribution of copper carbonate, chlorides and oxalates by SRFTIR, *Applied Physics A*, 99, 363-375.

[54] M. P. Merrifield, Original Treatises on the Arts of Painting, II, London 1849.

[55] C. Pelosi, G. Agresti, U. Santamaria, E. Mattei (2010) Artificial yellow pigments: production and characterization through spectroscopic methods of analysis, *E-Preservation Science*, 7, 108-115.

[56] M. Maguregui, U. Knuutinen, K. Castro, J. M. Madariaga (2010) Raman spectroscopy as a tool to diagnose the impact and conservation state of Pompeian second and fourth style wall paintings exposed to diverse environments (House of Marcus Lucretius), *Journal of Raman Spectrosc*opy, 41, 1400-1409.

[57] M. Maguregui, K. Castro, H. Morillas, J. Trebolazabala, U. Knuutinen, R. Wiesinger, M. Schreinerd, J.M. Madariaga (2014) Multianalytical approach to explain the darkening process of hematite pigment in paintings from ancient Pompeii after accelerated weathering experiments, *Analytical Methods*, 6, 372-378.

[58] O. Gómez-Laserna, I. Arrizabalaga, N. Prieto-Taboada, M A. Olazabal, G. Arana, J. M. Madariaga (2015) In situ DRIFT, Raman, and XRF implementation in a multianalytical methodology to diagnose the impact suffered by built heritage in urban atmospheres, *Analytical and Bioanalytical Chemistry*, 407, 5635-5647.

[59] V. Hayez, J. Guillaume, A. Hubin, H. Terryn (2004) Micro-Raman spectroscopy for the study of corrosion products on copper alloys: setting up of a reference database and studying works of art, *Journal of Raman Spectrosc*opy, 35, 732-738.

[60] R. Mazzeo, P. Baraldi, R. Lujan C. Fagnano (2004) Characterization of mural painting pigments from the Thubchen Lakhang temple in Lo Manthang, Nepal, *Journal of Raman Spectrosc*opy, 35, 678-685.

[61] D. Bersani, P. P. Lottici, G. Antonioli, E. Campani, A. Casoli, C. Violante (2004) Pigments and binders in the wall paintings of Santa Maria della Steccata in Parma (Italy): the ultimate technique of Parmigianino, *Journal of Raman Spectrosc*opy, 35, 694-703.

[62] S. Valadas, R. V. Freire, A. Cardoso, J. Mirão, C. B. Dias, P. Vandenabeele, A. Candeias (2015) On the Use of the Unusual Green Pigment Brochantite ($Cu_4(SO_4)(OH)_6$) in the 16th-Century Portuguese-Flemish Paintings Attributed to The Master Frei Carlos Workshop, *Microscopy and Microanalysis,* 21, 518-525.

CHAPTER 6

In situ and laboratory analyses for the understanding of a controversial restoration work

As discussed in detailed in the chapter 1, the wall paintings belong to a category of artworks particularly at risk since they are generally preserved *in situ*, and therefore, their conservation depends both on the characteristic of original materials used and on the environmental conditions [1, 2]. Thus, it can be very complex to determine their state of conservation, because the causes of damage are multiple.

First of all, they are exposed to natural decay factors such as variation of humidity and temperature [3], biological attacks [4, 5] or atmospheric pollutants in the air [6]. Furthermore, the chromatic change of the pigments caused by the natural aging and/or anthropogenic agents actions are widely known phenomena [7-9]. In addition, some studies have highlighted the inadequacy of obsolete conservation products used in the past, which were incompatible and even harmful for the conservation of the works of art [10], thus, new non-reactive and removable treatments have been proposed [11, 12].

Moreover, in the past years some restoration works have been carried out without a careful diagnose study. In fact, the restorers have been focusing for a long time on visual observation and on their experience. Unfortunately, this approach has caused incorrect diagnoses and, accordingly, the application of unsuitable conservation procedures to the artworks [13]. This is the reason why due to the complexity in the conservation of wall paintings, integrated analytical approaches have become an essential step for the identification of the degradation's causes and, especially, for the election of the conservation treatments required [14].

This chapter presents the results of a multianalytical methodology for the study of wall paintings, based on the use of Raman and X-ray fluorescence spectroscopy *in situ,* SEM-EDS microscopy and Raman spectroscopy laboratory measurements. The paintings belong to the late Gothic period and they are preserved in the Saint Stephen's church in Ribera de Valderejo (Álava, Basque Country). This research was focused on characterizing the plaster composition, the colour palette used by the artists and the materials employed during the recent restoration works.

6.1 *In situ* analyses

Portable Raman and X-ray fluorescence spectroscopy were selected to perform the *in situ* study of the chromatic palette and to identify the original and new pigments employed in the past restoration works. As summarise in the section 3.1.1, since the paintings located in the apse wall are characterized by a grey colour, the analyses were conducted mainly in those areas, in order to verify any degradation process (see Figure 6.1).

The Raman analysis carried out in deteriorated areas, in which the paint layer is lost, showed that the original preparation mortar (arriccio, used to make the wall flat) is composed of a mixture of calcite and siliceous material. The acquired spectra showed the features of calcium carbonate ($CaCO_3$, Raman bands: 1086, 712, 282 and 156 cm^{-1}) (Figure 6.2a) and quartz (SiO_2, Raman bands: 206, 262, 356, 465 cm^{-1}) (Figure 6.2b). Unlike other studied churches in the Basque territory, gypsum was not found in this mortar [15, 16].

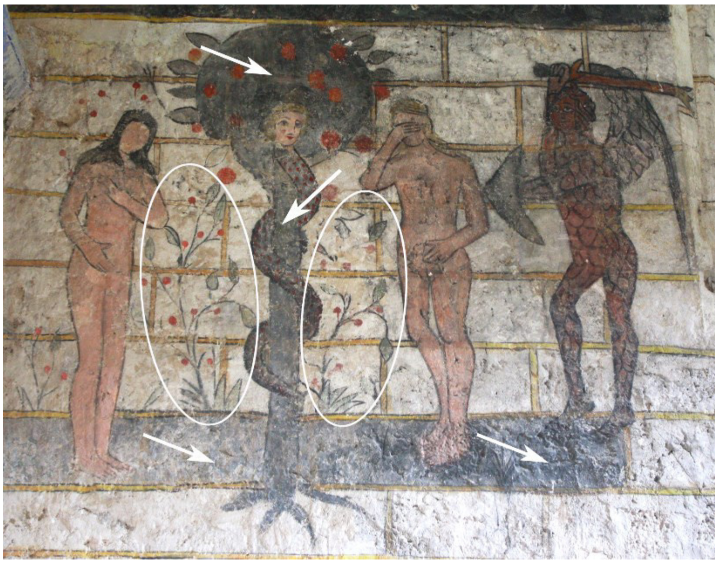

Figure 6.1: Representation of *Original Sin* in the apse area in which are visible grey areas (pointed by arrows) and green areas (pointed by circles).

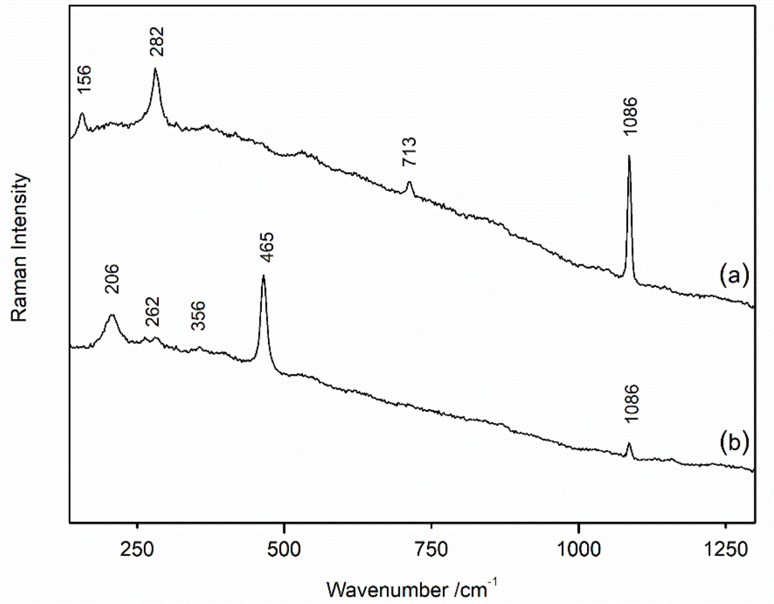

Figure 6.2: Raman spectra acquired in the preparation mortar give evidence of calcite (a) and quartz with the contribution of calcite (b).

Raman analyses were also carried out in order to identify the composition of the white layer of plaster that still covers the majority of the nave and the west wall. This layer was applied to cover the deteriorated paintings in the past. It is composed of two different sub-layers. The Raman spectra acquired in the exterior part showed the well-defined peaks of gypsum ($CaSO_4 \cdot 2H_2O$, 1008 and 415 cm^{-1}). The part underneath has a heterogeneous granulometry and a reddish colour. The Raman analyses showed, in addition to gypsum, the features of quartz and of iron oxide hematite (α-Fe_2O_3, Raman bands: 224, 245, 292, 410, 495, 612 cm^{-1}).

The analysis conducted *in situ* allowed the identification of the pigments used in the wall paintings. A first screening was done by X-ray fluorescence to determine the elemental composition.

In the red areas, which appear particularly bright, arsenic and mercury were detected by ED-XRF. In most red areas, vermilion (HgS, Raman bands: 342, 281, 252, 110 cm^{-1}) was identified using Raman spectroscopy. In other points, the Raman analysis showed that the red colour was produced by a mixture of a yellow pigment and a red one, orpiment (As_2S_3, Raman bands: 200, 290, 308, 352, 380 cm^{-1}) and vermilion, respectively (Figure 6.3a).

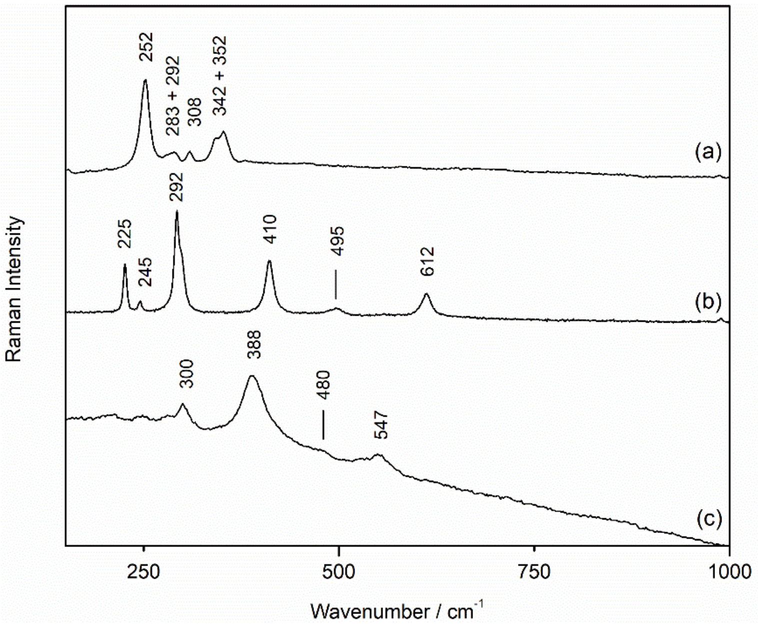

Figure 6.3: Raman spectra of original pigments identified in yellow and red areas: vermilion plus orpiment (a), hematite (b) and goethite (c).

The ED-XRF analysis performed in the orange areas of the apostles' robes in the *Apostolate* representation, showed evidence of iron and mercury. In this case, the shade is given by vermilion used together with the red iron oxide hematite (α-Fe_2O_3 Raman bands: 225, 245, 292, 410, 495, 612 cm^{-1}) (Figure 6.3b). In addition to orpiment, in the yellow areas, where iron was present, the yellow iron oxide goethite (α-FeO(OH), Raman bands: 300, 388, 480, 547 cm^{-1}) was identified (Figure 6.3c). From a comparison with other studies in mural paintings of the Gothic period, we can affirm that the pigments identified in the Saint Stephen's church are fairly compatible with this period [17].

Thanks to the portable devices used *in situ*, it was possible to identify the modern pigments used during the restoration works in recent times. In most of the analysed points, although they present different colours, ED-XRF analyses did not always show the key elements of the respective colorants. In fact, only calcium, zinc, barium and iron were detected.

The Raman analysis conducted in the yellow areas revealed the use of the arylamide yellow ($C_{17}N_3O_3H_8$, Raman bands: 460, 510, 786, 953, 1136, 1215, 1246, 1307, 1387, 1482, 1521, 1595, 1620, 1670 cm^{-1}) (Figure 6.4a) while in the blue areas the use of ultramarine blue ($Na_{6-10}Al_6Si_6O_{24}S_n$, Raman bands: 365, 546, 580 cm^{-1}) (Figure 6.4b) was noticed. Moreover, a synthetic red pigment was found. Thanks to further comparisons with the literature [18], this pigment was identified as the organic pigment red manganese ($C_{18}H_{11}ClN_2O_6SMn$, Raman bands at 358, 495, 742, 969, 1039, 1180, 1233, 1263, 1330, 1364, 1484, 1554, 1600 cm^{-1}) (Figure 6.4c) known also as a naphtol pigment (C.I.PR48:4). The white pigment barium sulphate ($BaSO_4$, Raman bands: 453, 460, 618, 987, 1040) (Figure 6.4e) was also identified frequently in the surface together with calcium carbonate. The green areas visible on the mural paintings, with evidences of colour reintegration, are very few and represent the leaves of the plants over a white background. Analysis with Raman spectroscopy identified only the synthetic pigment phthalocyanine green ($C_{32}H_3Cl_{13}CuN_8$, Raman bands: 220, 262, 289, 330, 345, 684, 740, 775, 814, 956, 978, 1082, 1212, 1282, 1336, 1388, 1503, 1536) (Figure 6.4d).

As already mentioned, some areas of the mural paintings are unusually dark-grey. For example, in the part that represents a tree's trunk. However, in this area only a mixture of carbon black (Raman bands: 1300, 1590 cm^{-1}), barium sulphate and anatase (TiO_2, Raman bands: 142, 196, 395, 514, 638 cm^{-1}) were detected by Raman spectroscopy.

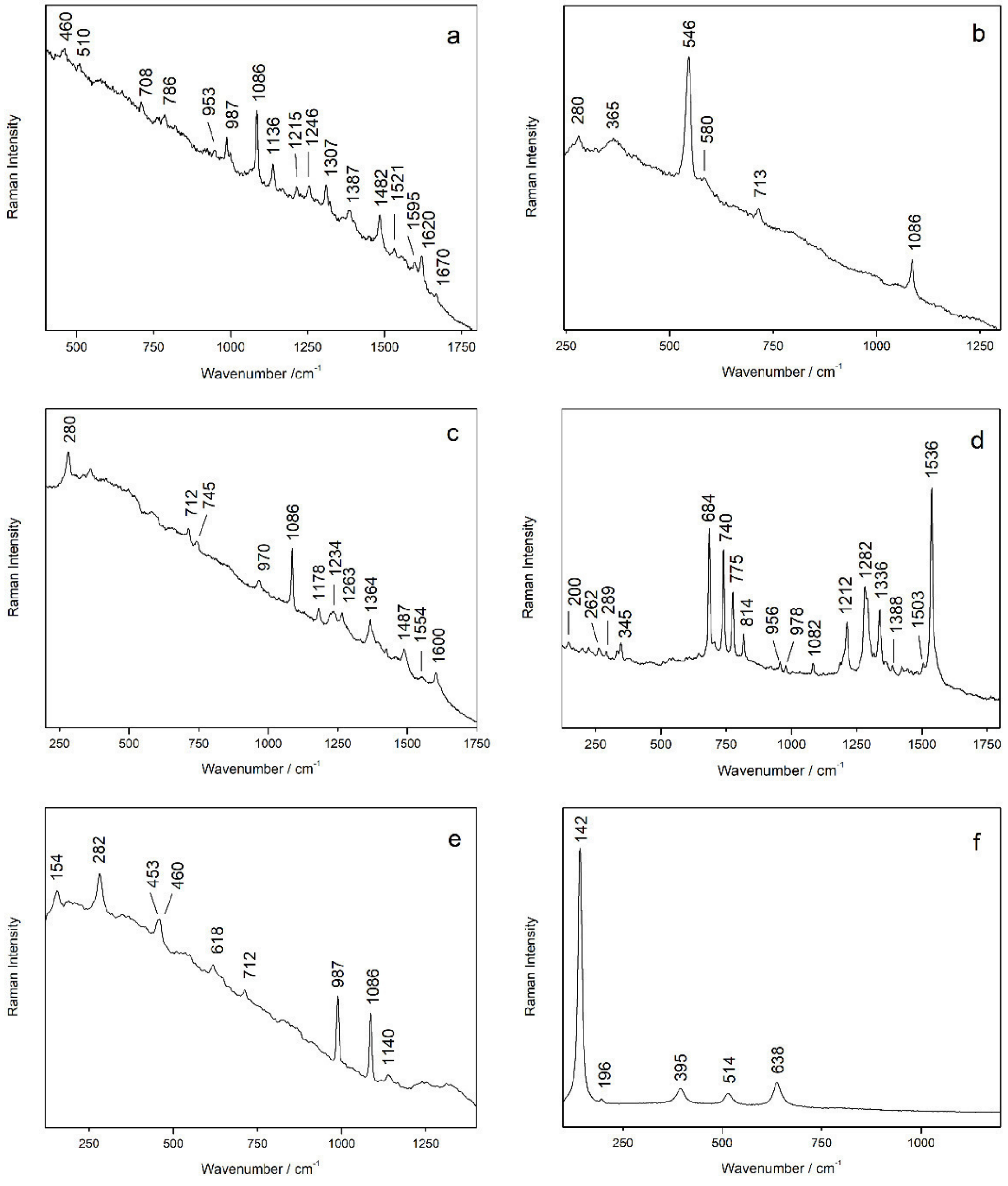

Figure 6.4: Raman spectra of modern pigments identified in wall paintings: arylamide yellow with the most intense peaks of calcium carbonate and barium sulphate (a), ultramarine blue and calcite (b), red manganese with the most intense peak of calcite (c), phtalocianine green (d), barium sulphate together with the features of calcite (e) and anatase (f).

Other grey areas are rather extensive and suggested that this colour was caused by factors beyond the artwork. In fact, one grey area represents a garden and in the past it could have been green in colour. Therefore, special attention was given to the study of these areas in order to understand if the tone was an intentional act or if it was caused by a process of degradation of the raw materials used in the wall paintings. Raman analyses carried out in this grey area, representing grass, in addition to the features of calcite, provided evidence of a mixture of carbon black and barium sulphate. Moreover, the modern white pigment anatase was also identified (Figure 6.4f). There were not recorded spectra of any antique green pigment or blue or yellow pigments that may have been mixed to obtain a green colour [19]. During the analysis *in situ* some green areas painted over this grey background were discovered. However, these areas, representing leaves, were painted with the modern pigment phtalocyanine green; thus, we must assume that this green area is a reintegration.

Unfortunately, there were still doubts about the origin of the possible blackening, and analyses in the laboratory were fundamental. Some samples were taken and submitted to the laboratory. Besides, large amounts of arsenic were detected by X-ray fluorescence in different points of the grey areas (Figure 6.5), even with arsenic signals higher than in the areas where orpiment was found by Raman spectroscopy.

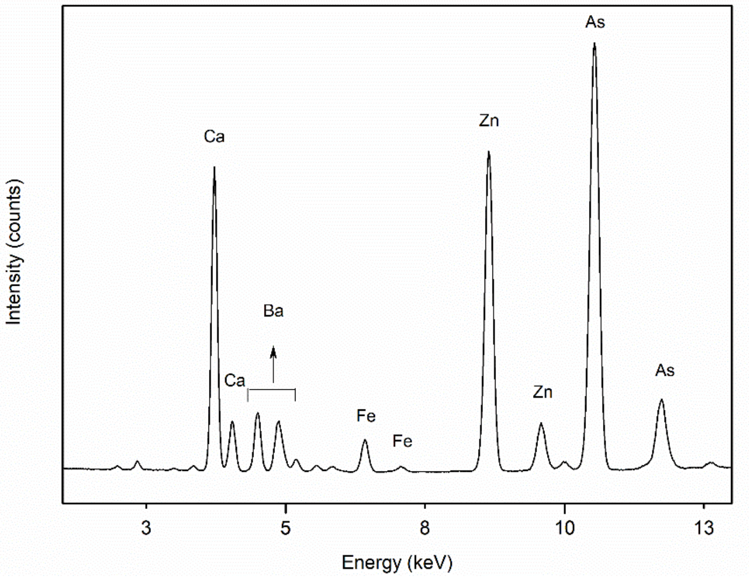

Figure 6.5: ED-XRF spectrum collected in grey areas.

Thus, despite the evident arsenic signals in these areas are evident, as pointed out by the result obtained *in situ*, it seemed to be scarcely plausible that the grey colour was caused by a blackening of orpiment, the only arsenic containing compound found in the wall paintings, since this pigment was detected only in red-orange areas, where the Raman analysis allowed to identify the orpiment in a perfect state of conservation. Moreover, it seemed that the grey colour was not due to any blackening process.

6.2 Laboratory analyses

According to the results obtained with the portable equipment, only the areas of greatest interest were sampled. In order to know the origin of the detected arsenic, to investigate the cause of grey coloration of the wall paintings and the absence of original green pigments, some micro samples were collected in the grey areas. They were embedded in resin and then they were analysed as cross sections using SEM-EDS microscopes and Raman spectroscopy in the laboratory. Moreover, another sample was taken in the green areas to verify the presence of original green pigments and it was analysed also as a cross section. In this way it was possible to study the stratigraphy to better distinguish the original green paint layer from chromatic retouching belonging to the modern times.

First of all, the grey samples were observed at the lowest magnification (200 x) using the scanning electron microscope. The image obtained allowed us to distinguish a complex stratigraphy. The elements' distribution in Figure 6.6 shows the composition of a grey sample in cross section.

The elemental maps show 3 layers (Figure 6.6). The mortar is characterised by the presence of calcium, carbon and silicon (not shown). The original paint layer presents a heterogeneous composition with evident grains of carbon in a matrix of sulphur and calcium. Over this, there is another layer with heterogeneous composition in which some grains of various sizes can be observed. The elemental maps show that the grains are composed by magnesium and arsenic. Together with Mg and As, there is a very thin layer containing Zn, S, Ba and Ti.

In addition, the analyses with SEM-EDS confirmed the presence of zinc in the outer layer together whit titanium and barium, which was also detected by ED-XRF during *in situ* analysis. Although the Raman spectrum of zinc sulphide was not collected (it has a very weak Raman signal), based on the SEM-EDS cross-sections results, it is possible to assume that the lithopone ($ZnS \cdot BaSO_4$), was used in a mixture with anatase since they coexist in the same layer. There are examples in the literature of the use of mixtures of lithopone and anatase in the modern age [20]. This thin painting layer applied in modern times is visible in all the analysed samples collected from the grey areas. Since the documentation regarding the past restoration works is incomplete, we cannot report the reason for this choice. However, we can assume that probably a white painting layer was applied by the restorers to attenuate the original and real black colour of the paintings.

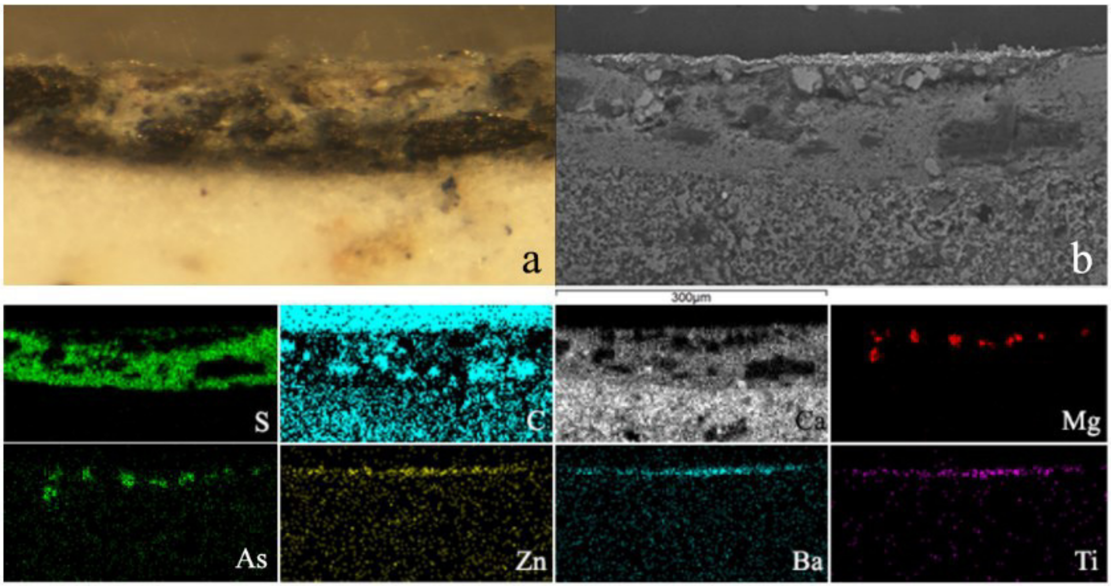

Figure 6.6: Optical microscope image (a) and secondary electron SEM image (b) obtained in a grey sample in cross-section. The elemental distribution maps show evidence of calcium, carbon and silicon (not shown) in the mortar, of sulphur and calcium in the original painting layer together with large amounts of carbon, of the grains composed by arsenic and magnesium, and of zinc, barium and titanium on the surface.

To complete the results obtained by means of SEM-EDS analysis in cross-section, further studies were carried out by Raman spectroscopy for the molecular characterization of this area.

The Raman spectra collected in this layer gave evidence of the massive presence of carbon black (Figure 6.7a) mixed with gypsum ($CaSO_4 \cdot 2H_2O$, Raman bands: 180, 415, 492, 618, 670, 1008, 1135 cm^{-1}) (Figure 6.7b). The observation of samples in the cross section allowed us to distinguish in the original painting, characterized by large grains in a sulphur matrix, small orange grains. The Raman spectra showed very defined features of cinnabar in scarce orange grains (Figure 6.7c).

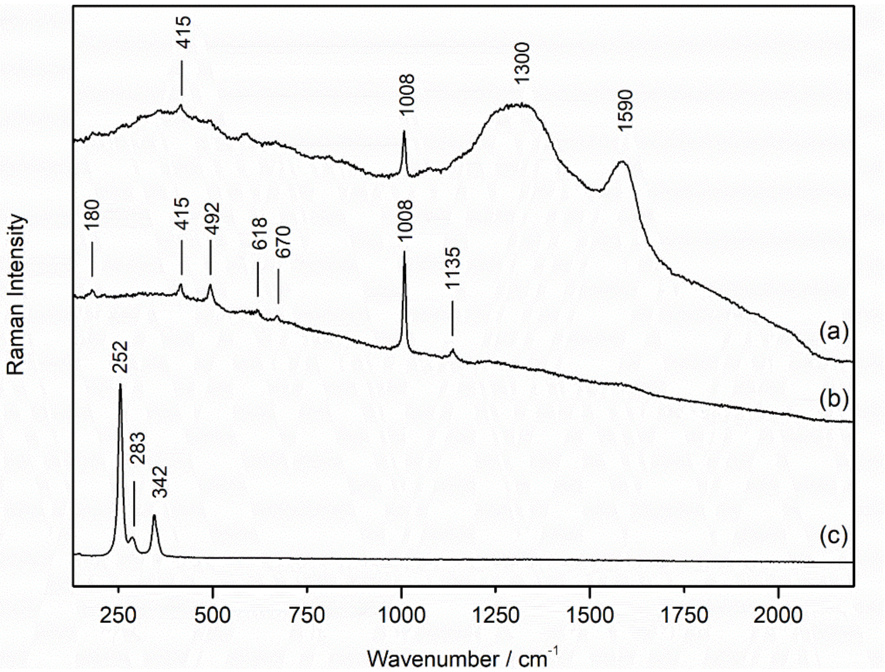

Figure 6.7: Raman spectra of pigments detected in the original paint from samples collected in grey areas: carbon black with the contribution of gypsum (a), gypsum alone (b) and cinnabar (c).

In addition, the samples observed as cross-sections under the microscope did not show evidence of the use of a green pigment in the original painting layer, where no signals of green pigments (or mixtures of yellow and blue pigments) were recorded by Raman spectroscopy.

The fragment taken from green areas was also observed and analysed in cross-section by Raman spectroscopy in the laboratory. Below the green layer, consisting of phtalocyanine green, no original green pigments were identified.

From the results obtained it is possible to conclude that originally, the areas that now appear grey, were not green because no trace of green pigments were found. In fact, the original paint layer was painted with a black hue composed primarily of carbon black and gypsum and cinnabar in smaller amounts. In addition, the areas that were retouched in green (with phtalocyanine green) were originally white.

With regard to the grains composed of arsenic and magnesium found over the original painting layer, several Raman analyses were conducted in the laboratory. They showed the presence of magnesium arsenate (Raman bands at 159, 206, 243, 271, 302, 366, 405, 428, 468, 810, 877 cm^{-1}), a highly toxic product, both for the human health and for the environment. Figure 6.8 shows a comparison with the spectrum of magnesium arsenate in mineral form (hornesite, $Mg_3(AsO_4)_2{\cdot}8H_2O$) [21, 22] and the spectrum recorded, in which the characteristic peaks of gypsum and carbon black are also present. There are not documents proving the use of this product during previous restoration works, but considering that this product is sold as a biocide, it may have been used to remove biological patinas [23]. It seems that the restorers left the product on site for the preservation of the frescoes and to prevent the formation of further biodeterioration processes or that some product remained on the wall paintings during the removal.

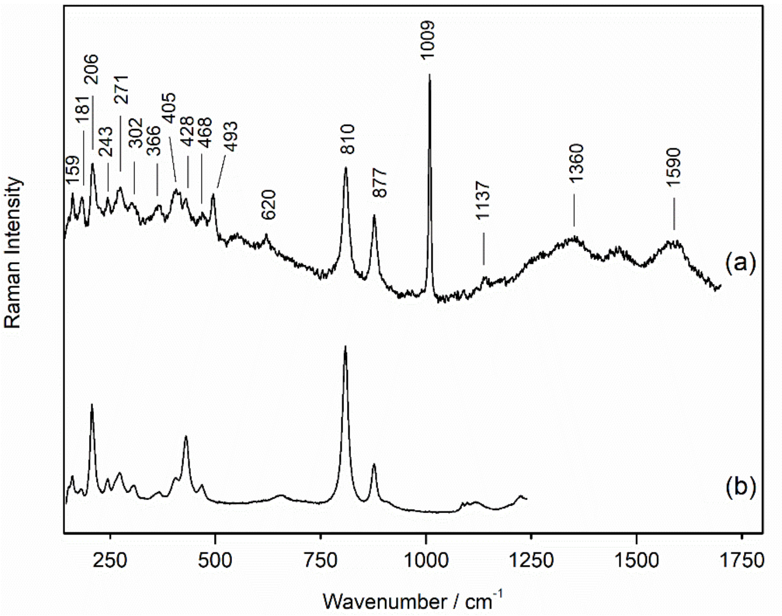

Figure 6.8: Raman spectra of the compound found in the wall painting (a) with the features of gypsum and carbon black and the spectra of mineral hornesite (b).

Table 6.1: Compounds determined by Raman spectroscopy *in situ* and in laboratory.

Reference	Type	Measurements	Location	Colour	Identified compounds
1	Original preparation mortar	*In situ*	Lateral nave	White-sand	Calcium carbonate and quartz
2	Modern plaster	*In situ*	Lateral nave	White	Gypsum, quartz and hematite
3	Polychromy	*In situ*	Apple in the tree (O.S.)	Red	Vermilion, vermilion plus orpiment
4	Polychromy	*In situ*	Camel (lateral nave)	Yellow	goethite
5	Polychromy	*In situ*	Apostles' robes (Ap.)	Orange	Vermilion, hematite
6	Polychromy	*In situ*	Bricklike painting (O. S.)	Yellow	Arylamide yellow
7	Polychromy	*In situ*	Columns (Lateral naves)	Blue	Ultramarine blue
8	Polychromy	*In situ*	Flower (O.S.)	Red	Red manganese
9	Polychromy	*In situ*	Leaves of the plants (O.S.)	Green	Phthalocyanine green
10	Polychromy	*In situ*	Tree canopy, tree’s trunk, grass on the background (O. S.)	Grey	Carbon black, barium sulphate, anatase
11	Polychrome and mortar	Laboratory (Cross section)	Tree canopy, grass on the background (O. S.)	Grey	Anatase, barium sulfate, calcite, magnesium arsenate, gypsum, carbon black
12	Polychrome and mortar	Laboratory (Cross section)	Leaves of the plants (O.S.)	Green	Calcite, phthalocyanine green

*Abbreviations: Representation of Original Sin (O.S), Apostolate (Ap.)

6.3 Final remarks

The results obtained confirm the reliability of the scientific approach for the evaluation of the state of wall paintings preservation. However, it should be noted that the simultaneous use of different elemental and molecular techniques allows a complete study of the materials (see Table 6.1).

By means of spectroscopic techniques, X-ray fluorescence and Raman spectroscopy, used *in situ*, it was possible to get a fairly complete evaluation of the original pigments used by the artists. The pictorial palette is homogeneous in the different parts of the church; hematite, goethite, vermilion, orpiment, gypsum and carbon black. Besides, all the pigments used in restorations works carried out in the modern era, such as arylamide yellow, phtalocyanine green, ultramarine blue, red manganese, barium sulphate, carbon black, and anatase were identified.

In addition, the *in situ* analyses permitted the identification of a very interesting area, from a diagnostic point of view, and a selective sampling was done to complete the study in the laboratory. This allowed us to avoid collecting other useless samples from the wall paintings. In this way, only some micro samples were collected and analysed as cross-section.

The laboratory techniques showed that the presence of a grey-dark colour in the wall paintings was caused neither by an external factor nor by a process of degradation of raw materials but by a voluntary act of the painters. By means of Raman spectroscopy measurements carried out on cross sections, we could verify that the original layer was painted mainly with gypsum and carbon black and with a lesser amount of vermilion. Thus, these parts of the wall paintings would have been originally dark-grey in colour because no green pigment or mixture (yellow and blue pigments) was ever identified. Probably, the lack of green pigments is due to an insufficient availability of the raw materials such as the green earths, malachite, celadonite or glauconite [24].

The only green colour found was phtalocyanine green, which was applied on the surface during a past intervention. In this case, a scientific approach with diagnostic instruments would have allowed to define the original appearance of mural paintings. In fact, the restorers conducted the restoration work starting from a visual observation and from a personal point of view assuming that the grass and the foliage must have been painted in green. They probably thought about a blackening phenomenon of the pigments, in particular about the degradation of the azurite into black tenorite as reported in literature [25]. It may have been mixed with a yellow pigment to obtain a green colour and probably for that reason the restorers used the phtalocyanine green for colour reintegration. Furthermore, the choice of painting some areas that originally were white with phtalocyanine green, as shown in the laboratory analysis, is a further evidence of an arbitrary choice of the restorers which is not compatible with the original appearance of the paintings.

In addition, the analyses in cross-section clarified an important aspect that was not possible to solve *in situ* with the spectroscopic techniques. In fact, it was possible to explain the presence of arsenic detected by the X-ray fluorescence analysis conducted *in situ*. Thanks to the elemental maps obtained by SEM-EDS, and to the molecular maps obtained by Raman spectroscopy, the use of the highly toxic substance magnesium arsenate, that was not documented, was identified.

This seems particularly serious because it is a very hazardous material for the environment and especially for human health. Thus, it was very important to document the presence of such product, especially to make sure that further restorations can be carried out safely and with appropriate precautions for the restorers in the future.

Moreover, magnesium arsenate is a rather invasive product and the restorers did not consider the possible damages that it could induct to the painted surfaces. Without an analytical approach we could not have information since the restoration documents at our disposal did not specify the substance used. For further restoration works, it is not only necessary to know the original materials but, above all, the materials used in the modern era and, as we have verified, a careful study of the materials can only be made with the use of complementary diagnostic techniques.

This work shows the importance of using scientific diagnostic techniques for the study of cultural heritage, especially to provide guidelines to the restorers for an appropriate intervention. In fact, the study of the original materials should be indispensable before making chromatic reintegration to ensure that the choices are compatible and respect the original appearance of the paintings. What we could verify is that, certainly, in the church of Ribera de Valderejo no physico-chemical analyses were carried out and, for this reason, inappropriate interventions were conducted in the past years.

References

[1] M. Maguregui, U. Knuutinen, I. Martínez-Arkarazo, A. Giakoumaki, K. Castro, J. M. Madariaga (2012) Field Raman analysis to diagnose the conservation state of excavated walls and wall paintings in the archaeological site of Pompeii (Italy), *Journal of Raman Spectroscopy*, 43, 1747-1753.

[2] S. R. Amato, D. Bersani, P. P. Lottici, P. Pogliani, C. Pelosi (2017) A Multi-Analytical Approach to the Study of the Mural Paintings in the Presbytery of Santa Maria Antiqua Al Foro Romano in Rome, *Archeometry*, 59, 1-15.

[3] M. Zarzo, A. Fernández-Navajas, F. J. García-Diego (2011) Long-Term Monitoring of Fresco Paintings in the Cathedral of Valencia (Spain) Through Humidity and Temperature Sensors in Various Locations for Preventive Conservation, *Sensors* 11, 8685-8710.

[4] L. Zucconi, M. Gagliardi, D. Isola, S. Onofri, M. C. Andaloro, C. Pelosi, P. Pogliani, L. Selbmann (2012) Biodeterioration agents dwelling in or on the wall paintings of the Holy Saviour's cave (Vallerano, Italy), *International Biodeterioration and Biodegradation*, 70, 40-46.

[5] M. Maguregui, U. Knuutinen, J. Trebolazabala, H. Morillas, K. Castro, I. Martínez-Arkarazo, J. M. Madariaga (2012) Use of in situ and confocal Raman spectroscopy to study the nature and distribution of carotenoids in brown patinas from a deteriorated wall painting in Marcus Lucretius House (Pompeii), *Analytical and Bioanalytical Chemistry*, 402, 1529-1539.

[5] J. Watt, J. Tidblad, V. Kucera, R. Hamilton ed., The Effects of Air Pollution on Cultural Heritage, *Springer* US, 2009.

[7] M. Maguregui, U. Knuutinen, K. Castro, J. M. Madariaga (2010) Raman spectroscopy as a tool to diagnose the impact and conservation state of Pompeian second and fourth style wall paintings exposed to diverse environments (House of Marcus Lucretius), *Journal of Raman Spectroscopy*, 41, 1400-1409.

[8] L. Cartechini, C. Miliani, B. G. Brunetti, A. Sgamellotti, C. Altavilla, E. Ciliberto, F. D'acapito (2008) X-ray absorption investigations of copper resinate blackening in a XV century Italian painting, *Applied Physics*, 92, 243-250.

[9] S. Aze, J. M. Vallet, A. Baronnet, O. Grauby (2006) The fading of red lead pigment in wall paintings: tracking the physico-chemical transformations by means of complementary micro-analysis techniques, *European Journal of Mineralogy*, 18, 835-843.

[10] C. Milanesi, F. Baldi, S. Borin, L. Brusetti, F. Ciampolini, F. Iacopini, M. Cresti (2009) Deterioration of medieval painting in the chapel of the Holy Nail, Siena (Italy) partially treated with Paraloid B72, *International Biodeterioration and Biodegradation*, 63, 844-850.

[11] R. Giorgi, M. Baglioni, D. Berti, P. Baglioni (2010) New Methodologies for the Conservation of Cultural Heritage: Micellar Solutions, Microemulsions, and Hydroxide Nanoparticles, *Accounts of Chemical Researc*, 43, 695-704.

[12] N. Prieto-Taboada, C. Isca, I. Martínez-Arkarazo, A. Casoli, M. A. Olazabal, G. Arana, J. M. Madariaga (2014) The problem of sampling on built heritage: a preliminary study of a new non-invasive method, *Environmental Science and Pollution Research*, 21, 12518-12529.

[13] M. Pérez-Alonso, K. Castro, M. Álvarez, J.M. Madariaga (2004) Scientific analysis versus restorer's expertise for diagnosis prior to a restoration process: the case of Santa Maria Church (Hermo, Asturias, North of Spain), *Analytica Chimica Acta*, 524, 379-389.

[14] H. G. M. Edwards, M. T. Domenech-Carbó, M. D. Hargreaves, A. Domenech-Carbó (2008) A Raman spectroscopic and combined analytical approach to the restoration of severely damaged frescoes: the Palomino project, *Journal of Raman Spectroscopy*, 39, 444-452.

[15] M. Irazola, M. Olivares, K. Castro, M. Maguregui, I. Martínez-Arkarazo, J. M. Madariaga (2012) In situ Raman spectroscopy analysis combined with Raman and SEM-EDS imaging to assess the conservation state of 16th century wall paintings, *Journal of Raman Spectroscopy*, 43, 1676-1684.

[16] M. Pérez-Alonso, K. Castro, J. M. Madariaga (2006) Investigation of degradation mechanisms by portable Raman spectroscopy and thermodynamic speciation: The wall painting of Santa María de Lemoniz (Basque Country, North of Spain), *Analytica Chimica Acta*, 571, 121-128.

[17] M.L. Franquelo, A. Duran, L.K. Herrera, M.C. Jimenez de Haro, J.L. Perez-Rodriguez (2009) Comparison between micro-Raman and micro-FTIR spectroscopy techniques for the characterization of pigments from Southern Spain Cultural Heritage, *Journal of Molecular Structure*, 924-926, 404-412.

[18] W. Fremout, S. Saverwyns (2012) Identification of synthetic organic pigments: the role of a comprehensive digital Raman spectral library, *Journal of Raman Spectroscopy*, 43, 1536-1544.

[19] M.C. Edreira, M.J. Feliu, C. Fernández-Lorenzo, J. Martín (2003) Spectroscopic analysis of roman wall paintings from Casa del Mitreo in Emerita Augusta, Mérida, Spain, *Talanta,* 59, 1117-1139.

[20] L. Boselli, S. Ciattini, M. Galeotti, M. R. Lanfranchi, C. Lofrumento, M. Picollo, A. Zoppi (2009) An unusual white pigment in La Verna Sanctuary frescoes: an analysis with micro-Raman, FTIR, XRD and UV-VIS-NIR FORS, *E Preservation. Science,* 6, 38-42.

[21] B Lafuente, R.T. Downs, H. Yang, N. Stone (2015) The power of databases: the RRUFF project. In: Highlights in Mineralogical Crystallography, T Armbruster and R M Danisi, eds. Berlin, Germany, W. De Gruyter, 1-30.

[22] R. L. Frost, W. Martens, P. A. Williams, J. T. Kloprogge (2003) Raman spectroscopic study of the vivianite arsenate minerals, *Journal of Raman Spectroscopy*, 34, 751-759.

[23] C.T. Duval (1970) Chemical Relationships and Nomenclature of Pesticides–Acaricides, Molluscicides, Rodenticides, etc, *PANS Pest Articles & News Summaries*, 16, 451-469.

[24] I. Aliatis, D. Bersani, E. Campani, A. Casoli, P. P. Lottici, S. Mantovani, I.G. Marino, F. Ospitali (2009) Green pigments of the Pompeian artists’ palette, *Spectrochimica. Acta Part A*, 73, 532-538.

[25] E. Mattei, G. de Vivo, A. De Santis, C. Gaetani, C. Pelosi, U. Santamaria (2008) Raman spectroscopic analysis of azurite blackening, *Journal of Raman Spectroscopy*, 39, 302-306.

CHAPTER 7

Study of natural impact on wall paintings and building materials of the abandoned church of Ribera de Valderejo

The present chapter concerns the study of the conservation state of Saint Stephen's church in the village of Ribera de Valderejo (Álava, Basque Country) and of the wall paintings preserved inside of it. The town is located in a rural area and it is in a state of abandonment, therefore, in these environmental conditions the preservation of artworks is complex.

The interest for the presence of degradation processes in the church of Ribera de Valderejo was born during the study of murals paintings, discussed in the chapter 6, when the presence of accumulation of soluble salts on the surface of wall paintings was noticed together with an extensive colonization of microorganism. Thus, in order to identify the causes that provoked them, considering primarily its natural environment, a deepen research only on the state of preservation of the building was carried out.

The diagnostic of the conservation state of the building heritage is a current topic that has been discussed in several previous works with the aim to identify the degradation processes and the mechanisms that provoked them [1, 2]. Certainly, nowadays, a special attention is paid on damage caused by anthropogenic factors due to the increase of contaminants in the atmosphere [3, 4]. In contrast, the degradation of cultural heritage assets in rural areas does not depend primarily on anthropogenic agents but also on their natural surrounding environment.

Independent of the area, rural or industrial, the artworks located in the open air are difficult to preserve and the impact of environmental agents such as the variation of the soil moisture, the presence of macro and microorganism, the variations of temperatures and humidity, the presence of salt weathering and the biological attacks can be harmful without a conservative strategy [5]. Thus, the identification of the degradation processes described above is an essential step for the conservation of cultural heritage in particular in order to suggest the guidelines for an appropriate restoration work.

Over the last years, several diagnostic techniques have been successfully employed for the evaluation of conservation state of building materials and pictorial surfaces, especially thanks to the use of portable instruments due to their non-destructive and non-invasive characteristics [6]. In particular Raman spectroscopy has demonstrated its reliability for the characterization of secondary products found on historical building materials thanks to its high spectral resolution [7].

For this aim, in this chapter, building materials and decay products were characterized first using Raman spectroscopy and X-ray fluorescence portable devices and subsequently, some collected samples were analysed by laboratory techniques.

7.1 Results

The *in situ* analyses with portable devices (Raman spectroscopy, X-ray fluorescence) allowed us the study of the secondary products found in wall paintings and in building materials. On the other hand, Raman spectroscopy and X-ray diffraction were employed in the laboratory for a complete characterization of materials, in particular for secondary products like efflorescence salts, which were complex to analyse in the form of efflorescence. The analysis was focus on the determination of their composition and the factors that have caused them. Moreover, in order to make it possible to distinguish the composition of the original materials from the degradation products, the structural stone of the church and of the portal were also sampled.

7.1.1 Study of soluble and insoluble efflorescence salts

By using *in situ* Raman spectroscopy on mural painting surface it was possible to identify different degradation products. Hydrated calcium oxalate weddellite ($CaC_2O_4{\cdot}2H_2O$) was detected in some points of the original mortar. The most intense peaks were visible at 869, 910 and 1474 cm^{-1} (Figure 7.1).

The presence of weddellite and the most stable form whewellite ($CaC_2O_4{\cdot}H_2O$), may result from the concomitant biological activity of microorganisms, such as algae or bacteria, and environmental conditions. The microorganism can excrete oxalic acid ($H_2C_2O_4$) that reacts with the carbonaceous materials in the wall paintings, such as calcium carbonate, the main component of the plaster of the wall paintings [8].

In addition, the presence of nitrates was determined, both in the inner layers of the plaster and in the pictorial surfaces. In this case, the presence of the single feature at 1050 cm^{-1} can be attributed to nitrocalcite ($Ca(NO_3)_2{\cdot}6H_2O$) and niter (KNO_3) since both have the main band in this position (the intense fluorescence did not allow us to detect the bands of lower frequencies). However, both salts can be differentiated due to their different FWHM (Full Wide at Half Maximum) values, FWHM=8 cm^{-1} for

KNO_3 and FWHM=22 cm^{-1} for $Ca(NO_3)_2.6H_2O$ [9, 10] being niter, in this case, the nitrate present in the efflorescence. Besides, nitratine ($NaNO_3$) was identified on the wall paintings surface. Its identification was made thanks to the presence of the most intense peak at 1067 cm^{-1}, that is specific for this nitrate salt.

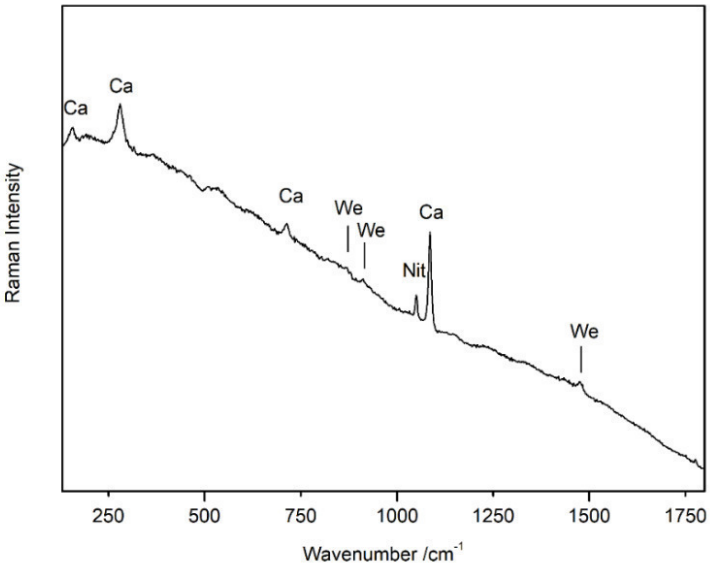

Figure 7.1: Raman spectrum collected on the plaster showed the presence of calcite (Ca), weddellite (We) and niter (Nit).

Further Raman analyses carried out in the laboratory confirmed the presence of niter (KNO_3, Raman bands at 715, 1050, 1343 and 1358 cm^{-1}) over the paintings. In addition, Raman analyses showed the presence of nitratine ($NaNO_3$, Raman bands at 190, 724, 1067 and 1385 cm^{-1}), detected also during the *in situ* analysis, over the pictorial surfaces (Figure. 7.2a). Sodium nitrate or nitratine may indicate a biodeterioration process by microorganisms acting on urine, manure, guano and vegetable waste. Probably, the fact that the church is completely open to the environment (without windows or door) favours the entry of animals such as birds or bats that can deposit the excrements on the walls and paintings. This nitratine compound has been identified even on prehistoric mural paintings [11] and on historical building materials [12].

The salt efflorescences that were taken from the structural walls inside the church had a similar composition. Raman analyses showed that they were mainly composed of gypsum ($CaSO_4{\cdot}2H_2O$, Raman bands at 413, 492, 615, 669, 1008 and 1135 cm^{-1}) and calcite ($CaCO_3$, Raman bands at 156, 282, 713 and 1086 cm^{-1}) (Figure 7.2b). The composition of salts found in the surface of wall paintings is strictly connected with the composition of a new plaster that was applied to cover the wall paintings. In fact, as already mentioned, it is composed almost entirely of gypsum. Thus, it is plausible to assume that this compound is also present on the pictorial surfaces. It must be taken into account that gypsum is partially soluble, and, by the action of moisture, rainwater and/or infiltration water, it can migrate and re-precipitate as efflorescence.

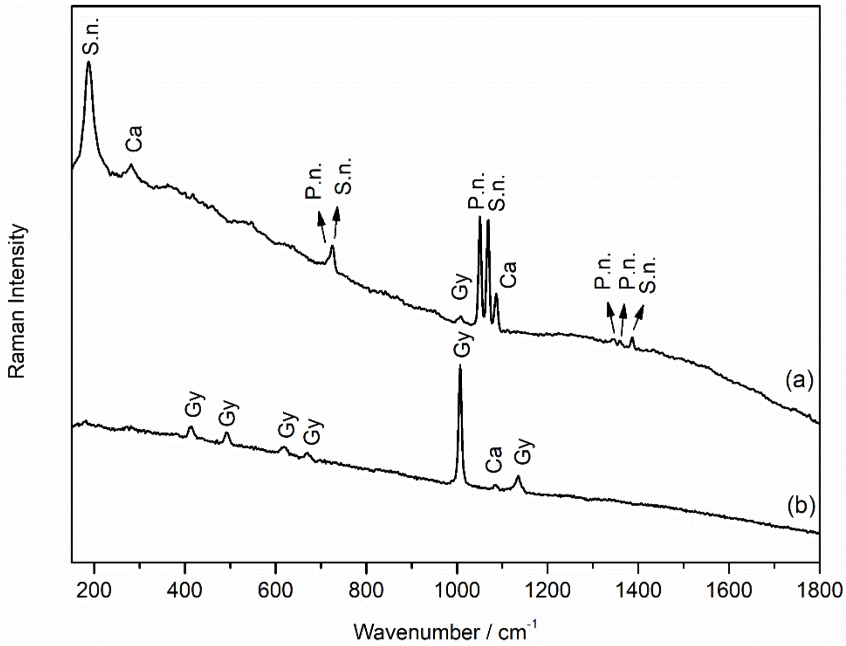

Figure 7.2: Raman spectra collected in the salt efflorescences showed the presence of sodium nitrate (S.n.) and potassium nitrate (P.n.) together with calcite and gypsum (a), calcium carbonate (Ca) and gypsum (Gy) (b).

A high percentage of nitrates, such as sodium nitrate and potassium nitrate together with reprecipitated calcium carbonate, were identified in the salt samples taken from the inner area of the portal too. This area is always exposed to the atmospheric agents and it is directly in contact with the soil, thus it is more exposed to the capillary rise of water from the ground than in the inner walls.

A screening by the X-ray fluorescence portable device was done in different points of the Romanesque portal where the crystallization of salts was particularly evident (Figure 7.3) in order to verify the elemental composition of the stone. All spectra collected in different areas showed a prevalence of calcium together with iron and potassium. The sulphur main peak was also evident (Figure 7.4).

Figure 7.3: Evidence of salt crusts on the portal stone.

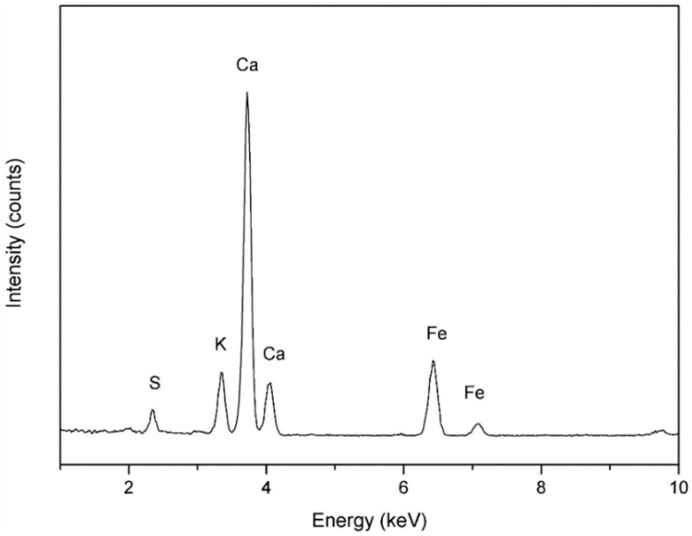

Figure 7.4: ED-XRF spectrum collected in the portal stone.

Raman analyses carried out in the laboratory showed that the salt samples taken from the stone of the Romanesque portal, are mainly composed of potassium sulphate (K_2SO_4, Raman bands at 455, 617, 983, 1102 and 1143 cm^{-1}) (Figure 7.5) and potassium nitrate (niter). Although sulphates were generally found at the bottom of the walls due to their lower mobility compared to nitrates, potassium sulphate was identified in higher area of the walls than potassium nitrate [13, 14].

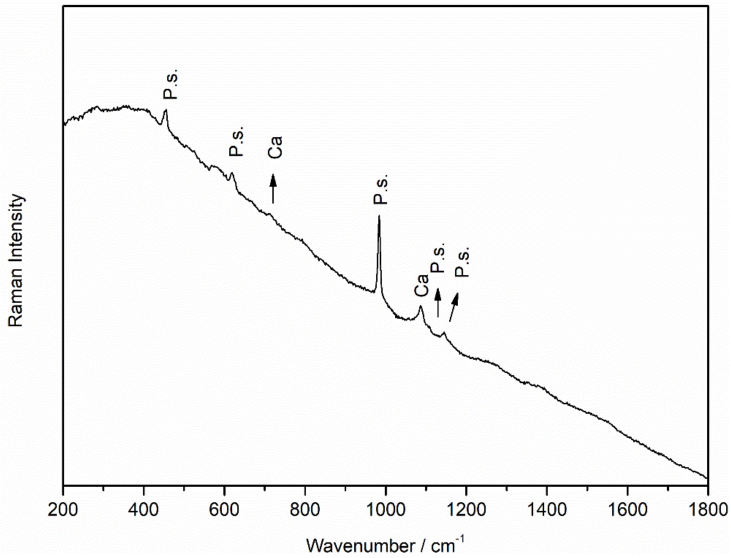

Figure 7.5: Raman spectra collected in the salt efflorescences showed the presence of potassium sulphate (P.s.) and calcite (Ca).

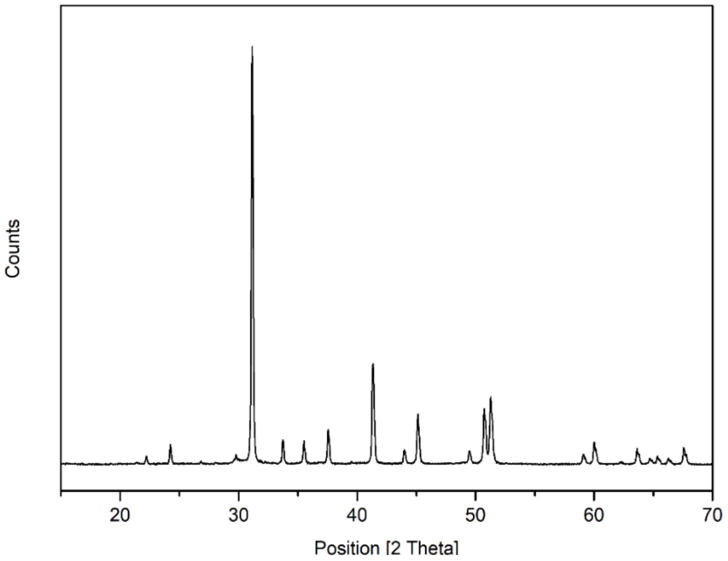

Figure. 7.6: X-ray diffraction pattern of the stone taken from the Romanesque portal show all the peaks belong to the mineral dolomite in addition to goethite and quartz.

Moreover, the stone used for the construction of the portal is mainly composed of mineral dolomite ($CaMg(CO_3)_2$) as demonstrated by both Raman and by X-ray diffraction analysis (Figure 7.6). In addition, the X-ray diffraction measurements pointed out the presence of quartz in small quantities (SiO_2, 26.65 2θ), and of iron oxide goethite (α-FeO(OH) 21.24, 36.68 2θ) that would be responsible of the yellow colour of the stone, explaining the presence of the iron detected by *in situ* ED-XRF analyses.

In contrast to *in situ* ED-XRF analyses, where the presence of potassium was evident, both Raman and X-ray diffraction analyses did not identify any potassium compound. This may be due to the fact that it is not a crystalline compound or that it is present in concentrations lower than 5%, therefore, hardly detectable with these techniques. However, the most likely hypothesis is that potassium comes from the soil and the plants that surround the church and it was not a component of the stone, as described below.

As previously mentioned, some original building materials samples were taken. The original structural stone sampled in a very deteriorated area of the apse wall, analysed by Raman spectroscopy, showed only the peaks of calcium carbonate in contrast to the dolomite found in the portal. X-ray diffraction analysis performed on the same sample gave the same results. In addition, Raman analyses carried out also on the mortar that binds the stones showed that it is mainly composed of calcite and a minor amount of gypsum. The features of calcium carbonate (156, 282, 713 and 1086 cm^{-1}) and calcium sulphate dihydrate (180, 415, 492, 618, 670, 1008 and 1135 cm^{-1}) were noticed in the recorded spectra.

In contrast to the analyses carried out in the materials from the portal, any traces of potassium or potassium compounds were found. This lack of potassium compounds in the original structural stones, as confirmed by Raman and XRD analysis, was a further confirmation of the environmental influence in the formation of potassium salt efflorescences that were found in the portal. In the same way, the presence of calcium sulphate dihydrate in the mortar validates the formation of potassium sulphates on the masonry. The rainwater that infiltrates in the stones drags potassium from the ground and from the roots of the plants and dissolves the sulphate ion of gypsum present in the mortar causing the development of potassium sulphate on the surface.

In contrast to other investigations [15], these results demonstrated that the degradation of the building was not due to anthropogenic contamination caused by the use of fertilizers rich in nitrates or sulphates, but by the natural and continuous accumulation of salts coming from the soils and from the natural decomposition of the vegetable covering.

7.1.2 Characterization of biopatinas

Different types of biological patinas were identified, with naked eye, over the paintings and extensively on stones in the interior walls of the church.

In bibliography different types of carotenoids (β-carotene, zeaxanthin and astaxanthin) have been identified as main responsible of chromatic alteration in cultural heritage materials [16]. They are a class of organic pigments produced by photosynthetic organisms such as algae, fungi or bacteria. Depending on the presence of oxygen in the molecule, they differ in non-oxygenated carotenoids (β-carotene, α-carotene, lycopene) and xanthophylls (luteins, zeaxanthin, astaxanthin). In recent studies, the presence of different types of carotenoids was investigated as markers of air quality [17]. In this sense, the research of Ibarrondo *et al.* [17] demonstrated, thanks to the use of Raman imaging, that the growth of xanthophyll astaxanthin in short time is faster in polluted areas.

All Raman spectra recorded *in situ* showed the three main features of carotenoids (carotene or xanthophyll), the common organic pigments found mainly in the materials preserved in the open air and synthesized by different biodeteriogens. The Raman spectra of carotenoids showed the most intense features located at 1507–1521 (ν_1), 1152–1158 (ν_2), and 1002–1005 (ν_3) cm^{-1} and they are assigned to the C=C stretching mode, to the C–C stretching mode and to the C–H in plane bending vibrational mode of carotenoids respectively [16].

Unfortunately, the *in situ* analyses did not allowed to identify the specific type of compound because the main Raman bands of carotenoids are in similar positions, and the bands of lower frequencies and the overtones must be considered for the accurate identification. Thus, some biological patinas were sampled and further analysis was carried out in the laboratory by Raman microspectroscopy.

Raman spectra gave evidence of zeaxanthin, a xantophyll carotenoid, and one of the most common carotenoid found in the nature. (Figure. 7.7 a). The Raman spectrum showed the most intense peaks at 1521 (ν_1 C=C), 1155 (ν_2 C–C) and 1004 (ν_3 C–H) the most affected ones by the Raman resonance effect. The other Raman bands were located at 960, 1187, 1207, 1267, 1285, 1347, 1386, 1443, 2153, 2345 and 2666 cm^{-1}.

Astaxanthin, another carotenoid of the xanthophylls class containing alcohol and keto groups with 12 conjugated C=C double bonds, was also identified in a green area of a patina. (Figure 7.7 b) The main Raman bands were located at 1507 (ν_1 C=C), 1152 (ν_2 C–C) and 1002 (ν_3 C–H), cm^{-1}. In addition, other peaks of lower Raman intensity that allowed to identify the compound were detectable at 883, 958, 1193, 1212, 1358, 1448, 1568, 2015, 2146, 2294, 2339, 2435, 2461, 2502, 2647, 2785, 2982 and 3015 cm^{-1}.

Raman analyses carried out in some samples in which some orange spots were evident using optical microscope, showed the presence of β-carotene (Figure 7.7 c) This type of non-oxidized carotenoid is the main pigment present in non-polluted areas. The most intense Raman bands are located at 1518 (ν_1 C=C) 1158 (ν_2 C–C) and 1005 (ν_3 C–H) cm^{-1}. The overtones at 2316 cm^{-1} ($2\nu_2$) and combination-tones at 2518 cm^{-1} ($\nu_1\nu_3$) and 2668 cm^{-1} ($\nu_1\nu_2$) were evident. In addition, the features at 874, 966, 1193, 1274, 1310, 1355, 1390, 1450, 1518, 1577, 2161, 2347, 2470 and 3030 cm^{-1} were also noticed.

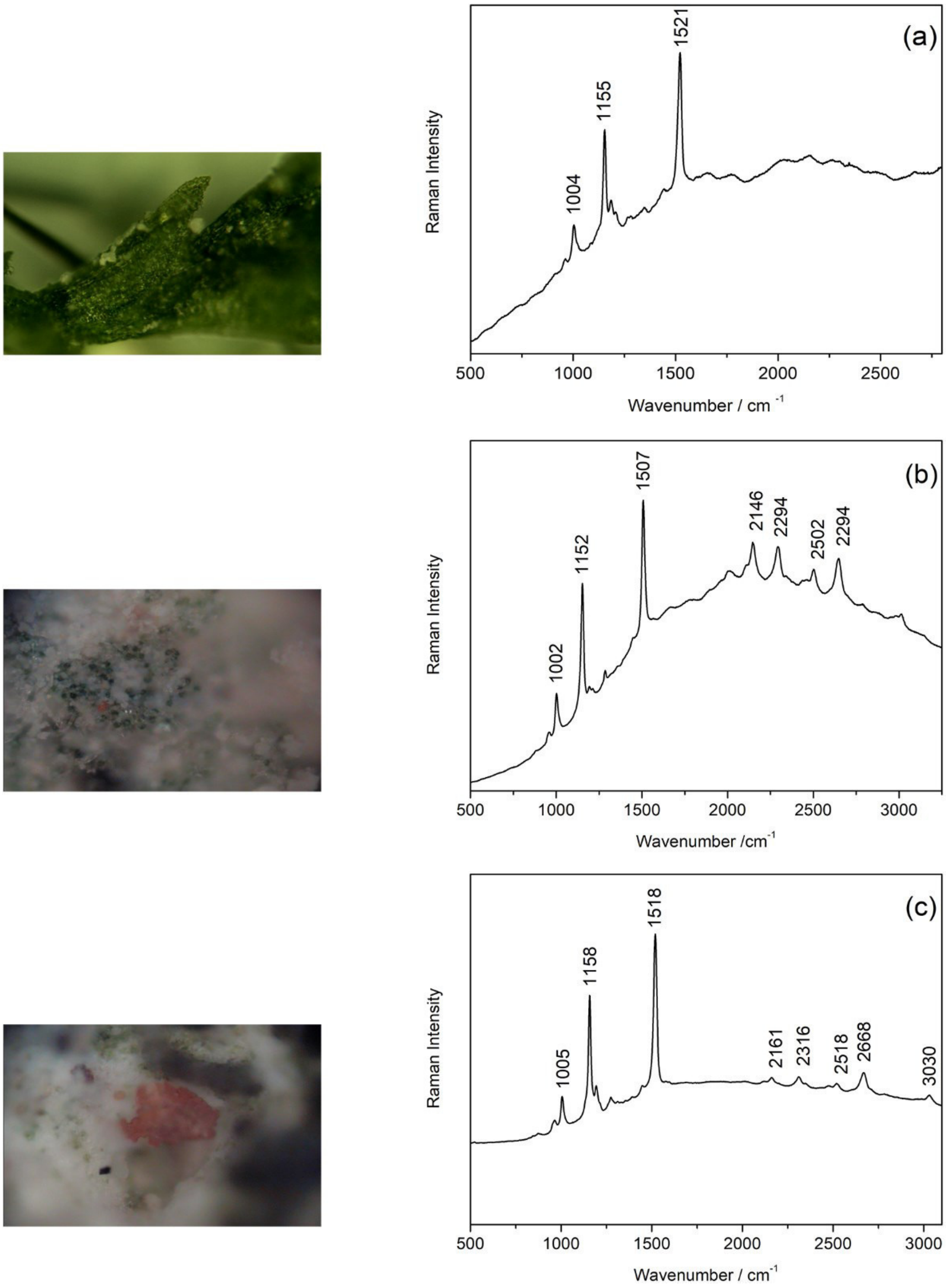

Figure 7.6: Images at optical microscope (50X) on the left and Raman spectra of carotenoids found on wall paintings surface and on structural walls: zeaxanthin (a), astaxanthin (b), β-Carotene (c) and the measuring points.

Photosynthetic organisms such as cyanobacteria, fungi and algae can synthesize carotenoids as a self-protective mechanism to defend against damage caused by air pollution or direct solar radiation. Moreover, the presence of carotenoids as auxiliary DNA repair agents has been recognised also in extreme environmental conditions [18].

The same biological patinas sampled for the Raman analyses were rubbed with cotton swabs and an in vitro growth assay in Petri dishes with Potato Destrose Agar was performed. Then, in order to identify the biological strains, a genomic DNA extraction was carried out. A high similarity (99%) was found with database entries of all biodeteriogens identified.

In two samples of black patinas taken from the wall paintings, fungi of the genus *Cladosporium cladorporioides* were identified (Figure 7.8a). It is a rather common genus of Ascomycetes fungi found on the mural paintings often together with *Aspergillum* or *Penicillum* genus and its spores can be found in the atmosphere, in the soil or in the water. In three green colour patinas, the fungi of the genus *Mortierella alpina* were found (Figure 7.8b). Both identified genes live as saprotrophs on dead organic materials in the soil.

Moreover, two bacteria genus were identified. The first belongs to the genus *Streptomyces sp.*, a genus of filamentous bacteria of the family Streptomycetaceae (order Actinomycetales) (Figure 7.8c). The second kind of bacteria was the *Bacillus amyloliquefaciens,* a microorganism of the *Bacillus* genus (Figure 7.8d). Both bacterial strains are characterized as gram positive bacteria [19] commonly found in the soil and vegetation.

Isolated strains, both fungal and bacterial, belong to spore formers, more properly called an endospore for the bacterial spore. They are certainly the most popular especially for their high rate of spore dissemination, and consequently, for the high colonization capability [20]. The spores are also produced to protect the cell and they allow biodeteriogens to adapt to adverse environmental conditions and survive for a long time [21].

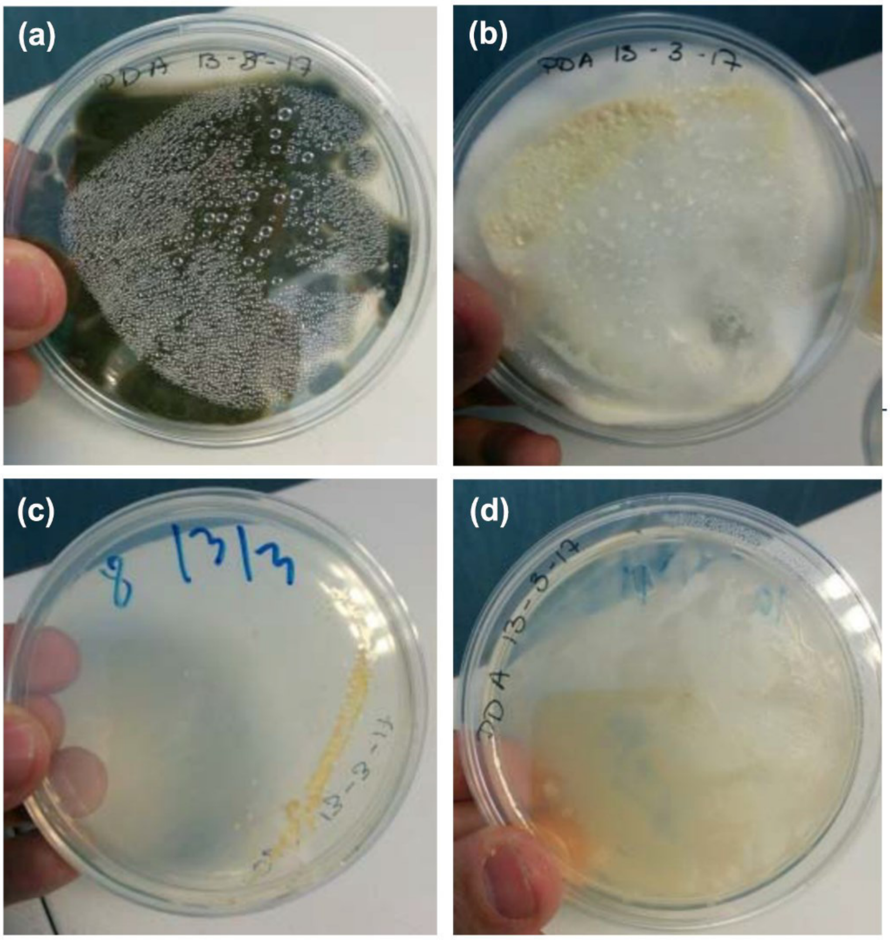

Figure 7.8: Fungi and bacteria strains isolated from wall painting and walls and cultured in PDA Petri dishes: *Cladosporium cladorporioides* (a), *Mortierella alpina (b), Streptomyces sp.* (c) and *Bacillus amyloliquefaciens* (c).

7.2 Final remarks

In contrast to the general opinion, mainly derived from the deterioration processes suffered by buildings and artworks in urban-industrial polluted areas, the preservation of an historical building in a rural area is very complex. The environmental impact can be extremely deleterious especially in absence of a conservation plan. This is the condition of the church of Saint Stephen now, as this multianalytical study using several diagnostic techniques has demonstrated, pointing out the causes of the degradation processes.

With regard to the study of the conservation state of the church, *in situ* analyses identified different degradation products, in particular salt efflorescences and organic patinas, that later were sampled and analysed in-depth in the laboratory. For example, an extensive presence of nitrate salts, potassium and sodium nitrate, was identified by Raman spectroscopy and, as evidenced by the obtained results, it seems to be a consequence of natural environmental impact rather than of the anthropogenic pollutants. Therefore, the main nitrate salts' sources, identified on the surface of the mural paintings and building materials, are nitrogen compounds, ammonium salts and nitrates, present in the soil from the decomposition of organic matter and from plants that absorb the ions through the roots.

The church is constantly exposed to conditions of the surrounding environment and, in addition, it is set directly on the ground in an agricultural area, thus, the ions coming from the soil and from the plants penetrate easily in the walls thanks to the phenomena of rain water infiltration and capillary rise. The water acts as a medium and transports the ions from the ground into the masonry. Besides, the temperature changes trigger dissolution-crystallization cycles and cause the development of white salts surfacing. In the case of the Saint Stephen church these phenomena are favoured by the presence of a masonry that has lost cohesion, and therefore, is characterized by cracks through which water can easily trace.

Moreover, the building is almost covered by vegetation, herbaceous and higher plants that contribute through the roots to transfer the substances. The prolongation of these phenomena over time has caused a massive loss of materials and the collapse of a part of the building.

The study of building materials was a further step to understand the causes that led to the formation of salts. In fact, as demonstrated by using Raman and XRD analyses, the environmental impact is so strong that the potassium sulphate, generated by the interaction of potassium from the soil and the gypsum of the mortar, generally located in lower parts of the masonry than nitrates, was found in the portal stone at about 2.50 meters high.

The research performed shown that the degradation of walls and mural paintings cannot be attributed only to the presence of saline efflorescence but also to an intense biological activity as documented by the molecular and microbiological techniques. For example, the presence of calcium oxalate weddellite identified *in situ* with portable devices appeared strictly connected to biodeterioration processes.

Raman spectroscopy has proven to be extremely efficient for the recognition of three different carotenoids, β-carotene, zeaxanthin and astaxanthin, identified in the biological patina samples. The identification of astaxanthin, the most oxidized of the carotenoid species, is particularly interesting. Until now, it was documented that it was formed, in a short time, in the presence of acidic environmental stress, such as a high SO_2 concentration in the atmosphere. We are not able to know how long the church has been in abandonment but, as documented in this study, the astaxanthin can develop in a long time in an uncontaminated countryside as well.

The detection of fungi and bacteria using analyses of PCR-amplified 18S and 16S rDNA fragments, contributed to better understand the genus of biodeterioration markers that grow within the church. These microorganisms may have a negative effect on the conservation of the mural paintings especially in a place where the atmospheric conditions cannot be controlled. They are causing not only a chromatic damage but also a structural damage caused by the production of mycelium, which can grow in the paintings and in the mortar.

References

[1] M. A. Rogerio-Candelera, M. Lazzari, E. Cano (eds.), Science and Technology for the Conservation of Cultural Heritage, CRC Press, Boca Raton (USA), 2013.

[2] I. Martínez-Arkarazo, M. Angulo, L. Bartolome, N. Etxebarria, M. A. Olazabal, J. M. Madariaga (2007) An integrated analytical approach to diagnose the conservation state of building materials of a palace house in the metropolitan Bilbao (Basque Country, North of Spain), *Analytica Chimica Acta*, 584, 350-359.

[3]. J. Aramendia, L. Gómez-Nubla, K. Castro, I. Martínez-Arkarazo, D. Vega, A. Sanz López de Heredia, A. García Ibáñez de Opakua, J. M. Madariaga (2012) Portable Raman study on the conservation state of four CorTen steel-based sculptures by Eduardo Chillida impacted by urban atmospheres, *Journal of Raman Spectroscopy*, 43, 1111-1117.

[4]. M. Sablier, P. Garrigue (2014) Cultural heritage and its environment: an issue of interest for Environmental Science and Pollution Research, *Environmental Science and Pollution Research*, 21, 5769-5773.

[5] L. K. Herrera, H. A. Videla, (2004) The importance of atmospheric effects on biodeterioration of cultural heritage constructional materials, *International Biodeterioration & Biodegradation*, 54, 125-134.

[6] J. M. Madariaga (2015) Analytical chemistry in the field of cultural heritage, *Analytical Methods*, 7, 4848-4876.

[7] M. Marszałek (2016), Identification of secondary salts and their sources in deteriorated stone monuments using micro-Raman spectroscopy, SEM-EDS and XRD, *Journal of Raman Spectroscopy,* 47, 1473–1485.

[8] R. M. Ion , S. Teodorescu, R. M. Ştirbescu, I. A. Bucurică, I. D. Dulamă, M. L. Ion (2017) Calcium Oxalate on Limestone Surface of Heritage Buildings, *Key Engineering Materials*, 750, 129-134.

[9 H. Morillas, M. Maguregui, O. Gómez-Laserna, J. Trebolazabal, J. M. Madariaga (2012) Characterisation and diagnosis of the conservation state of cementitious materials exposed to the open air in XIX century lighthouses located on the coast of the Basque Country: 'The case of Igueldo lighthouse, San Sebastian, North of Spain, *Journal of Raman Spectroscopy*, 43, 1630-1636.

[10] N. Prieto-Taboada, O. Gómez-Laserna, I. Martínez-Arkarazo, M. A. Olazabal, J. M. Madariaga (2013) Relevance of Cross-Section Analysis in Correct Diagnosis of the State of Conservation of Building Materials As Evidenced by Spectroscopic Imaging, *Analytical Chemistry,* 85, 9501-9507.

[11] A. Hernanz, M. Mas, B. Gavilán, B. Hernández (2006) Raman microscopy and IR spectroscopy of prehistoric paintings from Los Murciélagos cave (Zuheros, Córdoba, Spain), *Journal of Raman Spectroscopy*, 37, 492-497.

[12] A. Hernanz, I. Bratu, O. F. Marutoiu, C. Marutoiu, J. M. Gavira-Vallejo, H. G. M. Edwards (2008) Micro-Raman spectroscopic investigation of external wall paintings from St. Dumitru's Church, Suceava, Romania, *Analytical and Bioanalytical Chemistry,* 392, 263-268.

[13] A. Arnold, K. Zehnder, Monitoring Wall Paintings Affected by Soluble Salts, The Conservation of Wall Paintings, Proceedings of a symposium organized by the Courtauld Institute of Art and the Getty Conservation Institute, London, July 13-16, 1987, Sharon Cather, Editor.

[14] M. A. Vázquez , E. Galán , P. Ortiz , R. Ortiz (2013) Digital image analysis and EDX SEM as combined techniques to evaluate salt damp on walls, *Construction and Building Materials*, 45, 95-105.

[15] M. Veneranda, M. Irazola, M. Díez, A. Iturregui, J. Aramendia, K. Castro, J. M. Madariaga (2014) Raman spectroscopic study of the degradation of a middle age mural painting: the role of agricultural activities, *Journal of Raman Spectroscopy*, 45, 1110–1118.

[16] M. Maguregui, U. Knuutinen, J. Trebolazabala, H. Morillas, K. Castro, I. Martínez-Arkarazo, J. M. Madariaga (2012) Use of in situ and confocal Raman spectroscopy to study the nature and distribution of carotenoids in brown patinas from a deteriorated wall painting in Marcus Lucretius House (Pompeii), *Analytical and Bioanalytical Chemistry,* 402, 1529-1539.

[17] I. Ibarrondo, N. Prieto-Taboada, I. Martínez-Arkarazo, J. M. Madariaga (2016) Resonance Raman imaging as a tool to assess the atmospheric pollution level: carotenoids in Lecanoraceae lichens as bioindicators, *Environmental Science and Pollution Research*, 23, 6390-6399.

[18] H. G. M. Edwards (2007) A novel extremophile strategy studied by Raman spectroscopy, *Spectrochimica Acta Part A*, 68, 1126-1132.

[19] L. Laiz, D. Recio, B. Hermosin, C. Saiz-Jiménez (2000) Microbial Communities in Salt Efflorescences. In: Ciferri O., Tiano P., Mastromei G. (eds) *Of Microbes and Art*. Springer, Boston, MA.

[20] W. Wanfu, M. Xu, M Yantian, M. Lin, W. Fasi, M. Xiaojun, A. Lizhe, F. Huyuan (2010) Seasonal dynamics of airborne fungi in different caves of the Mogao Grottoes, Dunhuang, China, *International Biodeterioration & Biodegradation*, 64, 461-466.

[21] A. A. Gorbushina, J. Heyrman, T. Dornieden, M. González-Delvall, W. E. Krumbei, L. Laiz, Karin Petersen, C. Saiz-Jímenez (2004) Bacterial and fungal diversity and biodeterioration problems in mural painting environments of St. Martins church (Greene–Kreiensen, Germany) J. Swings, *International Biodeterioration & Biodegradation,* 53, 13-24.

CHAPTER 8

PALME software as an alternative tool for semi-quantification of salt efflorescence

As demonstrated in the previous chapter, the identification of salt deposits is a crucial first step in understanding the causes that led to the degradation process and even which chemical reactions have taken place between the environment and the artwork. Since in most cases, the causes of the presence of products of degradation are multiple, currently it is also important to quantify the precipitated salts to better understand the contribution of each factor on the phenomenon of deterioration that can be anthropogenic or natural, intrinsic or extrinsic to the material [1-3].

Many studies show the reliability of the vibrational spectroscopic techniques, FT-IR and Raman, for the study of salt efflorescences [4, 5]. Compared to FT-IR spectroscopy, the Raman technique has a number of advantages; the interpretation of spectra is easier and faster because there are not overlapping bands or overtones. Besides, it can be applied for analysing solid and liquid samples without pretreatment. Although the Raman technique can be considered the most one used for the study of saline deposits, performed in situ and in the laboratory, less researches use Raman spectroscopy for the quantitative analysis of these compounds. As the bibliography's demonstrates, the most widespread method used for semi-quantification with Raman spectroscopy is based on the so-called external calibration curves, where the intensity of the Raman signal is proportional to the concentration of the compound within the sample [6]. An example for this is the work of Veneranda *et al.*, where a quantitative study of salt deposits, present as degradation product on mural paintings, has been successfully performed with Raman spectroscopy using linear external calibration plots [7].

Quantitative Raman analysis has been performed always more frequently with samples in solution [8] and less in solid state [9]. In fact, to get good results homogeneous samples are needed and these can be hardly to obtain when you work with samples in solid state. However, the problem of the homogeneity of the solid phase samples can be overcome by using different procedures during Raman analysis. The use of a rotating sample holder, for example, allows to cover a wider area that represents the whole composition of the sample. Moreover, it is possible to record some spectra for each sample in different areas chosen randomly averaging the results obtained [10].

In this chapter Raman spectroscopy has been used to identify the different compounds present in such salts, but can also be used for the semi-quantification of such salt deposits based on the use of external calibration curves. Normally, this method takes time for the preparation of pellets composed both by mixtures of standard and or by real samples. In the present work we propose an innovative approach for semi-quantification of salts in the solid state by portable micro-Raman spectroscopy. It is based on the use of the PALME software (MONARIS-UPMC, Paris) that has been developed in order to obtain the quantitative information from the vibrational spectrum using a Multivariate Linear Regression approach (MLR). PALME software considers a mixture spectrum as a linear combination of the suspected pure materials spectra and in the field of Cultural Heritage studies it has been applied to various contexts [11-14]. In this investigation both calibration curves and PALME software have been applied to the quantitative analysis on samples of pure salts at different concentrations of calcium carbonate ($CaCO_3$), gypsum ($CaSO_4 \cdot 2H_2O$) and potassium nitrate (KNO_3) in order to compare the results obtained and verify which method can be considered the most reliable. In addition, both methods have been used to quantify real efflorescence salts found in the Saint Stephen's church (Ribera de Valderejo, Basque Country, Spain).

8.1 Methodology

8.1.1 Samples preparation

In order to perform the quantification analysis using external calibration curves and PALME software, a set of fourteen pellets composed by mixtures of commercial salt powders was prepared. As can be seen in Table 8.1, twelve pellets composed by mixtures at different concentrations of calcium carbonate ($CaCO_3$), gypsum ($CaSO_4 \cdot 2H_2O$) and potassium nitrate (KNO_3) (from 0 to 750 mg/g each) were prepared for the construction of calibration curves. Besides, two control pellets were used to assure the proposed method.

Table 8.1: Chemical composition of standard samples used for the external calibration procedure.

Calibration pellet	**Concentration of compounds % (w/w)**		
	$CaSO_4 \cdot 2H_2O$	**KNO_3**	**$CaCO_3$**
1	89.0	10.9	0
2	88.8	0	11.1
3	11.1	88.8	0
4	10.9	0	89.0
5	0	12.4	87.5
6	0	88.6	11.3
7	49.8	20.5	29.6
8	49.1	30.5	20.2
9	30.4	49.3	20.1
10	30.1	20.1	49.7
11	20.3	49.7	29.9
12	20.2	29.8	49.9
13	4.7	80.3	14.9

Calibration pellet	Concentration of compounds % (w/w)		
	$CaSO_4 \cdot 2H_2O$	KNO_3	$CaCO_3$
14	15	5.1	79.7
15	79.6	0	21.3
16	66.3	36.4	0
17	35	0	64.9
18	0	64.6	35.3
Control sample pellet			
1	39.6	39.9	20.4
2	69.3	30.6	0

The standard powders were weighed, aggregated, and mixed thoroughly in an agate mortar to obtain homogenous mixtures that weighs 0.2 g. The mixed compounds were then placed in a cylindrical die to form pellets, applying a pressure of 7 tn/cm^2 for 5 minutes.

Since the PALME software allows the analysis of mixture of spectra considering them as a sum of pure compounds spectra, it was necessary to prepare three reference pellets made of pure salts alone, calcium carbonate, gypsum and potassium nitrate respectively.

Finally, three real salt efflorescence samples, taken from the walls of Saint Stephen's church (Ribera de Valderejo, Basque Country, Spain), a building affected by both capillary and rainwater infiltration phenomena, were prepared in the form of pellets, like those used for calibration, for perform the semi-quantitative analysis.

Obviously, in order to perform the quantitative analysis, all Raman spectra, both of standard and of real samples, were recorded with the same acquisition parameters. All Raman spectra were acquired from 700 to 1400 cm^{-1} because this region collects the most intense features of the compounds of interest ($CaCO_3$, $CaSO_4.2H_2O$, KNO_3) used for the preparation of pellets. To assure reproducibility in the Raman spectra of the pellets, the analyses were performed coupling the Raman probe with a long-distance objective lens (4x) allowing to analyse areas of near 500 µm^2 where the required homogeneity is attained. Each spectrum was collected with 30 seconds of exposure time and 5 accumulations using the 10% of the nominal laser power. In order to obtain a good level of accuracy and to verify the repeatability of analysis, eighteen spectra were recorded in different points of each pellet.

8.2 PALME software

Software PALME was developed in order to obtain quantitative information from the vibrational spectrum of the mixture compound using a Multivariate Linear Regression approach (MLR) [15, 16]. As a first step, each reference spectrum is decomposed into elementary bands (the user can select the Gaussian or Lorentzian band profiles) and adjusted on the experimental spectrum. It defines the reference spectra profiles which are stored to be used for decomposition.

Then, the mixed spectrum is loaded and its adjustment procedure is performed by a linear combination of pure materials spectra using a least-squares criterion and the Levenberg-Marquardt algorithm. The software shows graphically (Figure 8.1) the decomposition of the spectrum.

The contribution of each pure component that is required to compose the experimental spectrum is expressed as two different coefficients, the weighting coefficient (*á*) and the area proportion depending on the employed spectroscopic technique. In the case of Raman spectroscopy, the contribution of each component pure on the mixture is expressed as a weighting coefficient (*á*) expressed as percentage. In order to achieve a good level of accuracy in the semi-quantitative analysis a series of spectra are collected in the same sample and the amount of analyte is given by the average of the coefficients.

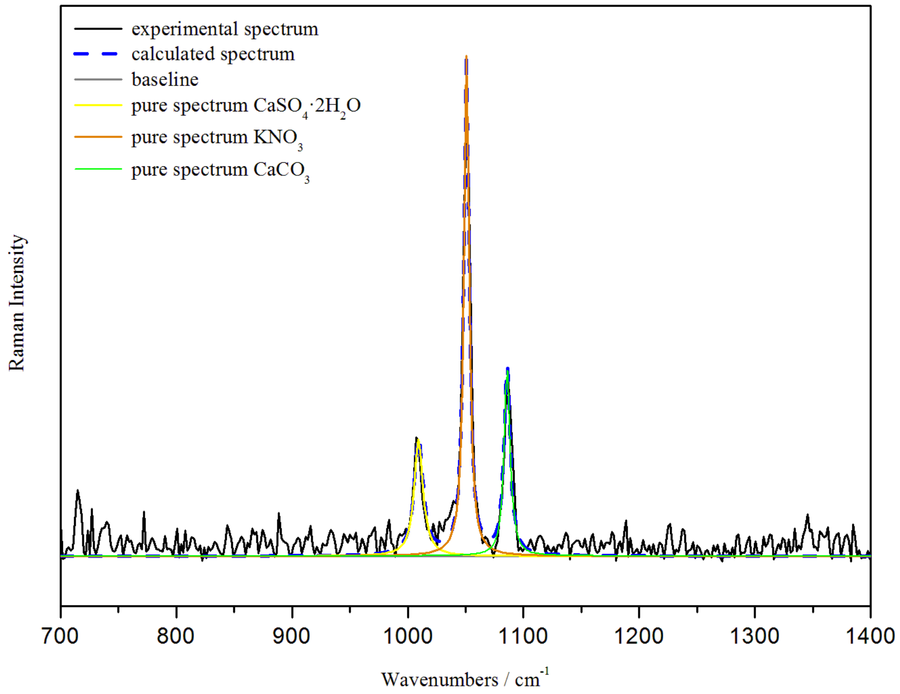

Figure 8.1: Spectral adjustment of Raman spectrum recorded on a pellet of real salt composed by a mixture of calcium carbonate, gypsum and potassium nitrate.

8.3 Results and discussion

In order to perform the quantification of each compound in the samples using calibration curves, 18 pellets were analysed using micro Raman spectroscopy. Six calibration curves were constructed, three evaluating the height (Figure 8.2) and three evaluating the integration area (Figure 8.3) of the main Raman band of calcium carbonate (1086 cm^{-1}, CO_3^{2-} ν_1), gypsum (1008 cm^{-1}, $SO_4^{2-}\nu_1$) and potassium nitrate (1050 cm^{-1}, NO_3^- ν_0), for each Raman spectrum recorded.

Due to the experimental uncertainty, the uncertainty of the intercept was always higher than 50% of % relative standard deviation (RSD); thus, the intercept of all calibration curves was fitted to 0 value. The changes in the slopes were within the estimated uncertainty of the results.

As demonstrated by previous studies carried out on salt efflorescence, it occurs a direct proportionality between the intensity of the main peaks of salts with their concentration [17]. Considering the height of the main Raman bands, the R^2 values for calcium carbonate, gypsum and potassium nitrate were 0.9544, 0.9788 and 0.9525 respectively.

Because the height of the Raman bands is influenced by the degree of crystallinity of the compounds, three calibration curves were built considering also the area of the peaks. As it can be seen, the values have a slightly improvement using the integration area of the main peaks. The R^2 were 0.9531 for $CaCO_3$, 0.9795 for $CaSO_4.2H_2O$ and 0.9606 for KNO_3. However, the general distribution of dots around the regression line is about the same for both extracted parameters (i.e. band intensities or areas), underlining that the measurement dispersion is more related to sample's characteristics than spectra treatment.

The obtained calibration curves showed that the linear correlation between both, peak integration area and height, is reasonably good. Moreover, taking into account that the work is based on the study of solid samples, the results obtained were quite good. In fact, it is much more difficult to achieve a good level of homogeneity of the samples with powders in the solid state compared to samples in solution. However, with regard to the homogeneity, the relative standard deviation of the signals of the analytes of interest in each pellet varied between 4%-10%, which can be acceptable for solid samples.

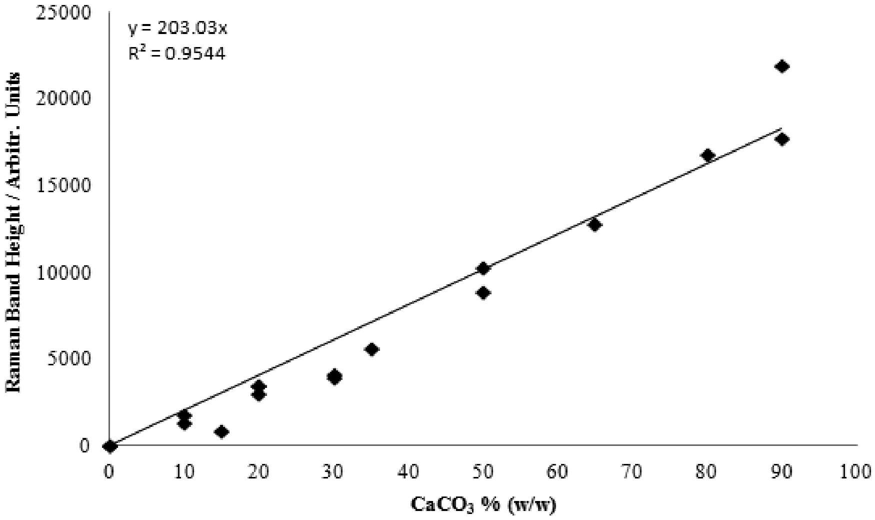

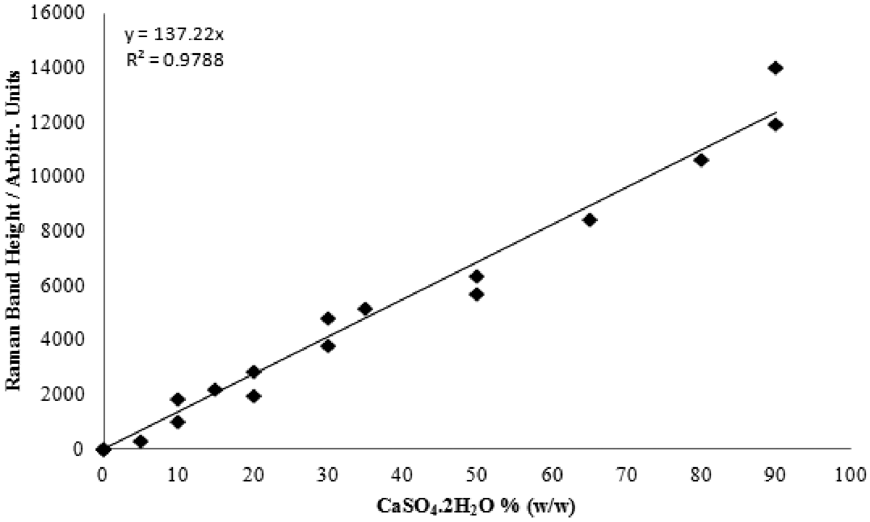

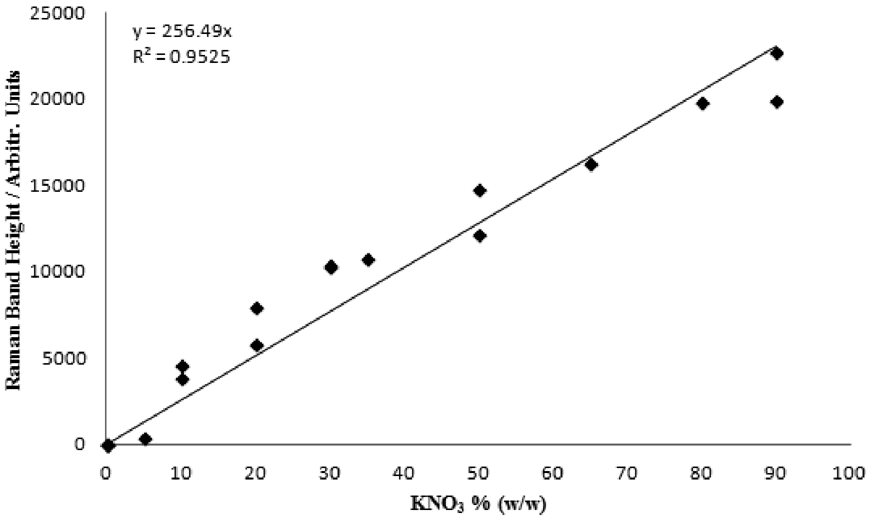

Figure 8.2: Raman calibration curves built evaluating the height of main Raman bands of calcium carbonate ($CaCO_3$), gypsum ($CaSO_4.2H_2O$) and potassium nitrate (KNO_3).

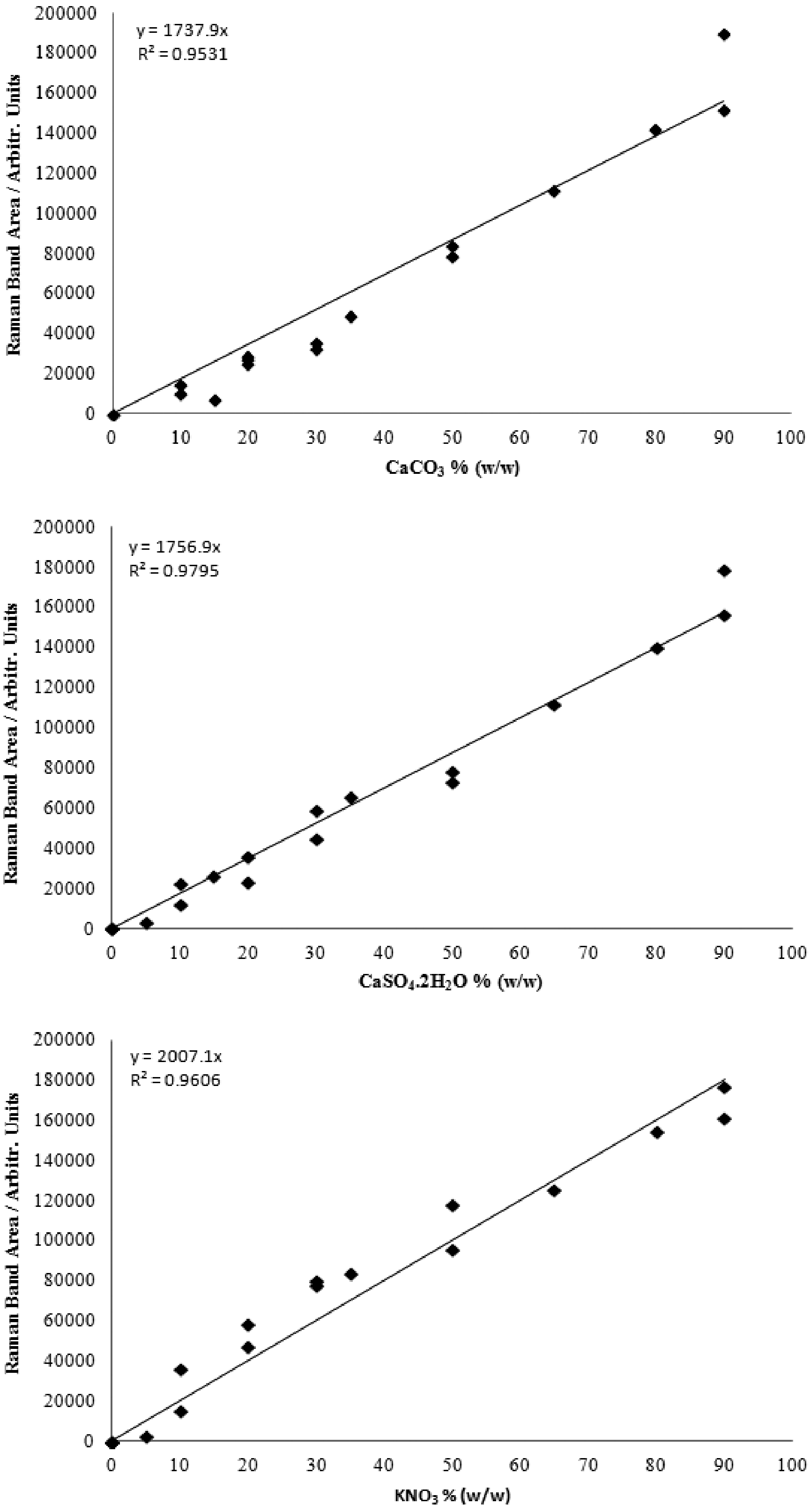

Figure 8.3: Raman calibration curves built evaluating the integration area of main Raman bands of calcium carbonate ($CaCO_3$), gypsum ($CaSO_4.2H_2O$) and potassium nitrate (KNO_3).

Two control pellets were also analysed by Raman spectroscopy in order to verify the reliability of the method. The quantitative results obtained respectively with the calibration curves, and with PALME software, concerning control samples with known concentration, are summarized in Table 8.2. Through the equation of the straight line, the contribution of each compound within the mixture was calculated. Concerning the control sample number 1 considering the integration area of main Raman bands the relative difference between the real concentration and the calculated one was for calcium carbonate 0.1%, for gypsum 3.1% and for potassium nitrate -12.7%. On the other hand, evaluating the height of Raman features the relative difference between real and calculated concentration was for calcium carbonate 1.3%, for gypsum and 0.4% and for potassium nitrate -9.5%. Concerning the control sample number 2 the relative difference between the theoretical and calculated percentages was for gypsum -5.4%, for potassium nitrate -25.2% considering the integration area of the Raman bands. Evaluating the height of Raman features the relative difference between real and calculated concentration was for gypsum -14.7% and for potassium nitrate -21.5%. Even though the results seem to present lack of accuracy, the paired test-t demonstrates that there are no significant differences between the obtained results and the real values. The results obtained analysing the control pellets show that the external calibration curves procedure is reliable for semi-quantitative analysis of salts samples in the solid state. Besides, the evaluation of the integration areas has returned results closer to the real ones confirming that they are more reliable for the semi-quantitative analysis of compounds.

Table 8.2: Results obtained with external calibration (8% of average %RSD) and with PALME software (4% of average %RSD) for control samples.

Control sample	**Compound**	**% (w/w) real**	**% (w/w) integration area**	**% (w/w) height**	**% (w/w) PALME**
Pellet 1	$CaCO_3$ $CaSO_4.2H_2O$ KNO_3	20.4 39.6 39.9	20.4 38.3 45.0	20.1 39.4 43.7	11.9 42.2 44.8
Pellet 2	$CaCO_3$ $CaSO_4.2H_2O$ KNO_3	0 69.3 30.6	6.0 73.1 38.3	5.7 79.5 37.2	0 67.4 32.5

Because PALME software only require the spectra from pure samples (reference spectra) it was applied directly on all Raman spectra from prepared pellets, both, those used for the construction of external calibration curve and those of control samples to determine the contribution of each salt in the mixtures. The reference spectra have to be recorded in the same conditions, i.e. with the same laser power and for the same number of accumulated scans, in order to obtain meaningful relative intensities between them. Treated experimental spectra do not require to be acquired with the same conditions as references, as only proportions between references spectra are used in the treatment. By working on site, according to situations, acquisition parameters could then be adjusted to obtain “good” spectra, offering more adaptability than using quantification through calibration curves. As the program needs the definition of a baseline to obtain the adjustment of spectra, they were corrected in the data pre-treatment step to exclude fluorescence background. The semi-quantification study of all spectra was performed through the deconvolution procedure. They were fitted with linear combinations of the reference Raman spectra for 700 to 1400 cm^{-1}. Decomposition was performed also for binary mixture. The software allows to keep out the corresponding pure spectrum before the quantitative analysis. The amount of each pure material required to form the experimental mixed spectrum is provided with the weight coefficient expressed as percentage.

Tables 8.2 and 8.3 show the average in percentage obtained collecting eighteen Raman spectra for each pellet compared with the real concentration of calcium carbonate, gypsum and potassium nitrate present in the standard samples. Polynomial trend line (Figure 8.4) reveals a good correlation between the real concentrations and the average of calculated values with PALME for all analysed pellets. Moreover, the paired test-t demonstrates that there are no significant differences between the obtained results and the real values.

Table 8.3: Real concentration of the pellets used for external calibration and calculated concentration by PALME (3% of average %RSD).

External calibration	Compounds	% (w/w) real	% (w/w) average PALME
Pellet 1	$CaCO_3$ $CaSO_4.2H_2O$ KNO_3	0 89.00 10.90	0 87.48 12.31
Pellet 2	$CaCO_3$ $CaSO_4.2H_2O$ KNO_3	11.10 88.80 0	7.13 92.77 0
Pellet 3	$CaCO_3$ $CaSO_4.2H_2O$ KNO_3	0 11.10 88.80	0 9.48 90.42
Pellet 4	$CaCO_3$ $CaSO_4.2H_2O$ KNO_3	89.00 10.90 0.00	83.82 16.08 0.00
Pellet 5	$CaCO_3$ $CaSO_4.2H_2O$ KNO_3	87.50 0 12.40	79.20 0 20.70
Pellet 6	$CaCO_3$ $CaSO_4.2H_2O$ KNO_3	11.30 0 88.60	6.00 0 93.90
Pellet 7	$CaCO_3$ $CaSO_4.2H_2O$ KNO_3	29.60 49.80 20.50	18.69 53.19 28.01
Pellet 8	$CaCO_3$ $CaSO_4.2H_2O$ KNO_3	20.20 49.10 30.50	12.47 48.85 38.32
Pellet 9	$CaCO_3$ $CaSO_4.2H_2O$ KNO_3	20.10 30.40 49.30	12.52 29.09 58.36
Pellet 10	$CaCO_3$ $CaSO_4.2H_2O$ KNO_3	49.70 30.10 20.10	36.14 35.49 28.47
Pellet 11	$CaCO_3$ $CaSO_4.2H_2O$ KNO_3	29.90 20.30 49.70	18.91 20.03 60.59
Pellet 12	$CaCO_3$ $CaSO_4.2H_2O$ KNO_3	49.90 20.20 29.80	35.89 23.23 40.41
Pellet 13	$CaCO_3$ $CaSO_4.2H_2O$ KNO_3	14.90 4.70 80.30	4.38 4.98 90.48

External calibration	Compounds	% (w/w) real	% (w/w) average PALME
Pellet 14	$CaCO_3$ $CaSO_4.2H_2O$ KNO_3	79.70 5.10 15.00	76.37 21.48 2.00
Pellet 15	$CaCO_3$ CaSO4.2H2O KNO_3	21.30 79.60 0	12.43 87.47 0
Pellet 16	$CaCO_3$ CaSO4.2H2O KNO_3	0 66.30 36.40	0 61.55 38.35
Pellet 17	$CaCO_3$ $CaSO_4.2H_2O$ KNO_3	64.90 35.00 0	55.93 43.97 0
Pellet 18	$CaCO_3$ $CaSO_4.2H_2O$ KNO_3	35.30 0 64.60	25.24 0 74.66

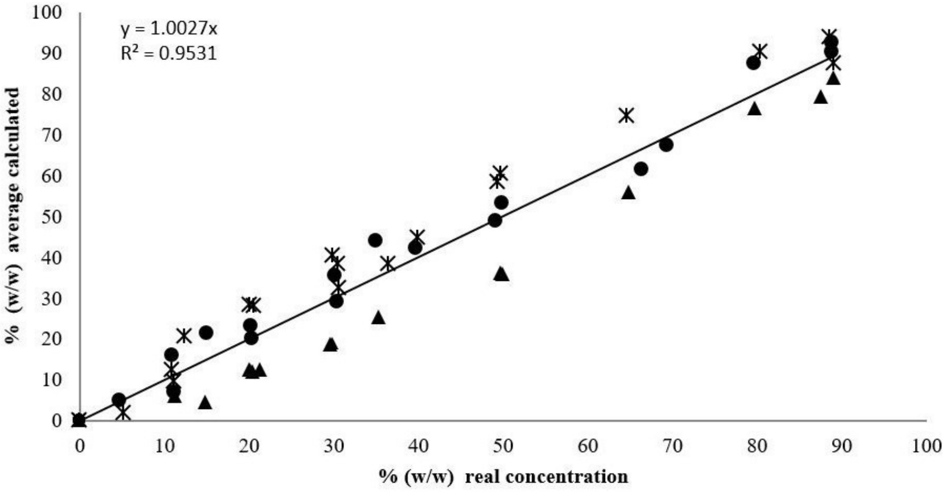

Figure 8.4: Trend line built with real concentration of the pellets used for external calibration and the average of concentration calculated by PALME software of calcium carbonate ($CaCO_3$), gypsum ($CaSO_4.2H_2O$) and potassium nitrate (KNO_3).

For a better comparison of the results between the two approaches, external calibration and PALME, a trend line was built using the concentration of calcite, gypsum and potassium nitrate calculated for control samples 1 and 2 with both methods. The x-axis represents the values obtained with external calibration procedure, evaluating integration area, and the y-axis represents the data obtained with PALME (Figure 8.5). The R^2 value 0.9514 demonstrates that there is an acceptable correlation between the concentration obtained with PALME and the area of the peaks. Therefore, both methods are comparable when you operate semi-quantitative analysis. Moreover, the paired test-t demonstrates again that there are no significant differences between both methods.

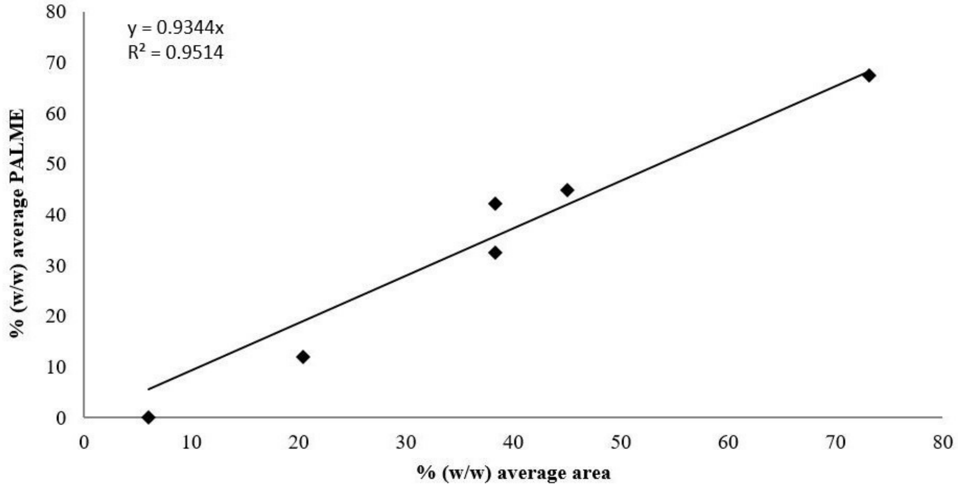

Figure 8.5: Trend line built with the average of concentrations of calcium carbonate ($CaCO_3$), gypsum ($CaSO_4.2H_2O$) and potassium nitrate (KNO_3) in the control sample calculated both evaluating the integration area of Raman bands and with PALME software.

Finally, three pellets prepared using real salt efflorescences, sampled in the Saint Stephen's church (Ribera de Valderejo-Basque Country), were analysed with both quantitative methods. These samples were previously characterized *in situ* by portable Raman spectrometer. The analysis showed the presence of calcium carbonate, gypsum and potassium nitrate, thus, they were semi-quantified by the developed external calibration procedure and the PALME software.

Both analytical procedures show that salt efflorescences, especially samples 2 and 3, are mainly composed of potassium nitrate followed by gypsum. Calcium carbonate is present in minor amount. For the sample 1 a slight trend reversal appears in the results obtained by calibration procedure and PALME for calcite and gypsum (Table 8.4). In this case, the R^2= 0.876 of the trend line built using concentrations of compounds, calculated with integration area of main Raman bands and with PALME software, confirmed a good correspondence between the data obtained from both methods (Figure 8.6). Once again, the paired test-t confirmed that there were no significant differences among the obtained results.

Although the research seems to show that the best results were obtained using calibration curves considering integration area of main Raman bands, paired test-t did not see significant differences, and the program PALME has significant advantages. In fact, it allowed to perform quantification analysis without preparing a set of reference pellets (with a calibration curve for each measurement conditions) with a considerable saving of time. Even if the variation between real and calculated data is higher with PALME it can be accepted when you work *in situ* for semi-quantitative analysis of mixtures of salts. However, the PALME software has proved to be an effective tool for identifying the main compounds in a mixture and this aspect is very important if PALME software is applied in the field of Cultural Heritage. Characterizing the concentrations of each mixture salts make it possible to classify the different causes that have caused the salt formation. The identification of each concentration therefore, allows to diagnose the most damaging cause of a porous material's deterioration. In this way, it can be possible to suggest the most appropriate method of intervention and in case to prevent the damage.

Table 8.4: Result obtained with external calibration (20% of average %RSD) and with PALME (10% of average %RSD) for real salt efflorescences from the sampled church.

Real samples	**Compounds**	**% (w/w) integration area**	**% (w/w) height**	**% (w/w) PALME**
Pellet 1	$CaCO_3$ $CaSO_4.2H_2O$ KNO_3	22.9 11.7 53.3	21.8 15.3 48.4	17.7 21.4 59.5
Pellet 2	$CaCO_3$ $CaSO_4.2H_2O$ KNO_3	18.0 25.3 59.7	17.2 35.3 58.6	10.2 33.6 56.9
Pellet 3	$CaCO_3$ $CaSO_4.2H_2O$ KNO_3	12.6 43.0 47.5	14.0 59.5 45.2	7.1 49.8 42.4

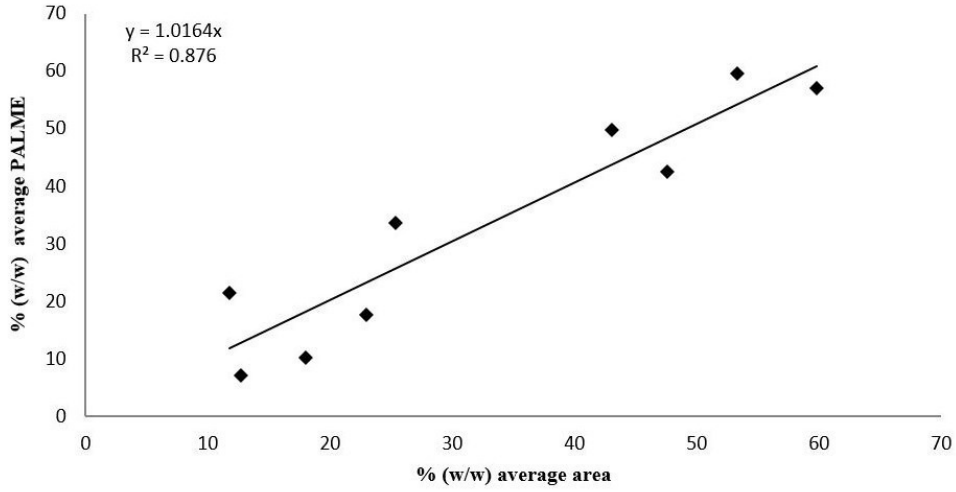

Figure 8.6: Trend line built with the average of concentrations of calcium carbonate ($CaCO_3$), gypsum ($CaSO_4.2H_2O$) and potassium nitrate (KNO_3) in the real salt efflorescence samples calculated both evaluating the integration area of Raman bands and with PALME software.

8.4 Final remarks

In this chapter, the PALME software was tested as a viable alternative to the external calibration curve procedures for the study of mixture of spectra recorded on salt samples in the solid state using portable micro Raman spectroscopy. This software was applied for the analysis of reference samples, at known concentration, and of real samples in order to establish the contribution of each compound in the mixture.

The results obtained by both quantification approaches were comparable in statistical terms revealing that the results obtained by the external calibration and the PALME software methods are reliable and repeatable. The results show that this new approach can be considered an appropriate tool for the semi-quantification of salt efflorescences and for the diagnosis of porous material employed as building materials.

The advantages of using the PALME software are evident. On the one hand, it can be applied on vibrational spectra without a previous preparation of the reference standard samples, which are instead required for the construction of the calibration curves. In this way, we can perform quantitative analysis in a very short time compared to other chemometric techniques. In fact, PALME does not need the preparation of the calibration curve, thus, it is a less time consuming approach.

On the other hand, one of the most important aspects highlighted in this research is that the use of portable Raman instrumentation coupled to PALME software could allow to perform semi-quantitative estimation of compounds, not only in the laboratory but also in situ. This feature is particularly useful in the field of the Cultural Heritage as it allows to carry out a quantitative study of salt deposits without needing a sampling and without using a laboratory analysis. Requiring only the reference spectra of quantified compounds, this reference database could be acquired prior to the field campaign. On site, it only requires for spectrum treatment the choice of the suspected compounds to obtain their quantification, without prerequisite on measurement conditions. Thanks to its non-invasiveness, speed in processing data and reliability features, the combination of Raman spectroscopy and PALME software for semi-quantification purposes is suggested for all fields of study, including Cultural Heritage, in which the sampling procedure is precluded or not recommended. Furthermore, compared to the reference technique of X-ray diffraction (XRD) and Rietveld analysis, such approach offers an alternative for the analytical quantification of mineral phases much more portable and without heavy data treatment.

References

[1] P. López-Arce, J. García-Guinea, D. Benavente, L. Tormo, E. Doehne (2009) Deterioration of dolostone by magnesium sulphate salt: An example of incompatible building materials at Bonaval Monastery, Spain, *Construction and Building Materials*, 23, 846-855.

[2] N. Prieto-Taboada, M. Maguregui, I. Martínez-Arkarazo, M. A. Olazabal, G. Arana, J.M. Madariaga (2011) Spectroscopic evaluation of the environmental impact on black crusted modern mortars in urban–industrial areas, *Analytical and Bioanalytical Chemistry*, 399, 2949-2959.

[3] H. Morillas, M. Maguregui, O. Gómez-Laserna, J. Trebolazabala, J. M. Madariaga (2012) Characterisation and diagnosis of the conservation state of cementitious materials exposed to the open air in XIX century lighthouses located on the coast of the Basque Country: The case of Igueldo lighthouse, San Sebastian, North of Spain, *Journal of Raman Spectrosc*opy, *43*, 1630-1636.

[4] M. Irazola, M. Olivares, K. Castro, M. Maguregui, I. Martinez-Arkarazo, J. M. Madariaga (2012) In situ Raman spectroscopy analysis combined with Raman and SEM-EDS imaging to assess the conservation state of 16th century wall paintings, *Journal of Raman Spectrosc*opy, 11, 1676-1684.

[5] R. Mazzeo, E. Joseph, V. Minguzzi, G. Grillini, P. Baraldi D. Prandstraller (2006) Scientific investigations of the Tokhung-Ri tomb mural paintings (408 A.D.) of the Koguryo era, Democratic People's Republic of Korea, *Journal of Raman Spectrosc*opy, 37, 1086-1097.

[6] J. H. Giles, D. A. Gilmore, M. B. Denton (1999) Quantitative analysis using Raman spectroscopy without spectral standardization, *Journal of Raman Spectroscopy*, 30, 767-771.

[7] M. Veneranda, M. Irazola, M. Díez, A. Iturregui, J. Aramendia, K. Castro, J. M. Madariaga, (2014) Raman spectroscopic study of the degradation of a middle age mural painting: the role of agricultural activities, *Journal of Raman Spectroscopy*, 45, 1110-1118.

[8] M. Kim, H. Chung, Y. Woo, M. S. Kemper (2007) A new non-invasive, quantitative Raman technique for the determination of an active ingredient in pharmaceutical liquids by direct measurement through a plastic bottle, *Analytica Chimica Acta*, 587, 200-207.

[9] C.G. Kontoyannis, N.Ch. Bouropoulos, P.G. Koutsoukos (1997) Use of Raman Spectroscopy for the Quantitative Analysis of Calcium Oxalate Hydrates: Application for the Analysis of Urinary Stones, *Applied Spectroscopy*, 51, 64-67.

[10] R. Szostak, S. Mazurek (2002) Quantitative determination of acetylsalicylic acid and acetaminophen in tablets by FT-Raman spectroscopy, *Analyst*, 127, 144-148.

[11] F. Salpin, F. Trivier, S. Lecomte, C. Coupry (2006) A new quantitative method: non-destructive study by Raman spectroscopy of dyes fixed on wool fibres, *Journal of Raman Spectroscopy*, 37, 1403-1410.

[12] C. Daher, V. Pimenta, L. Bellot-Gurlet (2014) Towards a non-invasive quantitative analysis of the organic components in museum objects varnishes by vibrational spectroscopies: Methodological approach, *Talanta*, 129, 336-345.

[13] J. Aramendia, L. Gómez-Nubla, L. Bellot-Gurlet, K. Castro, C. Paris, P. Colomban, J. M. Madariaga (2014) Protective ability index measurement through Raman quantification imaging to diagnose the conservation state of weathering steel structures, *Journal of Raman Spectroscopy*, 45, 1076-1084.

[14] J. Monnier, L. Bellot-Gurlet, D. Baron, D. Neff, I. Guillota, P. Dillmann (2011) A methodology for Raman structural quantification imaging and its application to iron indoor atmospheric corrosion products, *Journal of Raman Spectroscopy*, 42, 773-781.

[15] S. Döpner, P. Hildebrandt, A. Grant Mauk, H. Lenk, W. Stempfle (1996) Analysis of vibrational spectra of multicomponent systems. Application to pH-dependent resonance Raman spectra of ferricytochrome *c, Spectrochimica Acta Part A*, 51, 573-584.

[16] S. Bernard, T. Soulimane, S. Lecomte (2004) Redox and conformational equilibria of cytochrome c_{552} from *Thermus thermophilus* adsorbed on a chemically modified silver electrode probed by surface-enhanced resonance Raman spectroscopy, *Journal of Raman Spectroscopy,* 35, 47-52.

[17] A. Broggi, E. Petrucci, M. P. Bracciale, M. L. Santarelli (2012) FT-Raman spectroscopy for quantitative analysis of salt efflorescences, *Journal of Raman Spectrosc*opy, 43, 1560-1566.

CHAPTER 10

Final conclusions

As stated in chapter 2, the main objective of this thesis consisted in the study of some wall paintings from the Gothic period. In particular, two different scenarios were studied, one concerning the wall paintings preserved inside the Saint Stephen's church of Ribera de Valderejo (Álava, Spain) and the other one the wall paintings located inside the Saint Stephen's chapel of Montani (Bolzano, Italy). In both cases, an assessment of the state of conservation was carried out because the paintings presented some critical issues that were understood only thanks to a thorough scientific diagnostic study, together with the expertise of curators.

The wall paintings were studied trying to obtain the maximum information through portable non-destructive techniques including the identification of the critical areas of study to take as few samples as possible and to avoid unnecessarily damage to the painted surfaces, and therefore, safeguarding their integrity. The best *in situ* results were obtained through the simultaneous use of elemental and molecular spectroscopic techniques such as XRF and Raman spectroscopy. However, some important information could only be obtained through the use of laboratory techniques that are able to obtain information using a very limited amount of sample. For this purpose, the techniques applied *in situ* were extremely useful for the identification of particularly important areas, from the diagnostic point of view, where micro samples were required to collect.

Furthermore, the identification of the materials such as pigments, their choice and the way they were used in the figurative scenes, represents a tool to understand the social, economic and cultural aspects when the work of art was realized as well as the condition of the client or the cultural environment of the past. For this reason, the study of materials does not only concern technicians, but must be complementary to the studies of the historical and artistic surroundings in which a work of art is born. Therefore, an interdisciplinary approach between professionals who share different fields of knowledge seems essential in order to carry out a critical diagnostic study and establish the best conservation protocol. Fortunately, this PhD project has been developed with the collaboration of such professionals.

From a socio-cultural point of view two completely different cases have been studied and this is reflected in the current appearance of the paintings.

In the case of Saint Stephen's chapel of Montani, the great wealth of the client is demonstrated by the richness of the decorations and by the variety and quality of the pigments used. The study of wall paintings confirmed the presence of lead-based pigments which were identified by the restorers as responsible for an extensive phenomenon of blackening without having made any diagnostic analysis. Restorers even applied a lead white cleaning procedure without confirming the presence of lead white as an original pigment.

Fortunately, the application of the reconversion method of lead dioxide to lead white was applied only in small areas during the cleaning tests. Although this method was proposed in the 90s, it has not been widely used according to the existing bibliography. As demonstrated by this case study, probably at the local level, this treatment continues to be used, without carrying out any previous analyzes, and going against the minimum intervention concept, one of the restoration fundamentals. Thus, the decision of not continue with the treatment seems the most appropriate from a conservation point of view as the physical integrity of the surfaces was not guaranteed either because this blackened aspect is part of the history of the pictorial cycle and should be preserved despite strongly influencing the appreciation of the work of art.

In addition, the analysis carried out in the laboratory confirmed the presence of different lead based pigments but without detecting any trace of lead white. Furthermore, the results showed that blackening was caused not only by the presence of lead pigments (red lead) but also by the degradation process of iron pigments that had not been considered by restorers.

In the case of the Saint Stephen's church of Ribera de Valderejo the presence of both original and modern pigments was identified *in situ* as evidence of the fact that the paintings have undergone restoration works in the modern times. The current appearance of the paintings, characterized by a dark shade and due to the large use of carbon black, reflected a humble social context and the lack of raw materials in that period or region.

A further proof of the importance of applying diagnostic techniques for the study of original materials before carrying out restoration work, was confirmed by the fact that the pictorial retouching intervention did not respect the original appearance of the paintings. The analyses showed that no green pigment was originally used and that the restoration intervention with modern green pigments was not appropriate. Furthermore, XRF analysis identified the presence of arsenic in different parts of wall paintings and this was not compatible with the presence of arsenic pigments since only traces of them were identified. Through the use of chemical analysis imaging in the laboratory it was possible to identify the presence of an undocumented product based on arsenic, a biocide product, a substance potentially dangerous for the environment and for humans. In particular, in view of future restorations, restorers should take precautions in this regard.

The two scenarios investigated highlighted the importance of the application of non-destructive and micro-destructive diagnostic techniques for the study of original materials and degradation products, but above all, with the aim of guiding the restorers in the choice of the most appropriate restoration methods. This type of approach was not very common in the past years and the evaluations were carried out according to the experience of the restorer, causing, in some cases, inappropriate choices of procedures not compatible with the state of conservation of the works of art or with the work of art itself.

Nowadays the scientific diagnostic approach is an essential step in the planning of a conservation intervention and it will be necessary to insist in this direction with the aim to educate all those who work for the preservation of cultural heritage towards greater sensitivity by encouraging and promoting the use of any analytical technique, better if it is non-destructive. Is the labor of scientist to teach and spread the necessity of the analytical studies of any artwork before any intervention.

Another important aspect underlined in the thesis is that a greater attention must be directed at the surrounding environment without focusing only on wall paintings but extending the observation to phenomena that could affect them and to the degradation products that are located even in adjacent areas. Indeed, the investigations documented in this PhD thesis, demonstrate the importance of the study of secondary products in relation to the characteristics of the surrounding environment in order to evaluate its influence in the deterioration processes.

Unlike the church of Montani, the work on the church of St. Stephen required a thorough assessment of the state of conservation because it presents more critical problems caused by the state of abandonment of the entire building. The characterization of efflorescence is an important step because they are one of the major causes of deterioration of building materials, and because it is important to understand which are the factors that have caused their formation and try to limit them when it is possible. The lack of cohesion of the building materials was caused by continuous phenomena of both capillary rising from the ground and water infiltration phenomena favored by cracks opened by the presence of macro organisms (higher plants) that surround the church.

In particular, the study conducted in the church of Ribera de Valderejo would like to draw attention to a situation now over the edge. The massive presence of saline crystallization, of macro and microorganisms has caused irreversible damage over the years and in the absence of a recovery plan there is a real risk of collapse of the structure and that the wall paintings will be lost forever. It is important to highlight that all these problems have arisen in absence of direct or near pollution sources (such as greenhouse gases producers) in the middle of a natural park, which means that even in clean surroundings decay phenomena occur because soils, grass, microorganisms, rain are acting every day.

The studies carried out have shown phenomena of indirect degradation caused by the environmental and by the morphological conditions of the territory in which the buildings are located. This suggests that it would be necessary to study in a more detailed way also scenarios that do not show clear sources of contamination or that apparently do not appear to be damaged because they are placed in environments with a low level of anthropogenic pollutants.

Another important aspect of this PhD work is related with the new methodologies that have been tested (see the last two chapters of the thesis). The PALME program, used for the first time for the semiquantification of salt efflorescences, has proved to be an excellent tool thanks to its ease and speed of use. Furthermore, the main advantage is that it could be used in study campaigns in which the greater presence of a given salt can already suggest in situ the predominant factor of deterioration of the material under study.

The realization and the application of the microfluidic device for the detection of ammonium can represent a new research line even if the work presented in this

PhD thesis is a first step towards the experimentation of new non-invasive devices able to be applied directly to the surfaces both for the detection of contaminants and for their monitoring. The results are quite interesting, although, as will be explained below, further research is necessary. Indeed, thanks to the use of the device it was possible to determine the presence of ammonium, a substance very difficult to detect in mural paintings, generated by the environmental impact and highly dangerous for the integration of carbonated building materials.

Considering the results obtained, I can state that the established objectives have been successfully achieved. In addition, thanks to the experience gained in these years I think that have acquired the skills necessary to complete a critical scientific study starting from the analysis to be carried out in situ and the modalities of an effective sampling to conclude the analysis in the laboratory, completing the whole analytical process.

Future work

Currently, scientific research applied to the study of cultural heritage is focused, among other directions, on the development of new technologies and the experimentation of new materials in particular for the study and monitoring of the effects of contaminants in the atmosphere. This has been done in this PhD on two low polluted scenarios. But, at the end of a research that has developed the characterization of original and alteration materials and the evaluation of the state of conservation of wall paintings, the last chapter of the thesis has been dedicated to the development of a new methodology for the monitoring of ammonium.

Indeed, a microfluidic device was designed, and tested in the laboratory on mockups exposed to ammonium nitrate solutions for 7 months. It proved to be suitable for the detection of ammonium already from the first month of application.

However, further tests in the laboratory using mockups should be carried out by varying the ammonium nitrate solution concentration ranges, as well as the humidity, monitoring the sensor colour change through a photometric analysis, etc. To simplify the monitoring, once applied in a real case, the sensor should be monitored remotely through a micro-camera similar to those of which smartphones are equipped, with a considerable time saving.

As demonstrated by the results shown in chapter 9, the device also detected the ammonium when the mortar is in contact with vapors, thus, it is not clear if the detection comes from the outside of the device or through the mortar, by absorption. This drawback can be solved by modifying the experimental protocols and by improving the sensor design or by using different materials. In fact, the PMMA layer is rigid and does not adhere perfectly to the mockup so it could be replaced by a more flexible polymer such as PSA or COP used in the lamination process. Furthermore, it may be useful in the future to equip the device with an external sensor in direct contact with the environment so that the behavior of the two sensors can be compared.

The reduced realization time together with the easy use and remote control are characteristics for a device that could be placed on the market and it could be considered in the future its applicability also for the determination of other contaminants that affect cultural heritage.

CHAPTER 11

Scientific publications

1 I. Costantini, M. Veneranda, N. Prieto-Taboada, L. Bellot-Gurlet, K. Castro, J.M. Madariaga, (2016) Comparison of semiquantification experimental methodologies using micro-Raman spectroscopy: PALME software as an alternative tool for the study of salt efflorescence, *Journal of Raman Spectroscopy,* 47, 1415-1421.

2 I. Costantini, M. Veneranda, M. Irazola, J. Aramendia, K. Castro, J. M. Madariaga, (2018) The green grass was never green: How spectroscopic techniques should have assisted restoration works, *Microchemical Journal* 138, 154-161.

3 I. Costantini, K. Castro, J. M. Madariaga, Portable and laboratory analytical instruments for the study of materials, techniques and environmental impacts in mediaeval mural paintings (2018) *Analytical Methods*, 10, 4854-4870

4 J. M. Madariaga, I. Costantini, K. Castro (2019) Analysis of natural degradation of medieval mural paintings in the open air abandoned church of Ribera, North of Spain, Raman Spectroscopy in Art and Archaeology, Volume 2, 213-233, Willy, Chichester, UK.

ANNEX

Abbreviations

ATR: Attenuated Total Reflection spectroscopy

ATR-FT-IR: Attenuated Total Reflection–Fourier Transform InfraRed spectroscopy

CCD: Charge-coupled Device

COP: cyclo-olefin polymer

ED-XRF: Energy-Dispersive X-ray Fluorescence spectroscopy

ESEM-EDS: Environmental Scanning Electron Microscope-Energy dispersive system

FORS: Fiber-Optic Reflectance Spectroscopy

FT-IR: Fourier-Transform Infrared spectroscopy

FWHM: Full-Width at Half Maximum

GC-MS: Gas Chromatography Mass Spectrometry

GIS: Geographic Information System

HSL: hue, saturation, lightness

HSV: hue, saturation, value

IO-1: 1-ethyl-3-methylimidazolium ethyl sulfate

IO-2: trihexyltetradecyl-phosphonium dicyanamide

IR: Infrared spectroscopy

LA-ICP-MS: Laser-Ablation Inductively-Coupled Plasma Mass Spectrometry

LIBS: Laser-Induced Breakdown Spectroscopy

LMWOA: Low Molecular Weight Organic Acids

MALDI-TOF-MS: Matrix Assisted Laser Desorption Ionization-Time Of Flight Mass Spectrometry

NIR: Near Infrared spectroscopy

OM: Optical Microscopy

PMMA: polymethylmethacrylate

PSA: pressure-sensitive adhesive polymer

PY-GC-MS: Pyrolysis Gas Chromatography Mass Spectrometry

RGB: Red, Green, Blue

SEM: Scanning Electron Microscope

SEM-EDS: Scanning Electron Microscope-Energy dispersive system

TEM: Transmission Electron Microscopy

UV: Ultraviolet spectroscopy

VIS: Visible spectroscopy

Vis-RS: Visible reflectance spectroscopy

XRD: X-ray Diffraction

XRF: X-ray Fluorescence